CKDMIP: CKD tool performance evaluation

May 3, 2020

CKD tool: **ecCKD version 0.5**
Spectral domain: **Longwave**
Application: **Climate**
Evaluation dataset: **Evaluation-1**

Contents

Model 1:	ecCKD climate-fsck-9	**3**
Model 2:	ecCKD climate-fsck-14	**5**
Model 3:	ecCKD climate-fsck-21	**7**
Model 4:	ecCKD climate-fsck-27	**9**
Model 5:	ecCKD climate-fsck-40	**11**
Model 6:	ecCKD climate-fsck-59	**13**
Model 7:	ecCKD climate-wide-14	**15**
Model 8:	ecCKD climate-wide-19	**18**
Model 9:	ecCKD climate-wide-30	**21**
Model 10:	ecCKD climate-wide-43	**24**
Model 11:	ecCKD climate-wide-57	**27**
Model 12:	ecCKD climate-wide-87	**30**
Model 13:	ecCKD climate-narrow-22	**33**
Model 14:	ecCKD climate-narrow-28	**36**
Model 15:	ecCKD climate-narrow-37	**39**
Model 16:	ecCKD climate-narrow-48	**42**
Model 17:	ecCKD climate-narrow-69	**45**
Model 18:	ecCKD climate-narrow-101	**48**

Overview

This automatically generated document contains an evaluation of the performance of ecCKD for generating longave correlated k-distribution (CKD) gas-optics models targeting the application *Climate*: atmospheric heating rates are required to a minimum pressure of 0.02 hPa, and evaluation is performed for a wide range of greenhouse gas concentrations. The evaluation dataset is *Evaluation-1* from the Correlated K-Distribution Model Intercomparison Project (CKDMIP)[1]. Longwave radiative transfer is performed using four angles per hemisphere.

[1] `https://confluence.ecmwf.int/display/CKDMIP`

The ecCKD tool has been used to generate CKD models with the following band structure(s): *fsck* (one full-spectrum band), *wide* (5 bands) and *narrow* (13 bands). For each band structure, a number of CKD models have been generated, characterized by the total number of k terms (also known as g points).

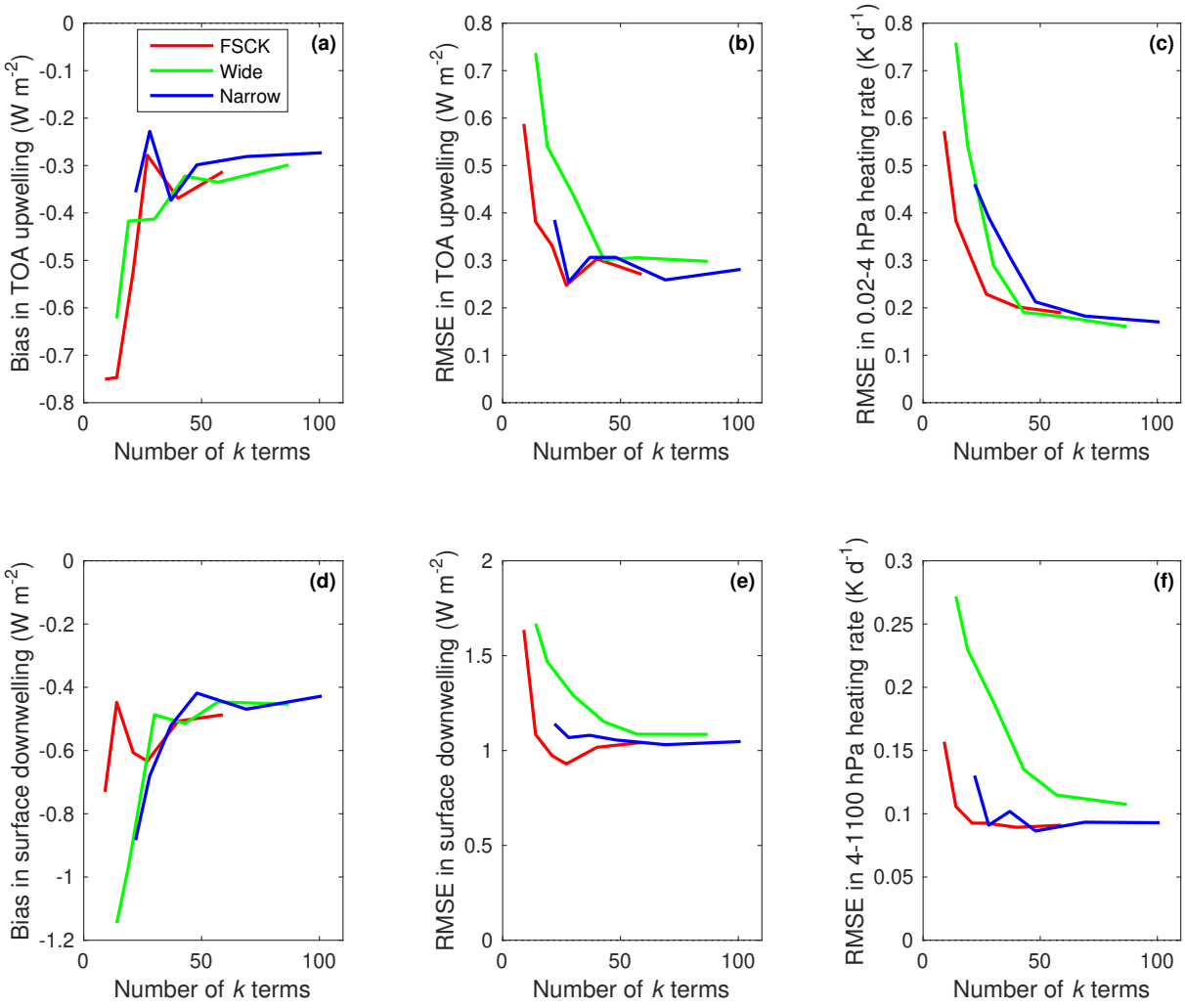

Biases and root-mean-squared errors (RMSE) in top-of-atmosphere (TOA) upwelling irradiance and surface downwelling irradiance, and RMSE in heating rate for two pressure ranges, for the various band structures as a function of the total number of k terms. It was computed from the CKDMIP scenarios 1–22, which cover climate conditions from glacial maximum up to the worst of the CMIP6 future scenarios, perturbing the individual greenhouse gases both together and separately.

Model 1: ecCKD climate-fsck-9

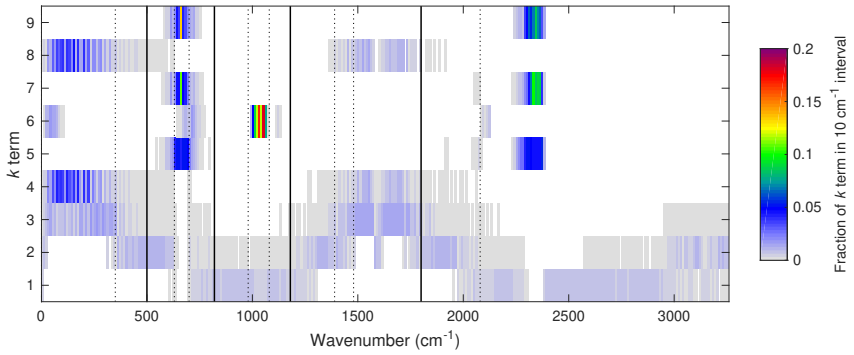

Illustration of the parts of the longwave spectrum that contribute to each k term of the climate-fsck-9 model.

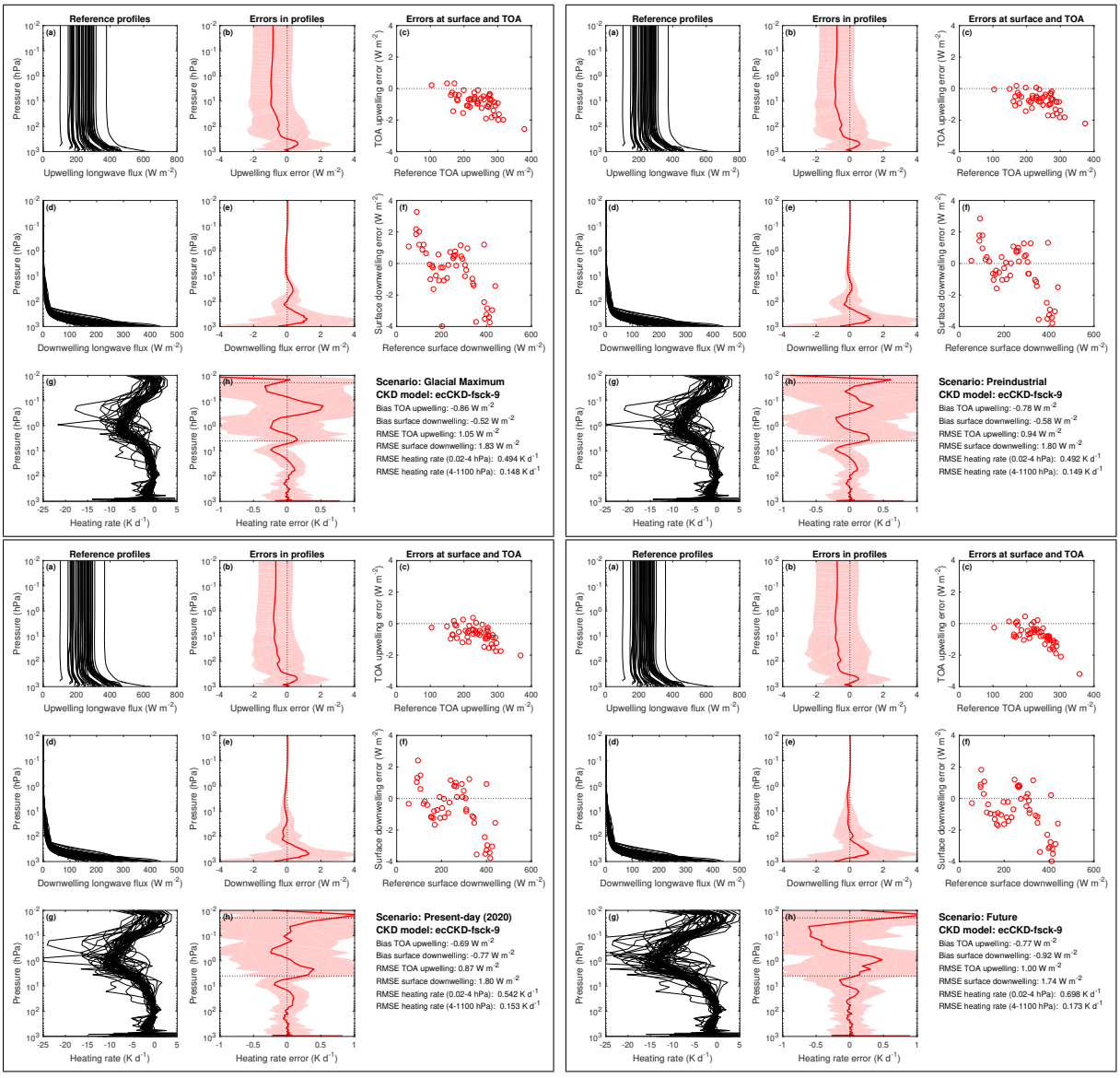

Each boxed groups of panels evaluate the climate-fsck-9 CKD model for a single CKDMIP scenario. The left three panels in each group show the irradiances and heating rates from the reference line-by-line calculations. The red lines in the middle three panels show the corresponding bias in these quantities from the CKD model. The shaded regions encompass 95% of the instantaneous errors. Panels c and f depict instantaneous errors in upwelling TOA and downwelling surface irradiances. Error metrics are provided in the lower right.

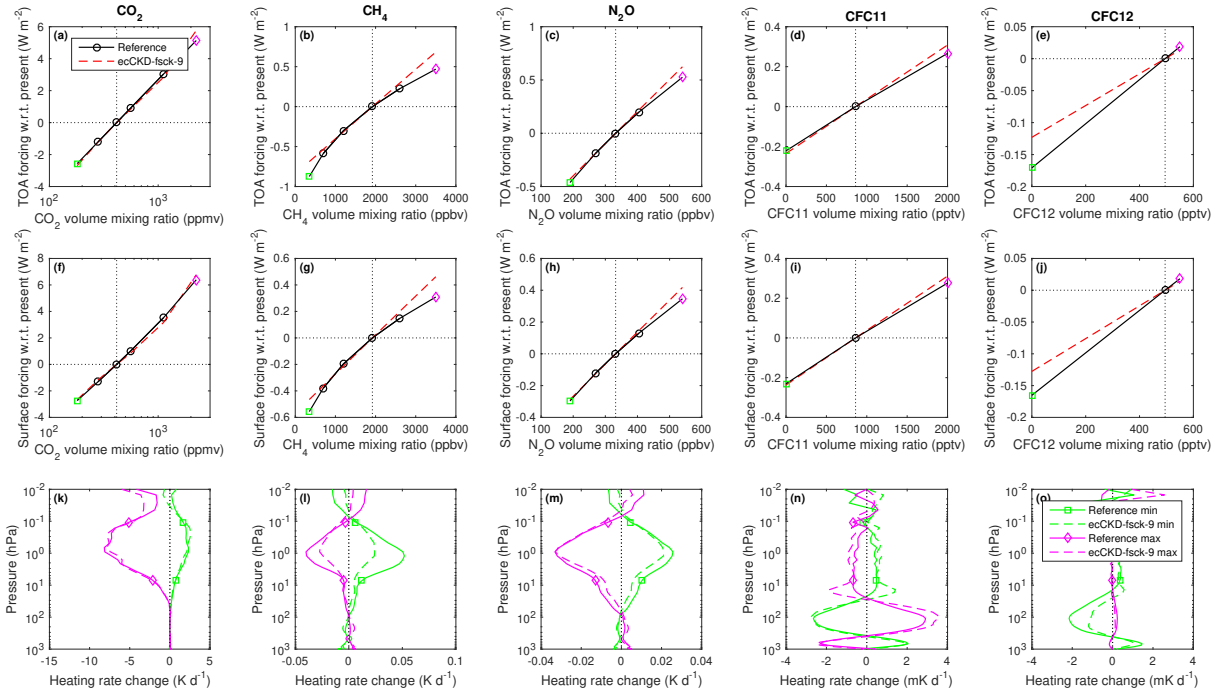

Comparison of reference line-by-line and calculations by the climate-fsck-9 model of the instantaneous clear-sky radiative forcing from perturbing each of the five well-mixed greenhouse gases from their present-day values, at (top row) top-of-atmosphere and (middle row) surface, averaged over the 50 profiles of the Evaluation-1 dataset. The bottom row shows the mean change to heating rate resulting from perturbing the concentration of a gas from its present-day value to either the maximum or minimum value in the range for that gas.

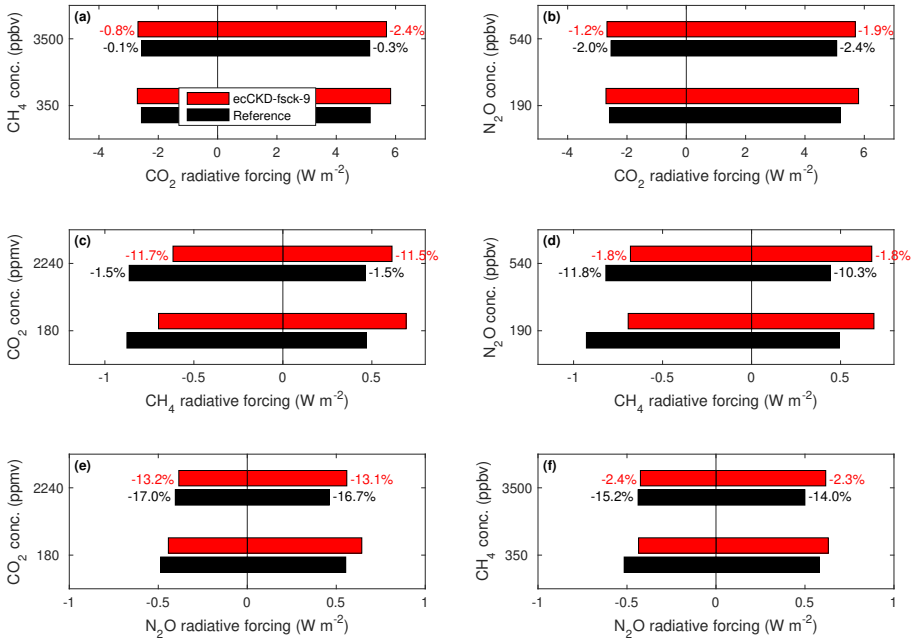

Evaluation of the representation of spectral overlap of CO_2, CH_4 and N_2O by the climate-fsck-9 CKD model. In each panel, the abscissa shows the TOA radiative forcing from perturbing a gas to either its climatic minimum or maximum value. These radiative forcings are computed keeping the concentrations of all other well-mixed gases at their present-day values, except for the gas on the ordinate, which is perturbed to its own climatic minimum or maximum values.

Model 2: ecCKD climate-fsck-14

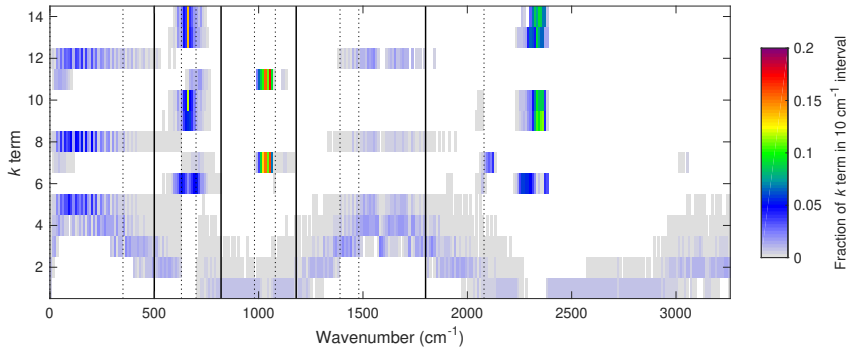

Illustration of the parts of the longwave spectrum that contribute to each k term of the climate-fsck-14 model.

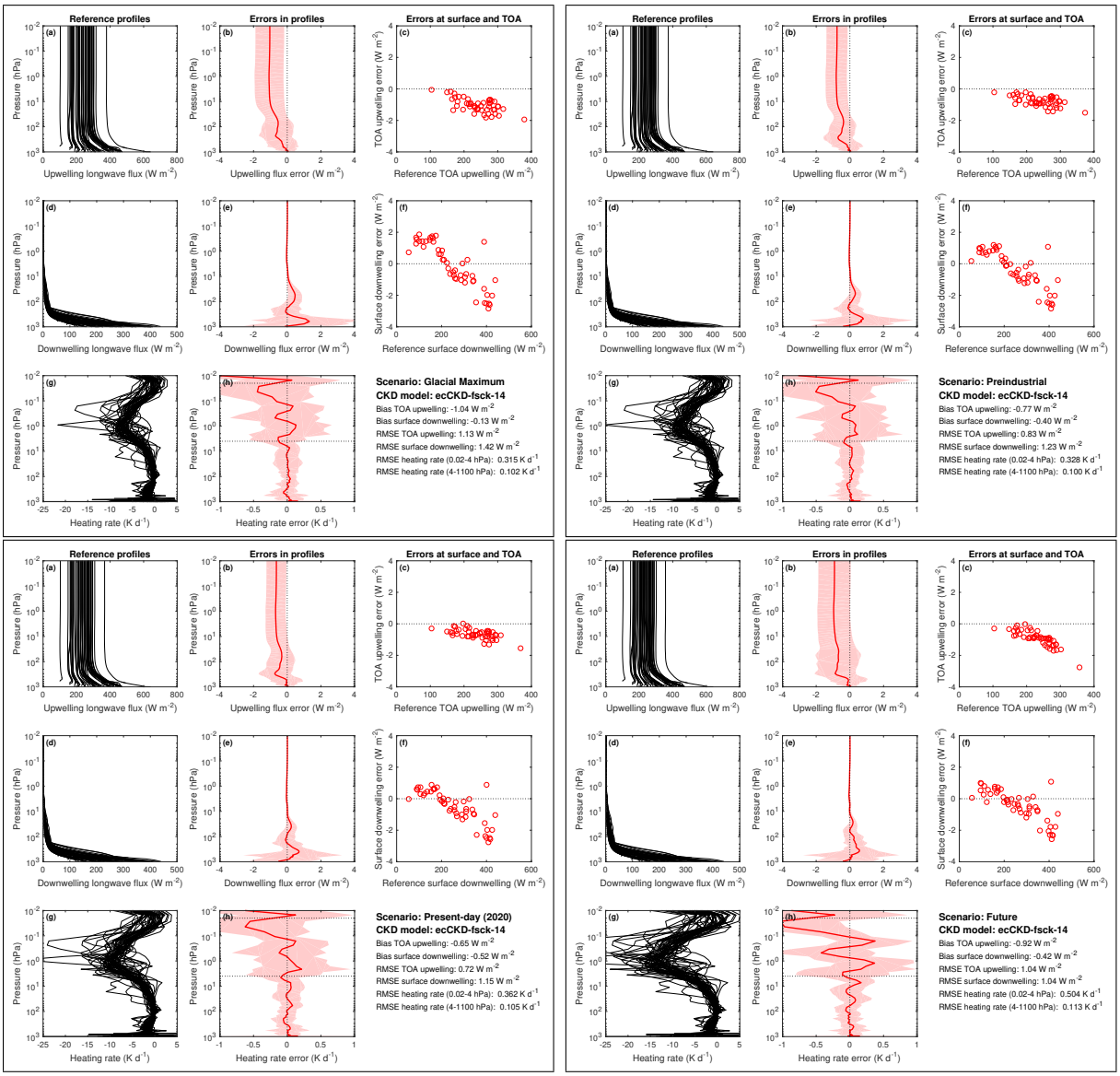

Each boxed groups of panels evaluate the climate-fsck-14 CKD model for a single CKDMIP scenario. The left three panels in each group show the irradiances and heating rates from the reference line-by-line calculations. The red lines in the middle three panels show the corresponding bias in these quantities from the CKD model. The shaded regions encompass 95% of the instantaneous errors. Panels c and f depict instantaneous errors in upwelling TOA and downwelling surface irradiances. Error metrics are provided in the lower right.

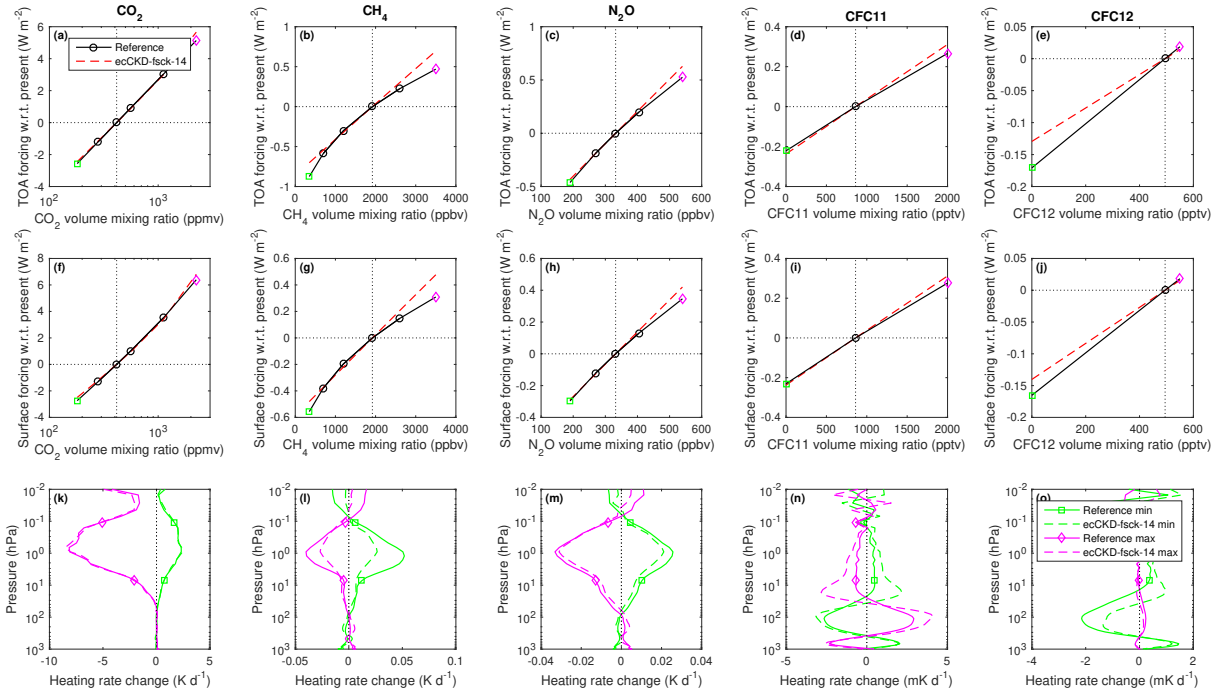

Comparison of reference line-by-line and calculations by the climate-fsck-14 model of the instantaneous clear-sky radiative forcing from perturbing each of the five well-mixed greenhouse gases from their present-day values, at (top row) top-of-atmosphere and (middle row) surface, averaged over the 50 profiles of the Evaluation-1 dataset. The bottom row shows the mean change to heating rate resulting from perturbing the concentration of a gas from its present-day value to either the maximum or minimum value in the range for that gas.

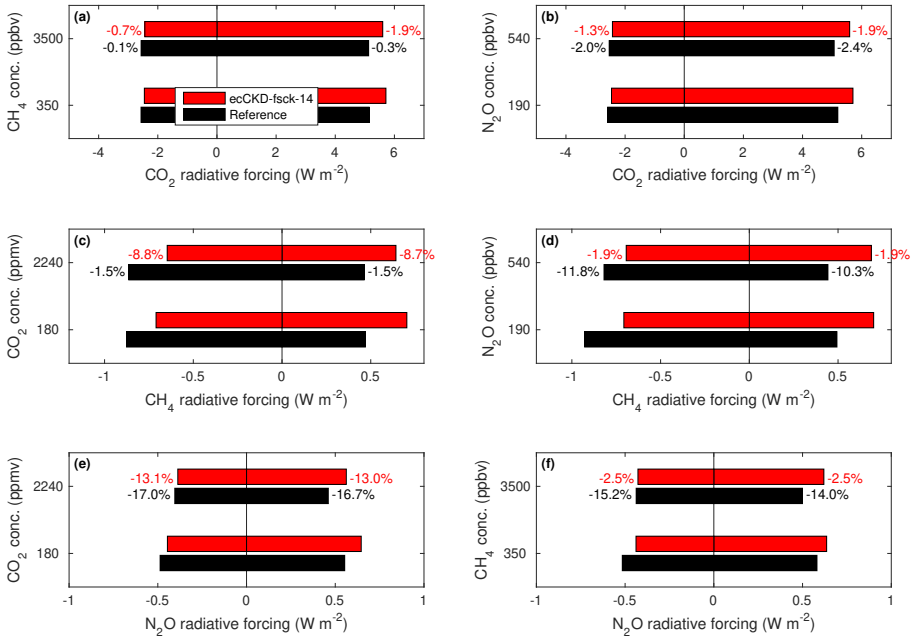

Evaluation of the representation of spectral overlap of CO_2, CH_4 and N_2O by the climate-fsck-14 CKD model. In each panel, the abscissa shows the TOA radiative forcing from perturbing a gas to either its climatic minimum or maximum value. These radiative forcings are computed keeping the concentrations of all other well-mixed gases at their present-day values, except for the gas on the ordinate, which is perturbed to its own climatic minimum or maximum values.

Model 3: ecCKD climate-fsck-21

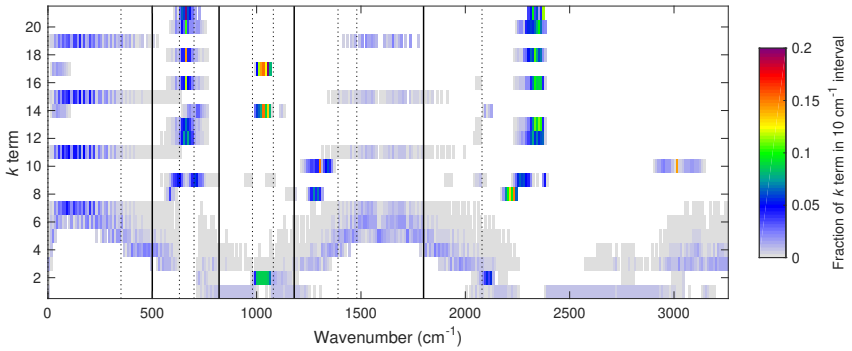

Illustration of the parts of the longwave spectrum that contribute to each k term of the climate-fsck-21 model.

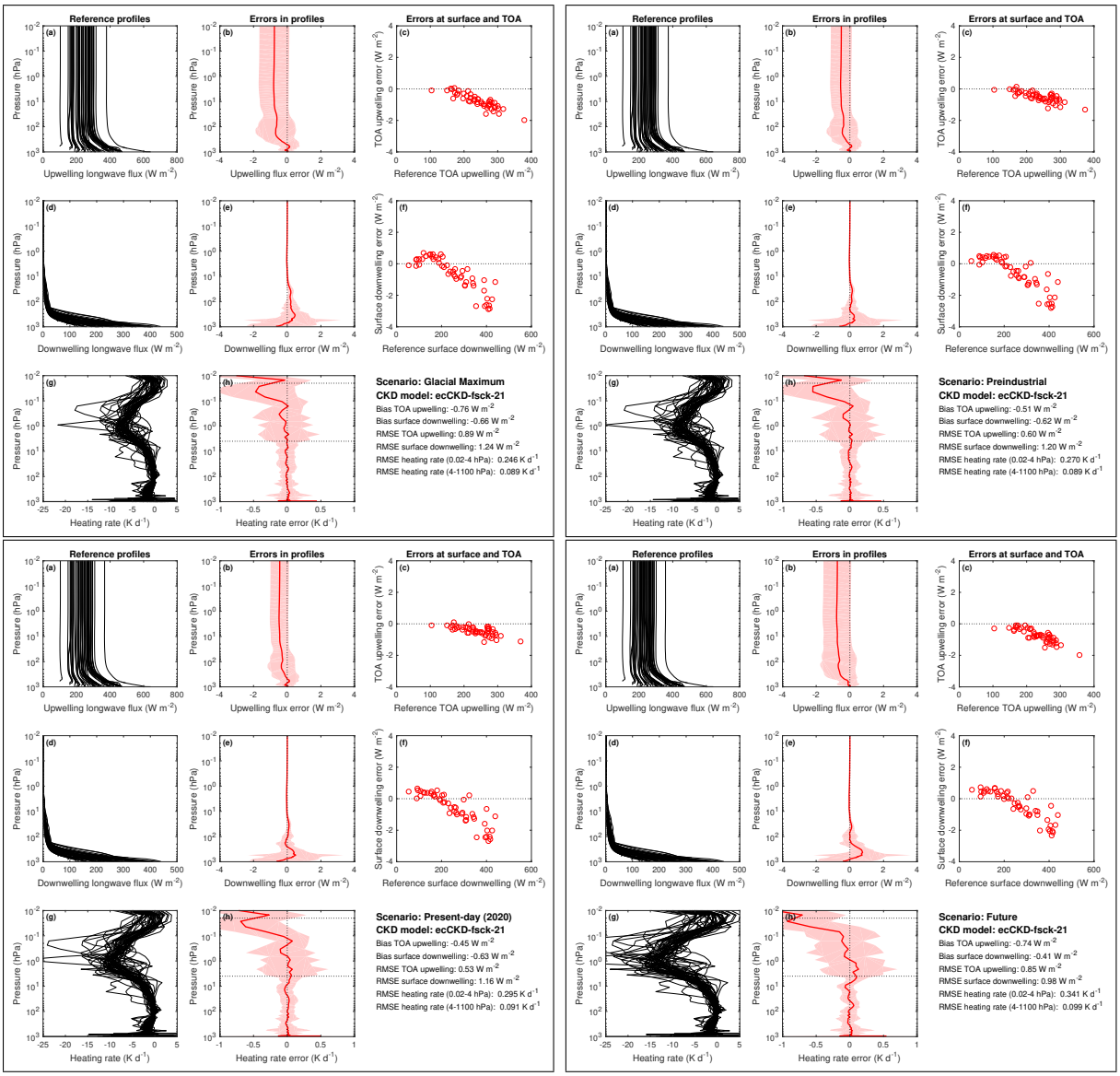

Each boxed groups of panels evaluate the climate-fsck-21 CKD model for a single CKDMIP scenario. The left three panels in each group show the irradiances and heating rates from the reference line-by-line calculations. The red lines in the middle three panels show the corresponding bias in these quantities from the CKD model. The shaded regions encompass 95% of the instantaneous errors. Panels c and f depict instantaneous errors in upwelling TOA and downwelling surface irradiances. Error metrics are provided in the lower right.

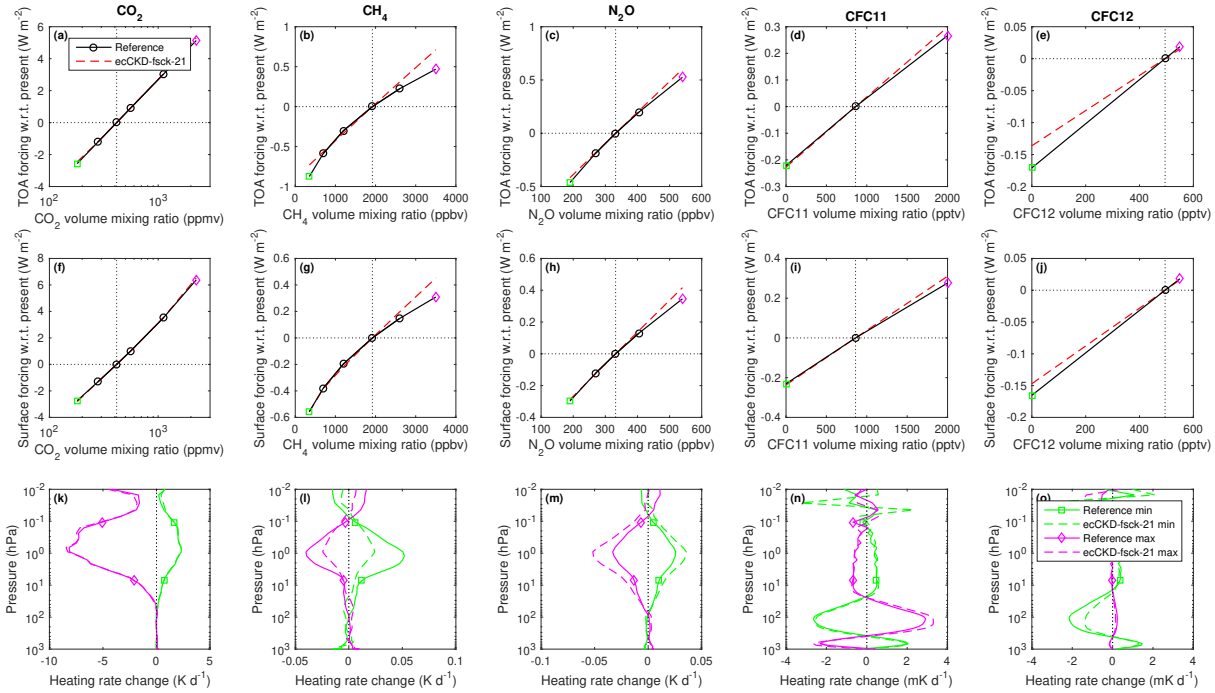

Comparison of reference line-by-line and calculations by the climate-fsck-21 model of the instantaneous clear-sky radiative forcing from perturbing each of the five well-mixed greenhouse gases from their present-day values, at (top row) top-of-atmosphere and (middle row) surface, averaged over the 50 profiles of the Evaluation-1 dataset. The bottom row shows the mean change to heating rate resulting from perturbing the concentration of a gas from its present-day value to either the maximum or minimum value in the range for that gas.

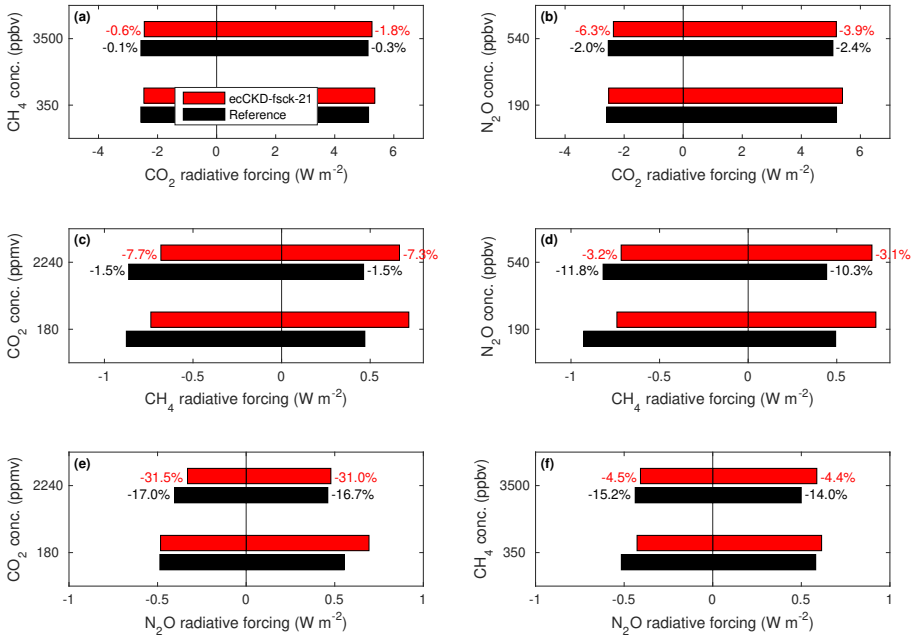

Evaluation of the representation of spectral overlap of CO_2, CH_4 and N_2O by the climate-fsck-21 CKD model. In each panel, the abscissa shows the TOA radiative forcing from perturbing a gas to either its climatic minimum or maximum value. These radiative forcings are computed keeping the concentrations of all other well-mixed gases at their present-day values, except for the gas on the ordinate, which is perturbed to its own climatic minimum or maximum values.

Model 4: ecCKD climate-fsck-27

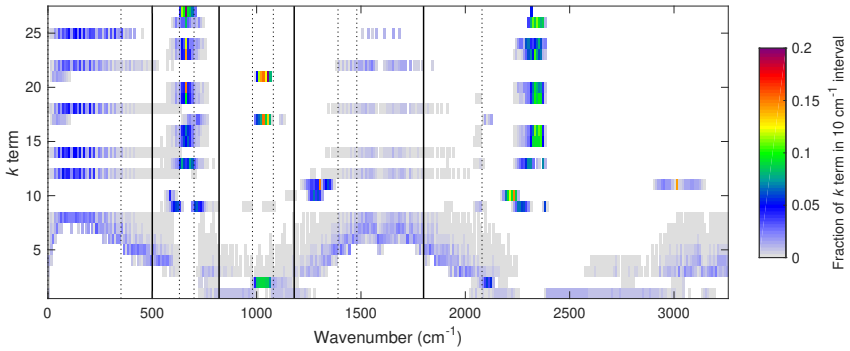

Illustration of the parts of the longwave spectrum that contribute to each k term of the climate-fsck-27 model.

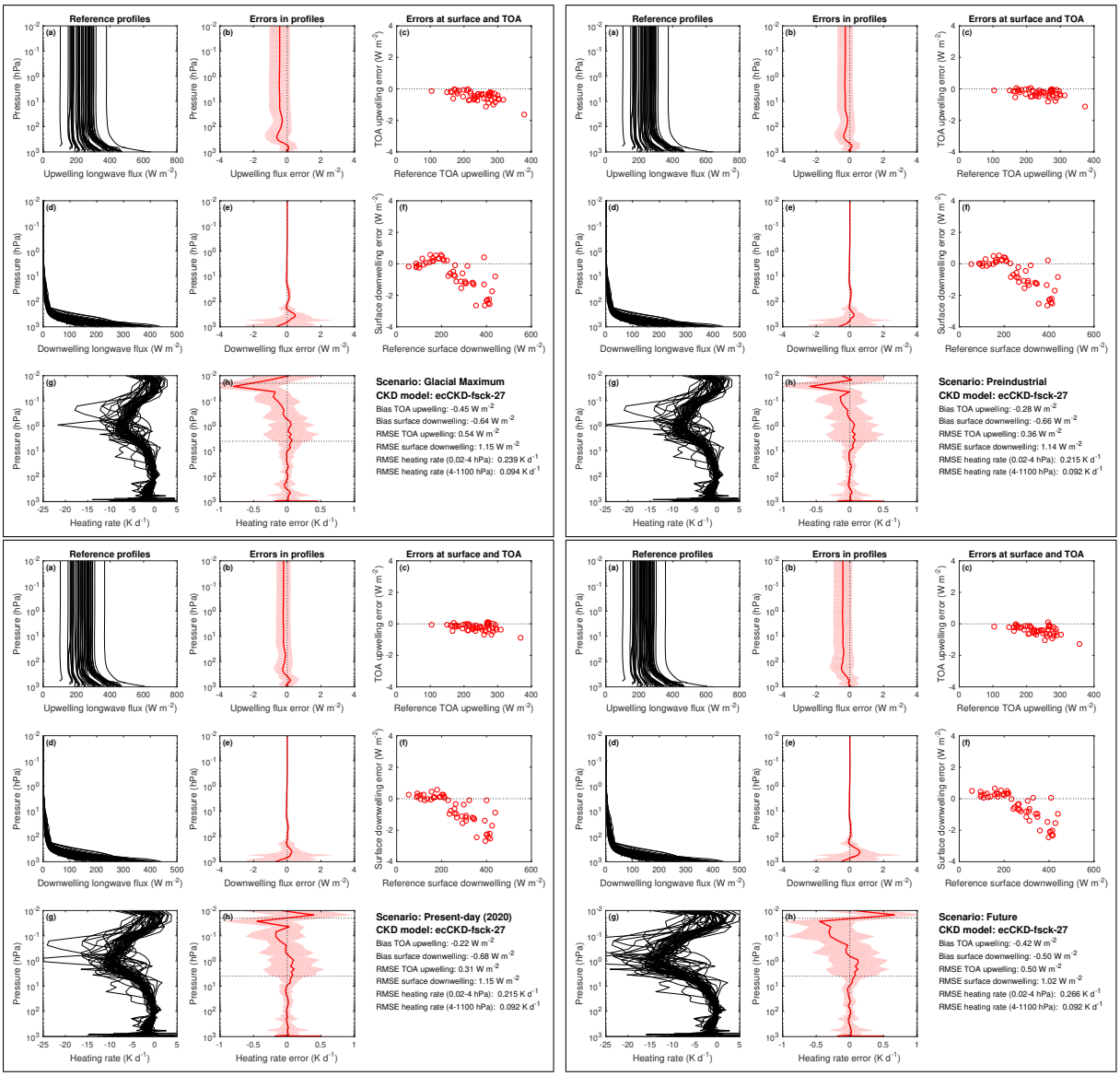

Each boxed groups of panels evaluate the climate-fsck-27 CKD model for a single CKDMIP scenario. The left three panels in each group show the irradiances and heating rates from the reference line-by-line calculations. The red lines in the middle three panels show the corresponding bias in these quantities from the CKD model. The shaded regions encompass 95% of the instantaneous errors. Panels c and f depict instantaneous errors in upwelling TOA and downwelling surface irradiances. Error metrics are provided in the lower right.

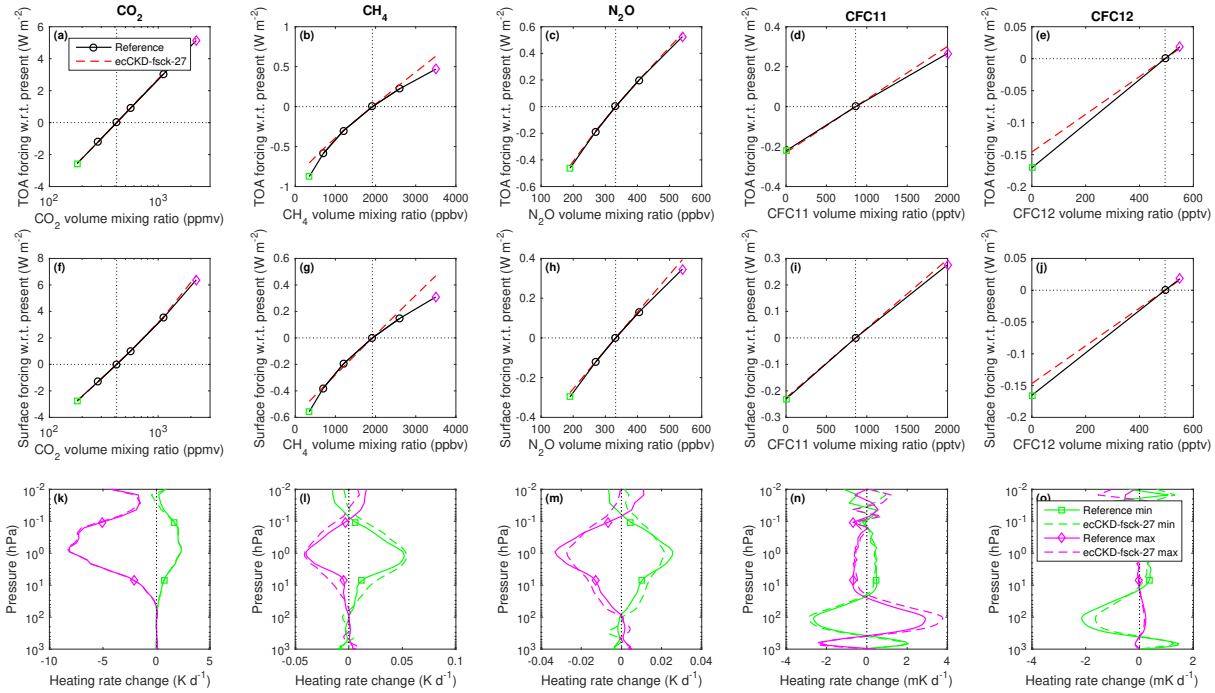

Comparison of reference line-by-line and calculations by the climate-fsck-27 model of the instantaneous clear-sky radiative forcing from perturbing each of the five well-mixed greenhouse gases from their present-day values, at (top row) top-of-atmosphere and (middle row) surface, averaged over the 50 profiles of the Evaluation-1 dataset. The bottom row shows the mean change to heating rate resulting from perturbing the concentration of a gas from its present-day value to either the maximum or minimum value in the range for that gas.

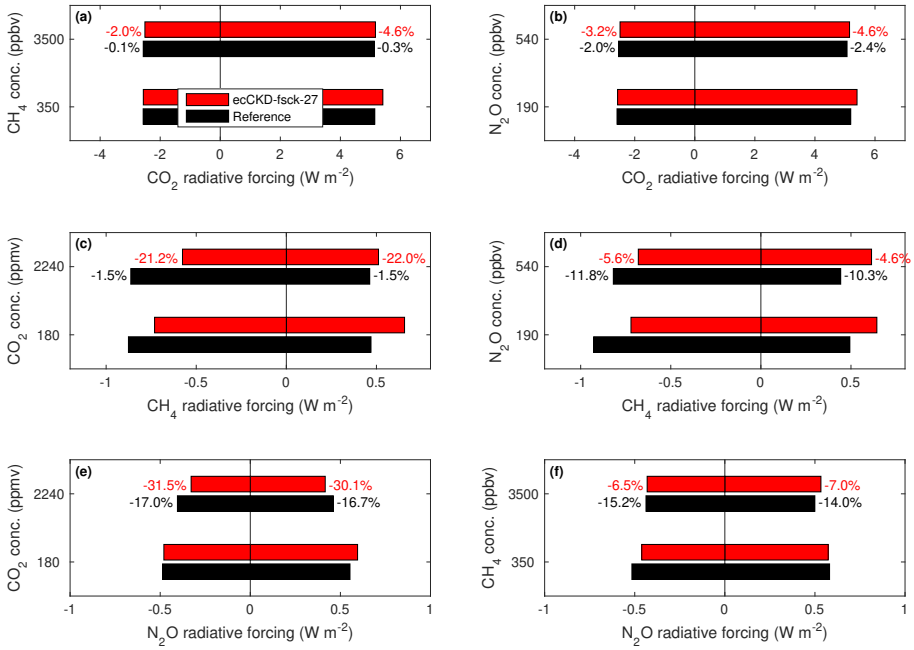

Evaluation of the representation of spectral overlap of CO_2, CH_4 and N_2O by the climate-fsck-27 CKD model. In each panel, the abscissa shows the TOA radiative forcing from perturbing a gas to either its climatic minimum or maximum value. These radiative forcings are computed keeping the concentrations of all other well-mixed gases at their present-day values, except for the gas on the ordinate, which is perturbed to its own climatic minimum or maximum values.

Model 5: ecCKD climate-fsck-40

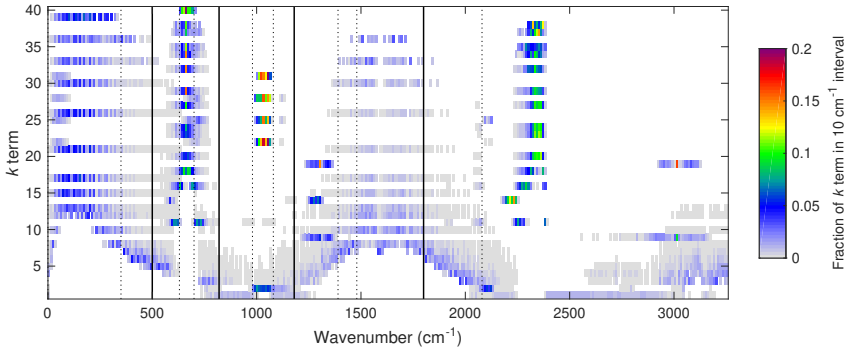

Illustration of the parts of the longwave spectrum that contribute to each k term of the climate-fsck-40 model.

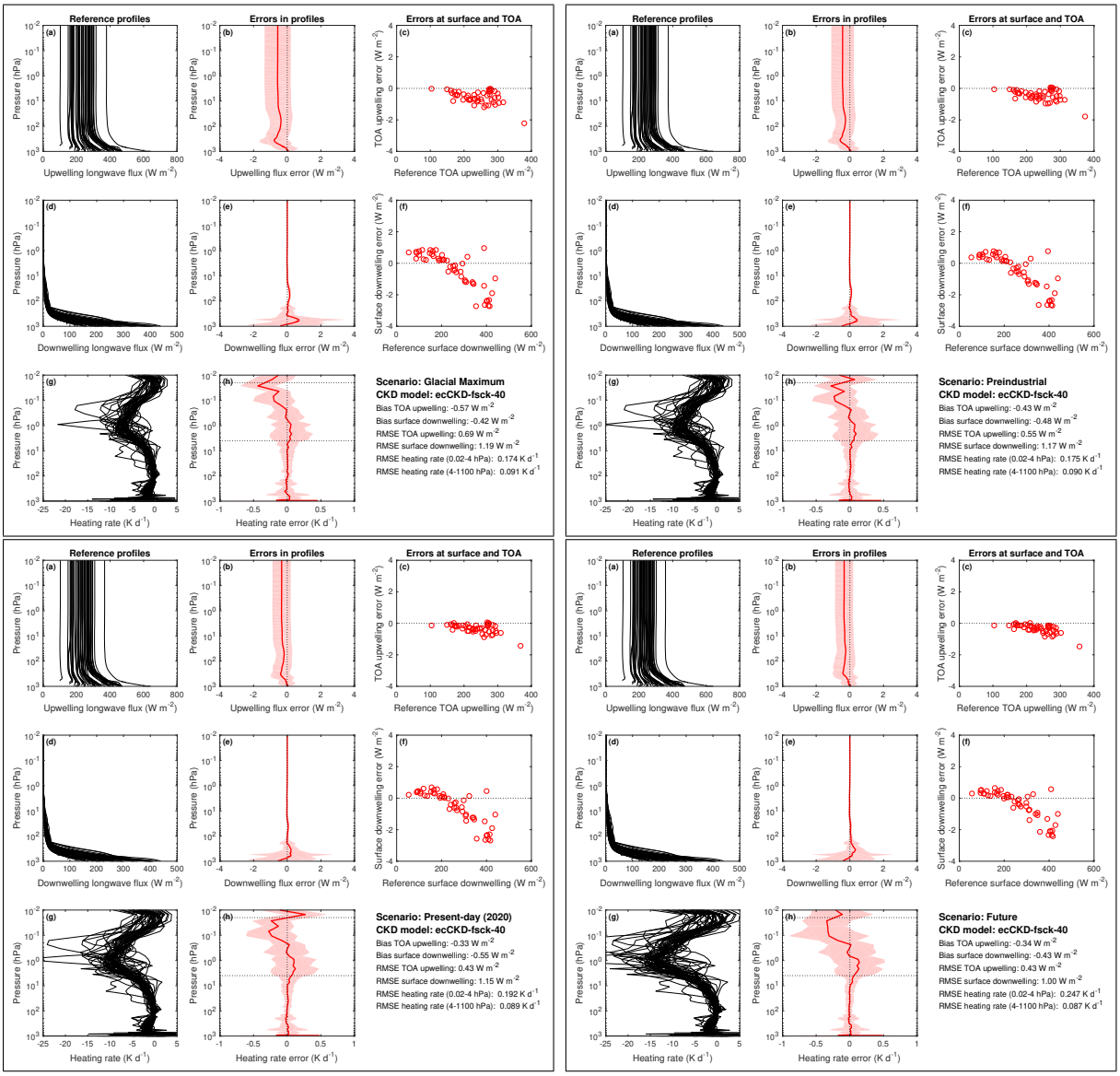

Each boxed groups of panels evaluate the climate-fsck-40 CKD model for a single CKDMIP scenario. The left three panels in each group show the irradiances and heating rates from the reference line-by-line calculations. The red lines in the middle three panels show the corresponding bias in these quantities from the CKD model. The shaded regions encompass 95% of the instantaneous errors. Panels c and f depict instantaneous errors in upwelling TOA and downwelling surface irradiances. Error metrics are provided in the lower right.

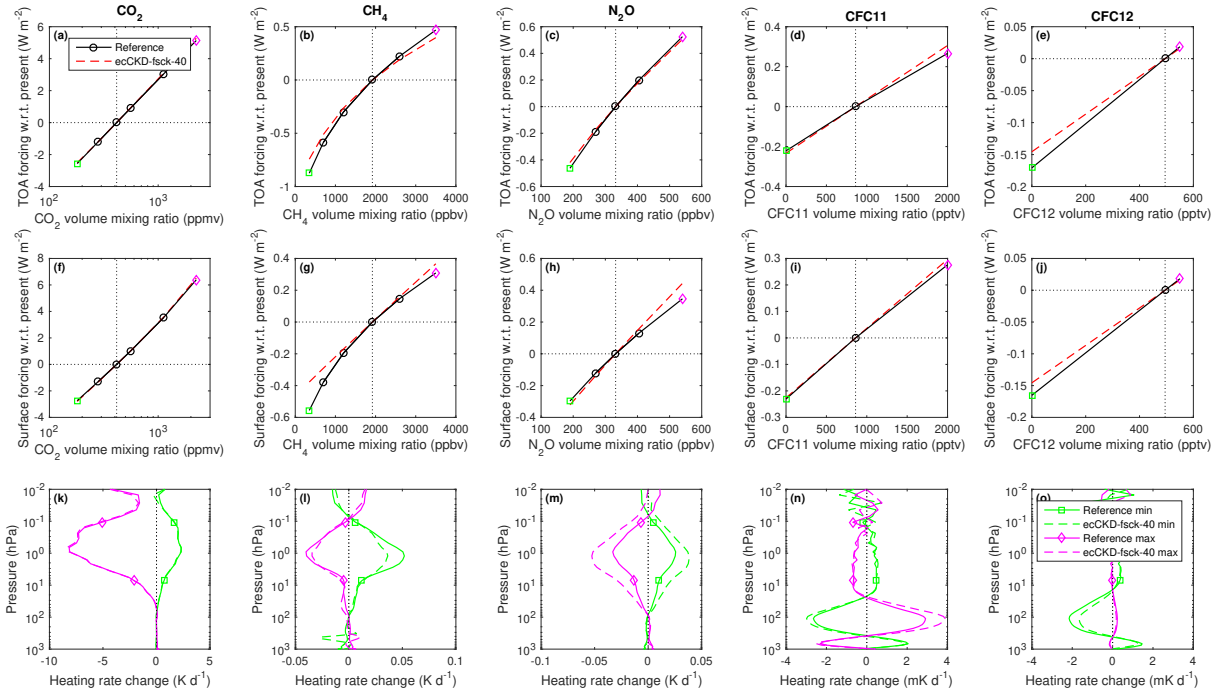

Comparison of reference line-by-line and calculations by the climate-fsck-40 model of the instantaneous clear-sky radiative forcing from perturbing each of the five well-mixed greenhouse gases from their present-day values, at (top row) top-of-atmosphere and (middle row) surface, averaged over the 50 profiles of the Evaluation-1 dataset. The bottom row shows the mean change to heating rate resulting from perturbing the concentration of a gas from its present-day value to either the maximum or minimum value in the range for that gas.

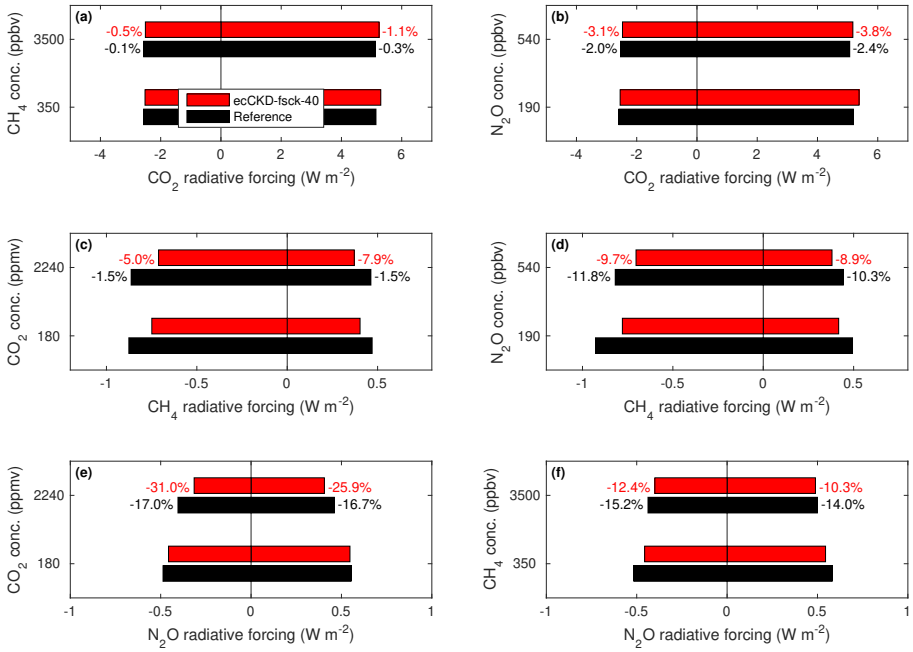

Evaluation of the representation of spectral overlap of CO_2, CH_4 and N_2O by the climate-fsck-40 CKD model. In each panel, the abscissa shows the TOA radiative forcing from perturbing a gas to either its climatic minimum or maximum value. These radiative forcings are computed keeping the concentrations of all other well-mixed gases at their present-day values, except for the gas on the ordinate, which is perturbed to its own climatic minimum or maximum values.

Model 6: ecCKD climate-fsck-59

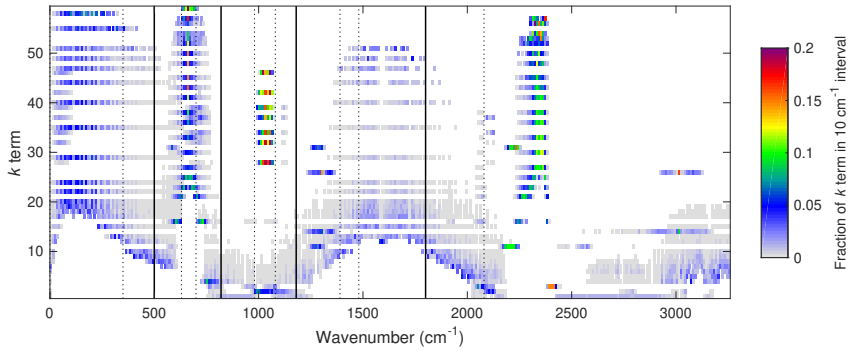

Illustration of the parts of the longwave spectrum that contribute to each k term of the climate-fsck-59 model.

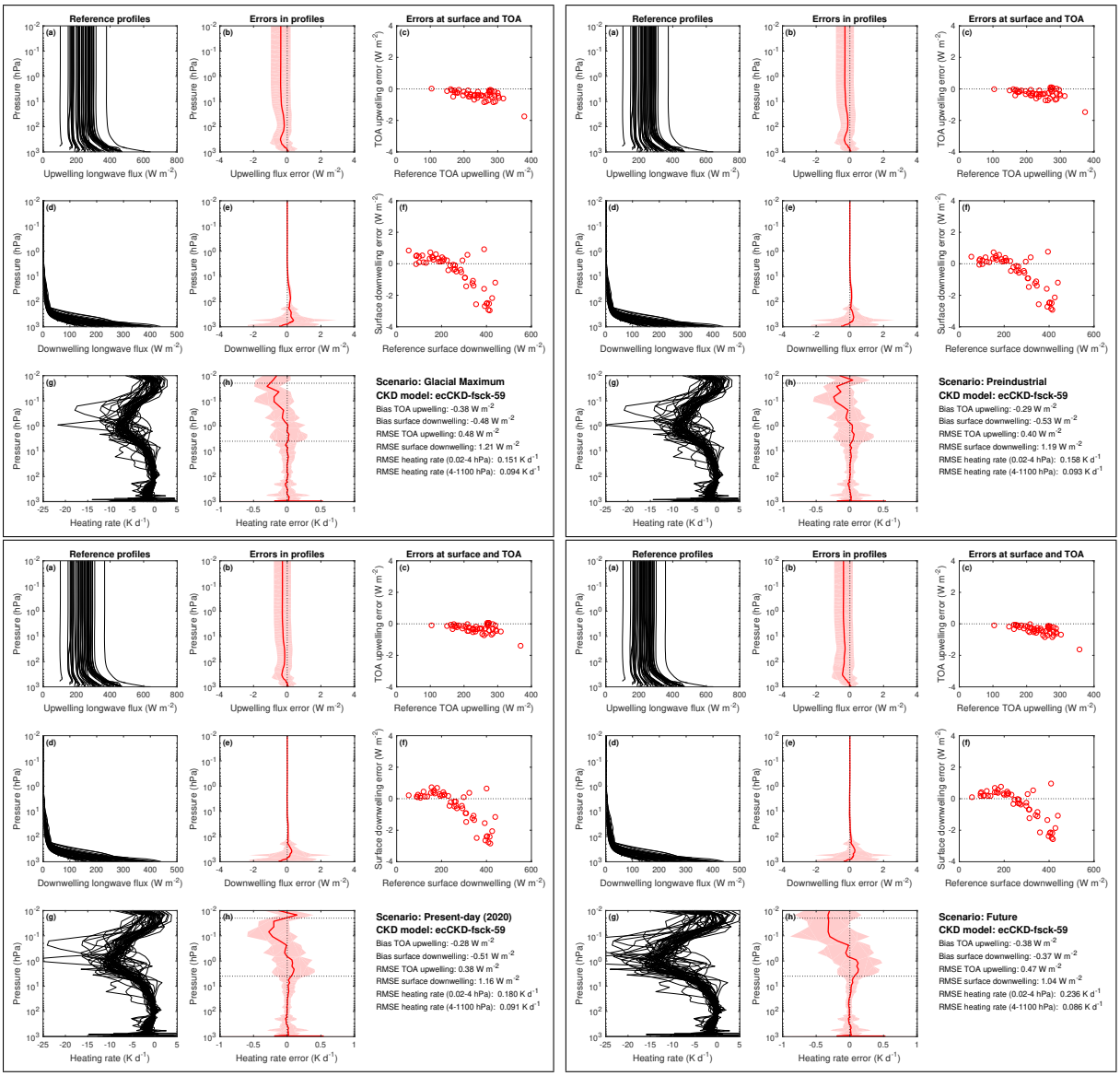

Each boxed groups of panels evaluate the climate-fsck-59 CKD model for a single CKDMIP scenario. The left three panels in each group show the irradiances and heating rates from the reference line-by-line calculations. The red lines in the middle three panels show the corresponding bias in these quantities from the CKD model. The shaded regions encompass 95% of the instantaneous errors. Panels c and f depict instantaneous errors in upwelling TOA and downwelling surface irradiances. Error metrics are provided in the lower right.

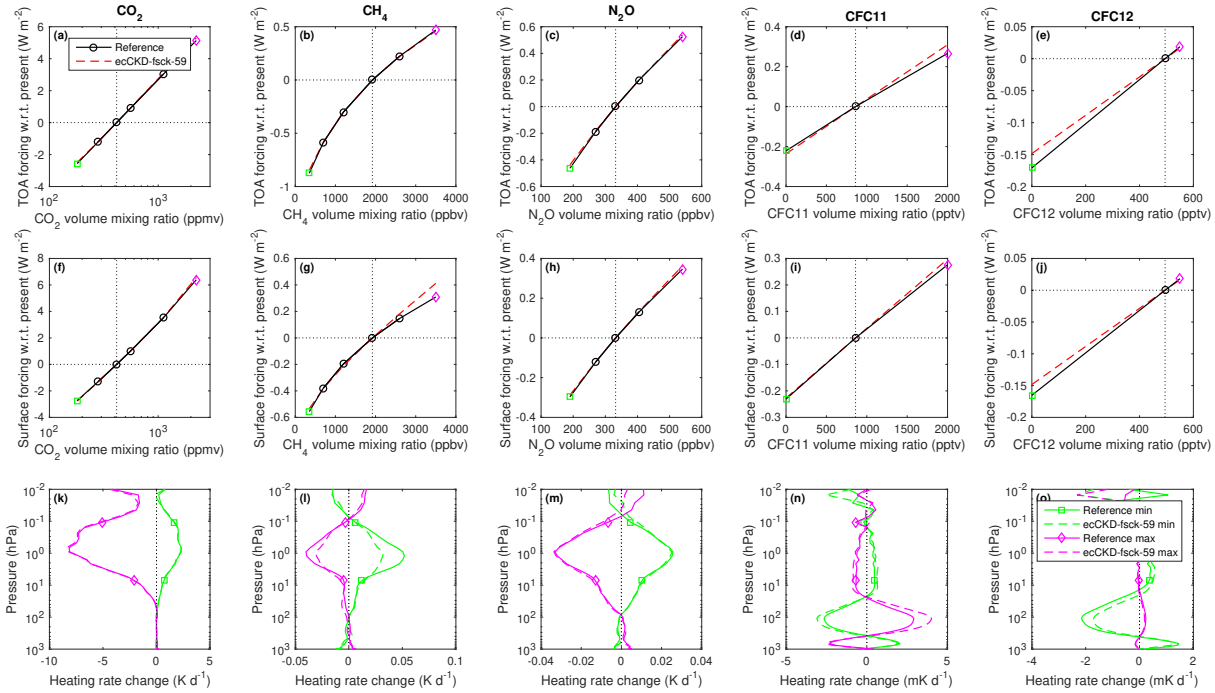

Comparison of reference line-by-line and calculations by the climate-fsck-59 model of the instantaneous clear-sky radiative forcing from perturbing each of the five well-mixed greenhouse gases from their present-day values, at (top row) top-of-atmosphere and (middle row) surface, averaged over the 50 profiles of the Evaluation-1 dataset. The bottom row shows the mean change to heating rate resulting from perturbing the concentration of a gas from its present-day value to either the maximum or minimum value in the range for that gas.

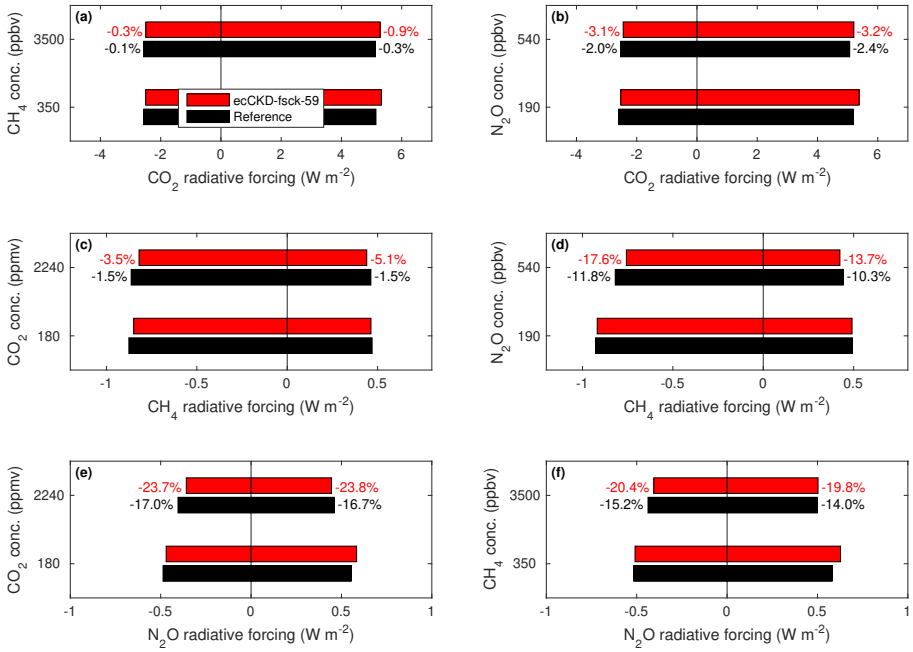

Evaluation of the representation of spectral overlap of CO_2, CH_4 and N_2O by the climate-fsck-59 CKD model. In each panel, the abscissa shows the TOA radiative forcing from perturbing a gas to either its climatic minimum or maximum value. These radiative forcings are computed keeping the concentrations of all other well-mixed gases at their present-day values, except for the gas on the ordinate, which is perturbed to its own climatic minimum or maximum values.

Model 7: ecCKD climate-wide-14

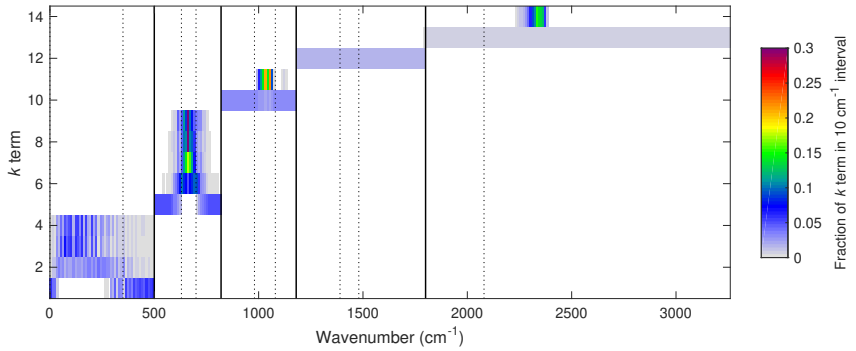

Illustration of the parts of the longwave spectrum that contribute to each k term of the climate-wide-14 model.

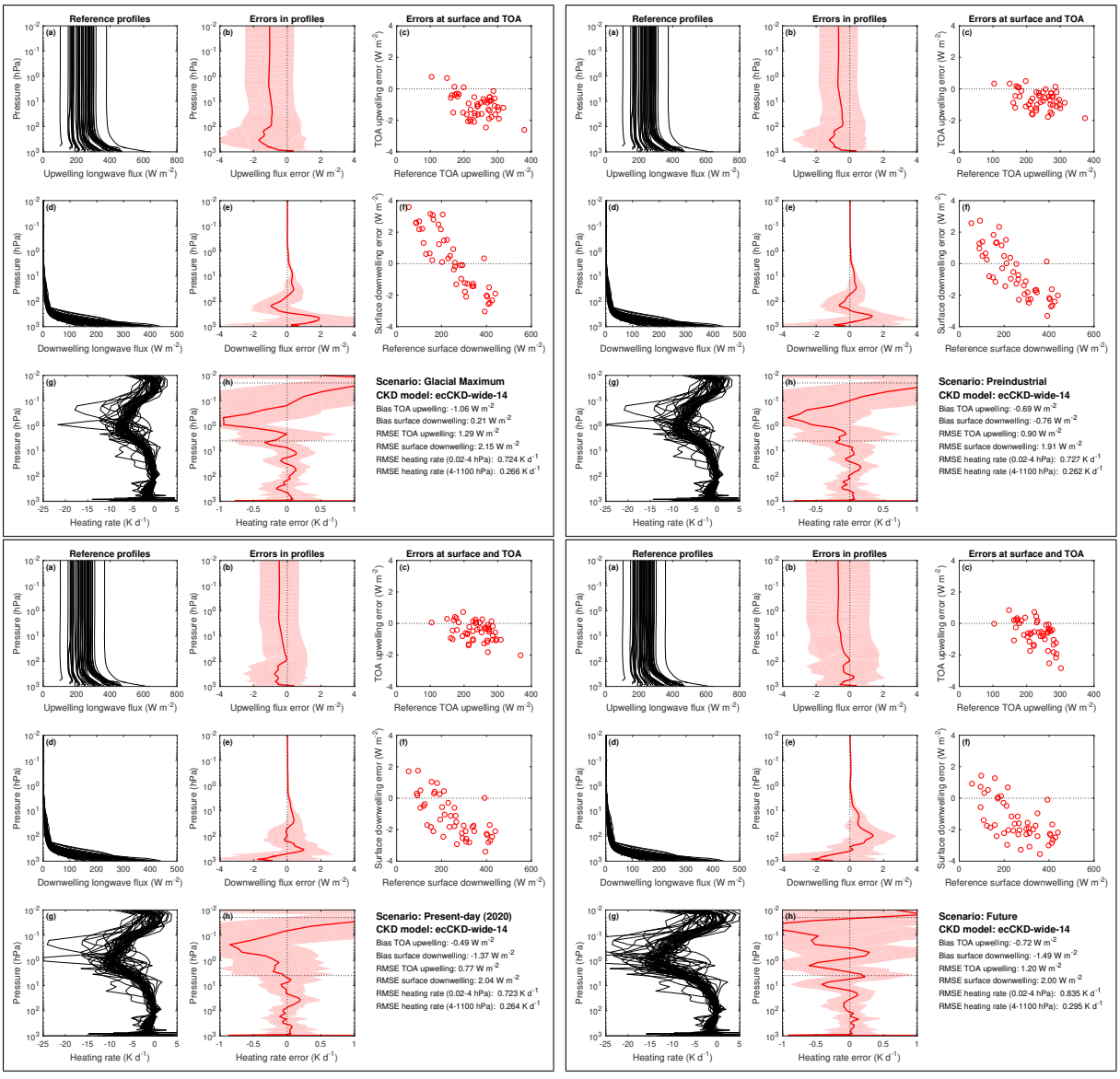

Each boxed groups of panels evaluate the climate-wide-14 CKD model for a single CKDMIP scenario. The left three panels in each group show the irradiances and heating rates from the reference line-by-line calculations. The red lines in the middle three panels show the corresponding bias in these quantities from the CKD model. The shaded regions encompass 95% of the instantaneous errors. Panels c and f depict instantaneous errors in upwelling TOA and downwelling surface irradiances. Error metrics are provided in the lower right.

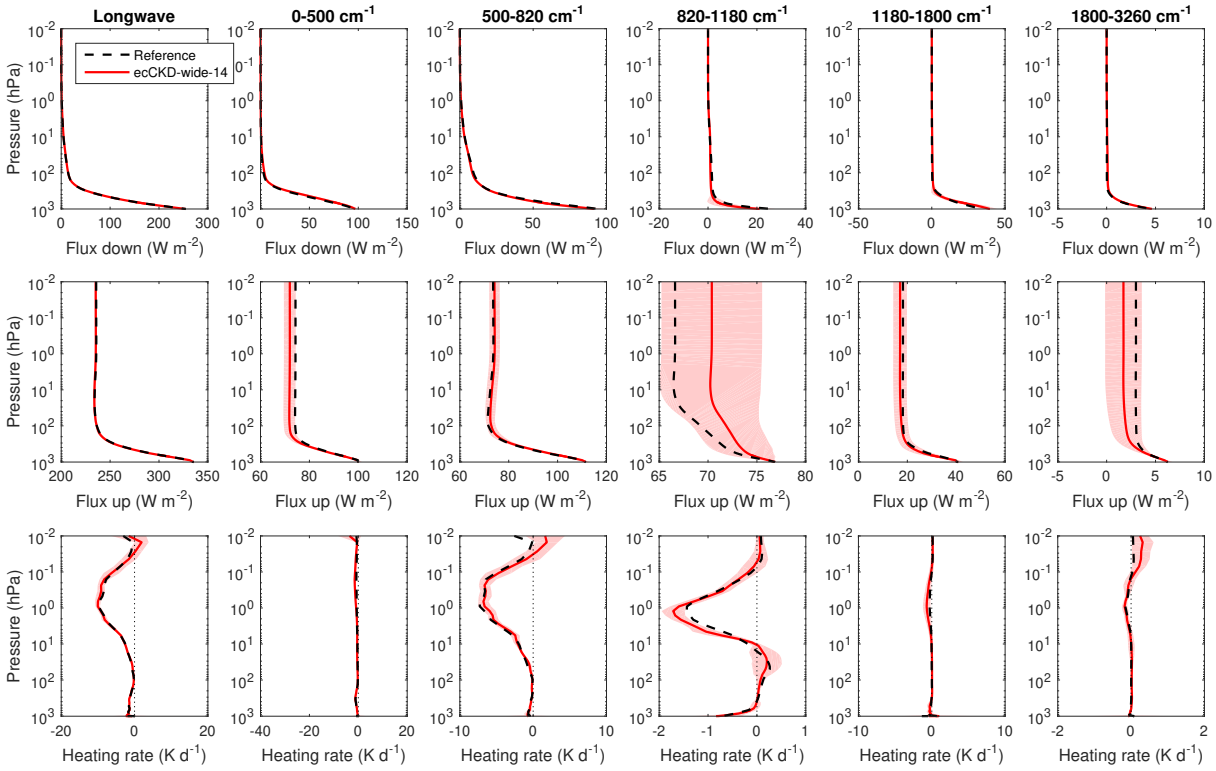

Evaluation of irradiances and heating rates for the broadband (leftmost column of panels) and the 5 wide longwave bands (other panels) of the climate-wide-14 CKD model. The black dashed and red solid lines correspond to the average of the 50 profiles for the "present-day" scenario, while the shaded regions encompass 95% of the error.

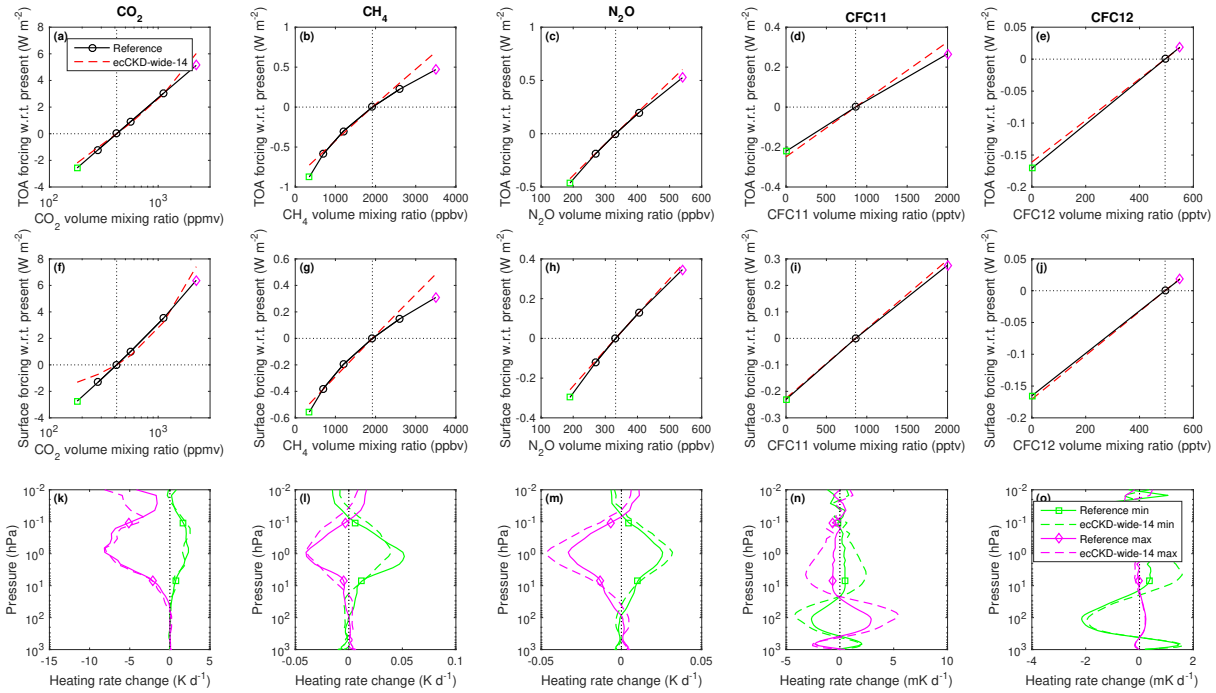

Comparison of reference line-by-line and calculations by the climate-wide-14 model of the instantaneous clear-sky radiative forcing from perturbing each of the five well-mixed greenhouse gases from their present-day values, at (top row) top-of-atmosphere and (middle row) surface, averaged over the 50 profiles of the Evaluation-1 dataset. The bottom row shows the mean change to heating rate resulting from perturbing the concentration of a gas from its present-day value to either the maximum or minimum value in the range for that gas.

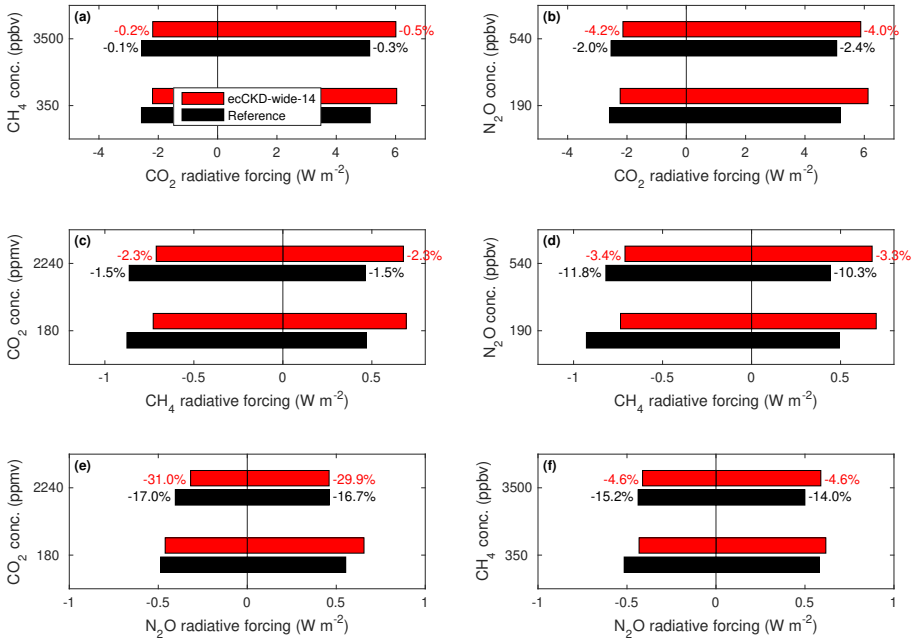

Evaluation of the representation of spectral overlap of CO_2, CH_4 and N_2O by the climate-wide-14 CKD model. In each panel, the abscissa shows the TOA radiative forcing from perturbing a gas to either its climatic minimum or maximum value. These radiative forcings are computed keeping the concentrations of all other well-mixed gases at their present-day values, except for the gas on the ordinate, which is perturbed to its own climatic minimum or maximum values.

Model 8: ecCKD climate-wide-19

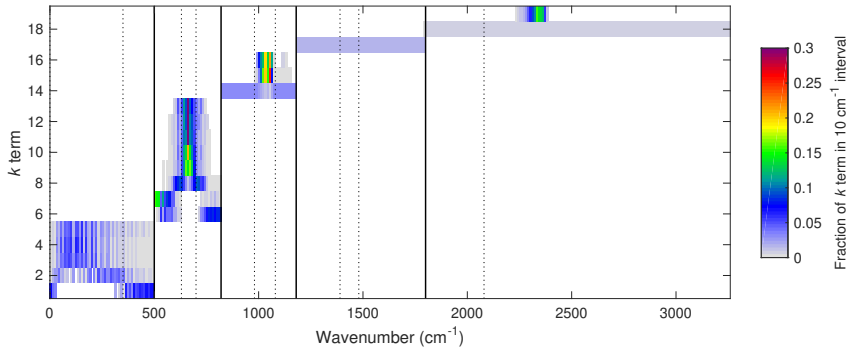

Illustration of the parts of the longwave spectrum that contribute to each k term of the climate-wide-19 model.

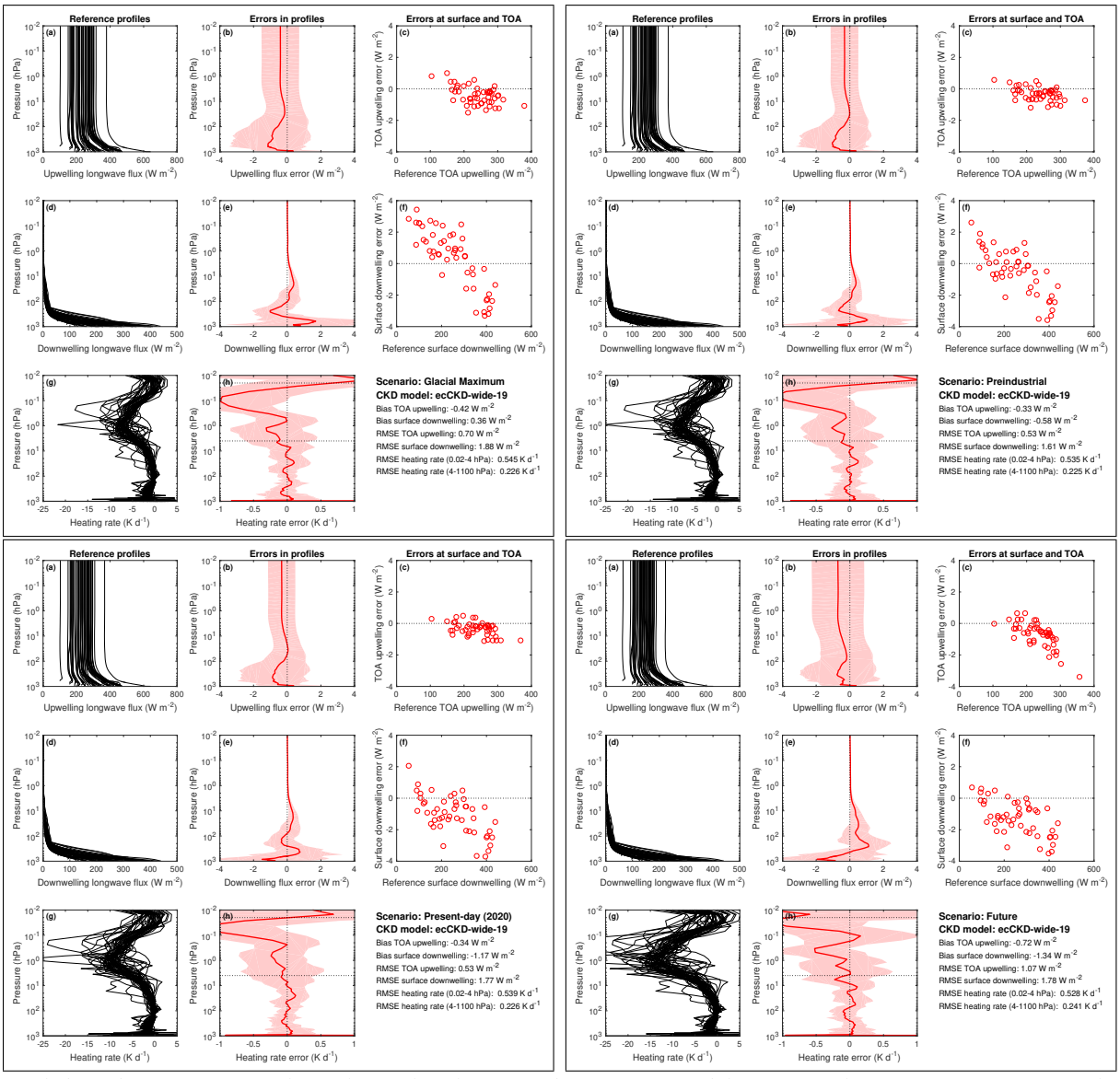

Each boxed groups of panels evaluate the climate-wide-19 CKD model for a single CKDMIP scenario. The left three panels in each group show the irradiances and heating rates from the reference line-by-line calculations. The red lines in the middle three panels show the corresponding bias in these quantities from the CKD model. The shaded regions encompass 95% of the instantaneous errors. Panels c and f depict instantaneous errors in upwelling TOA and downwelling surface irradiances. Error metrics are provided in the lower right.

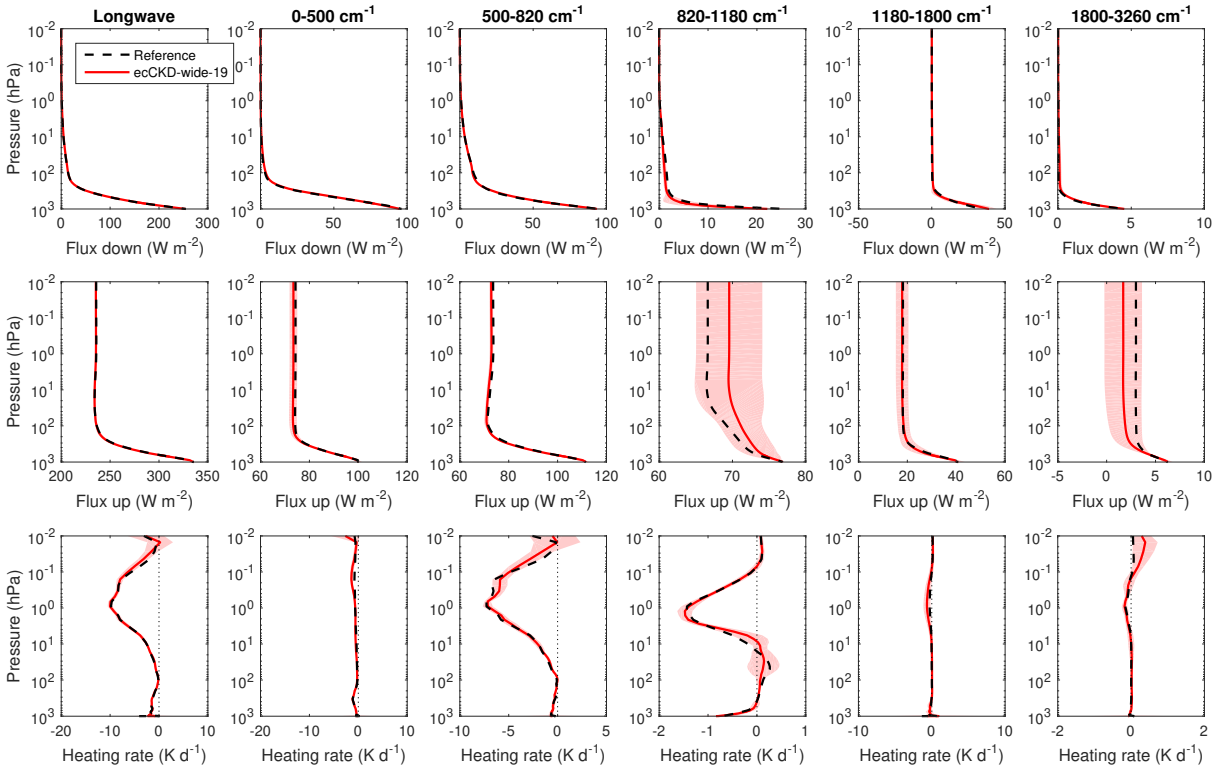

Evaluation of irradiances and heating rates for the broadband (leftmost column of panels) and the 5 wide longwave bands (other panels) of the climate-wide-19 CKD model. The black dashed and red solid lines correspond to the average of the 50 profiles for the "present-day" scenario, while the shaded regions encompass 95% of the error.

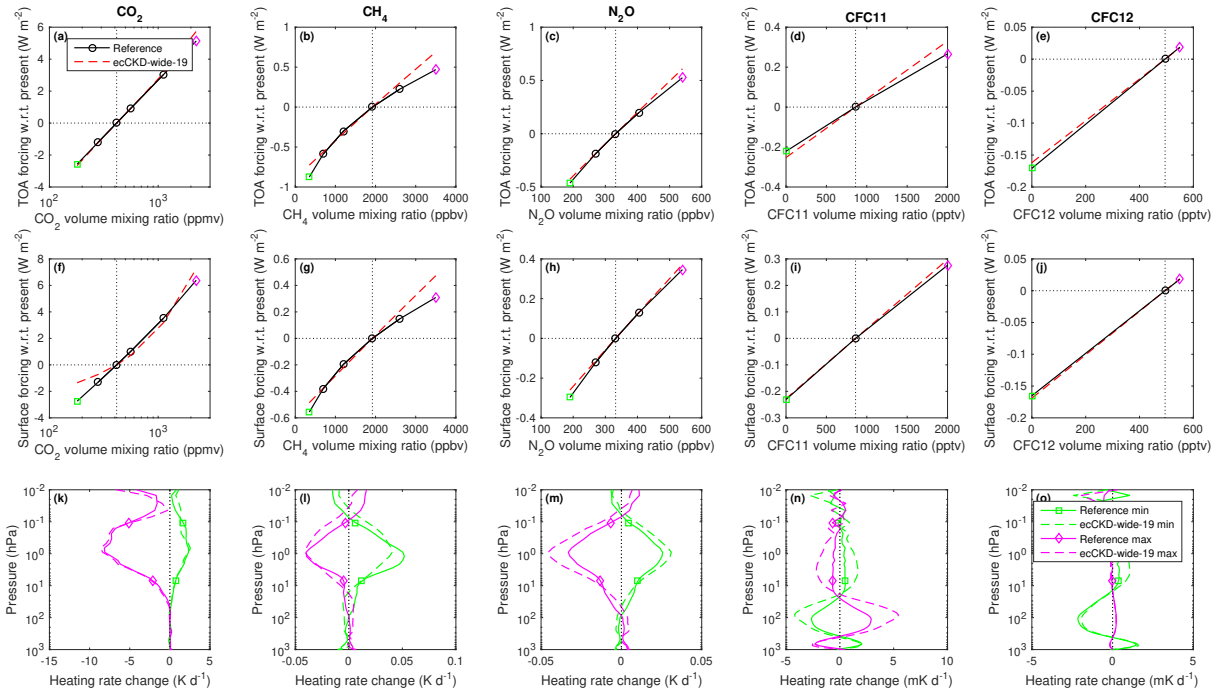

Comparison of reference line-by-line and calculations by the climate-wide-19 model of the instantaneous clear-sky radiative forcing from perturbing each of the five well-mixed greenhouse gases from their present-day values, at (top row) top-of-atmosphere and (middle row) surface, averaged over the 50 profiles of the Evaluation-1 dataset. The bottom row shows the mean change to heating rate resulting from perturbing the concentration of a gas from its present-day value to either the maximum or minimum value in the range for that gas.

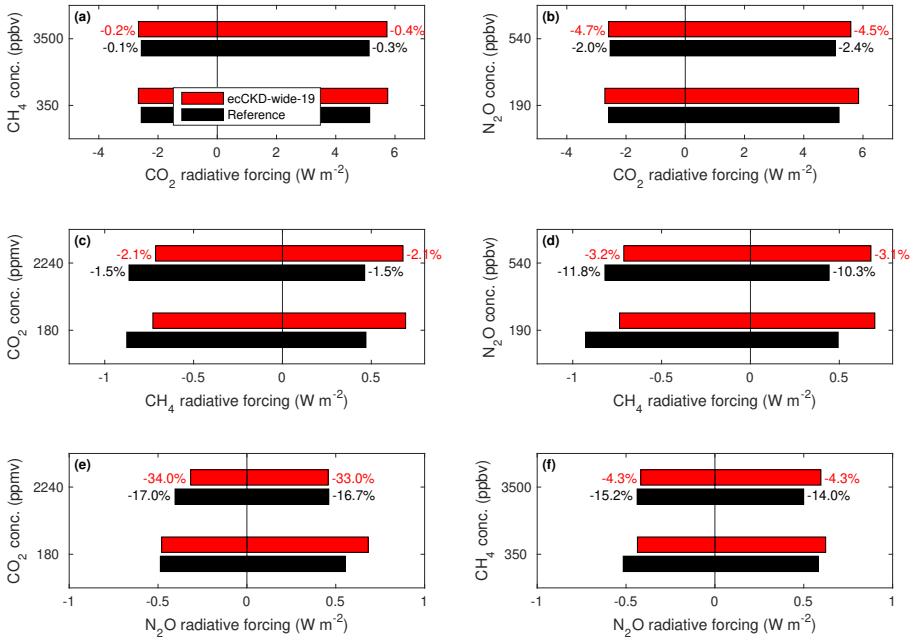

Evaluation of the representation of spectral overlap of CO_2, CH_4 and N_2O by the climate-wide-19 CKD model. In each panel, the abscissa shows the TOA radiative forcing from perturbing a gas to either its climatic minimum or maximum value. These radiative forcings are computed keeping the concentrations of all other well-mixed gases at their present-day values, except for the gas on the ordinate, which is perturbed to its own climatic minimum or maximum values.

Model 9: ecCKD climate-wide-30

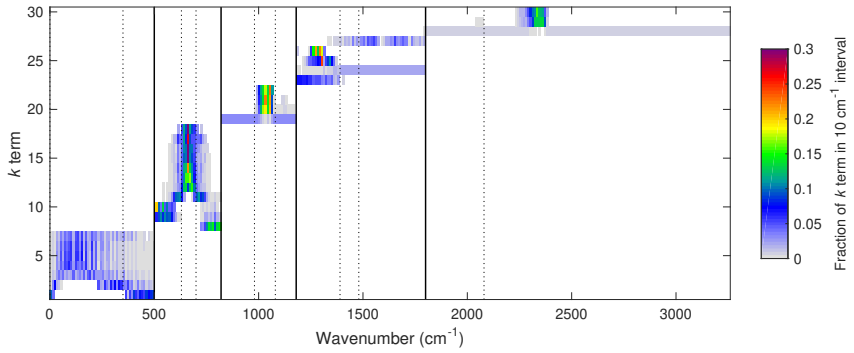

Illustration of the parts of the longwave spectrum that contribute to each k term of the climate-wide-30 model.

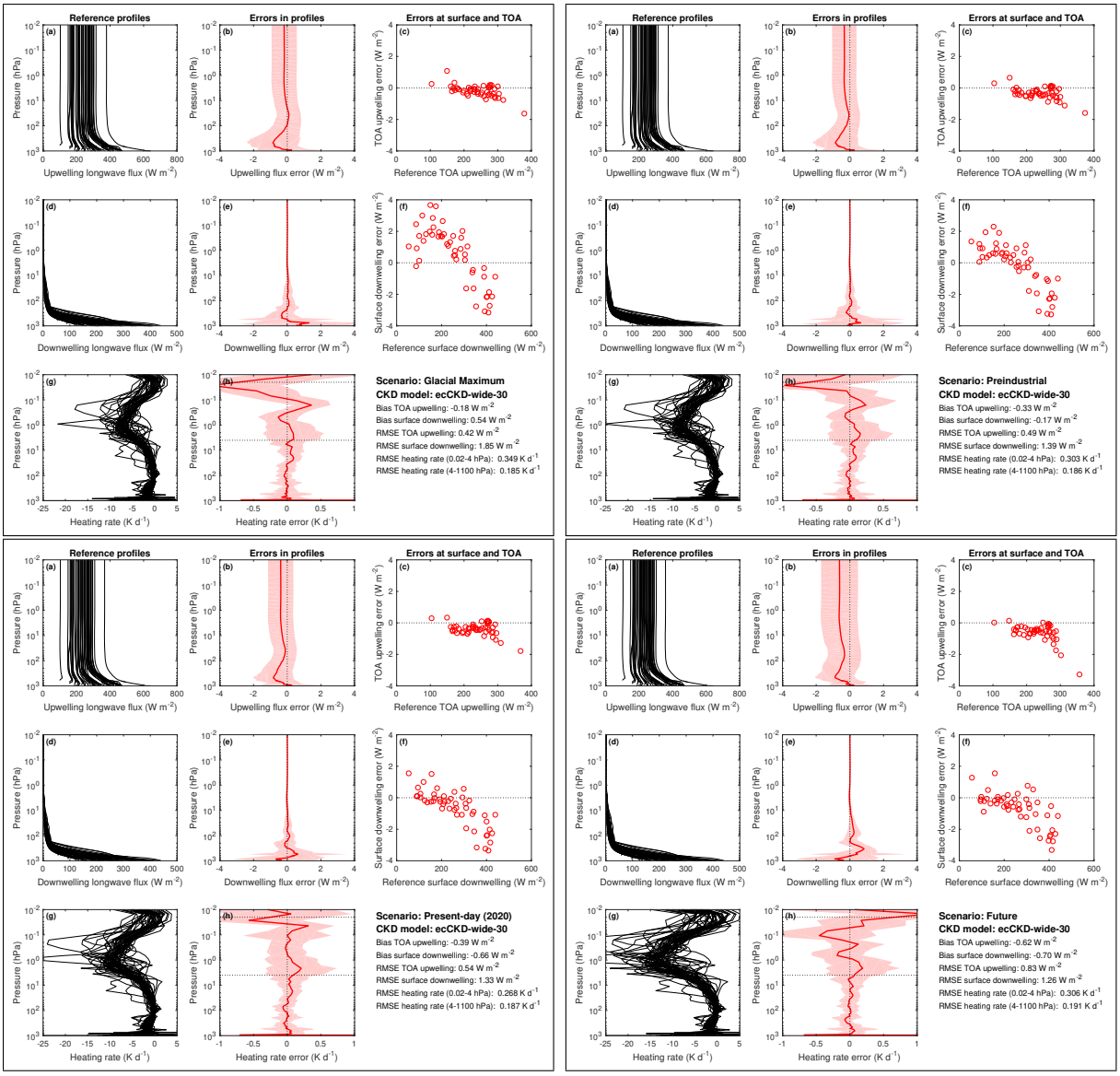

Each boxed groups of panels evaluate the climate-wide-30 CKD model for a single CKDMIP scenario. The left three panels in each group show the irradiances and heating rates from the reference line-by-line calculations. The red lines in the middle three panels show the corresponding bias in these quantities from the CKD model. The shaded regions encompass 95% of the instantaneous errors. Panels c and f depict instantaneous errors in upwelling TOA and downwelling surface irradiances. Error metrics are provided in the lower right.

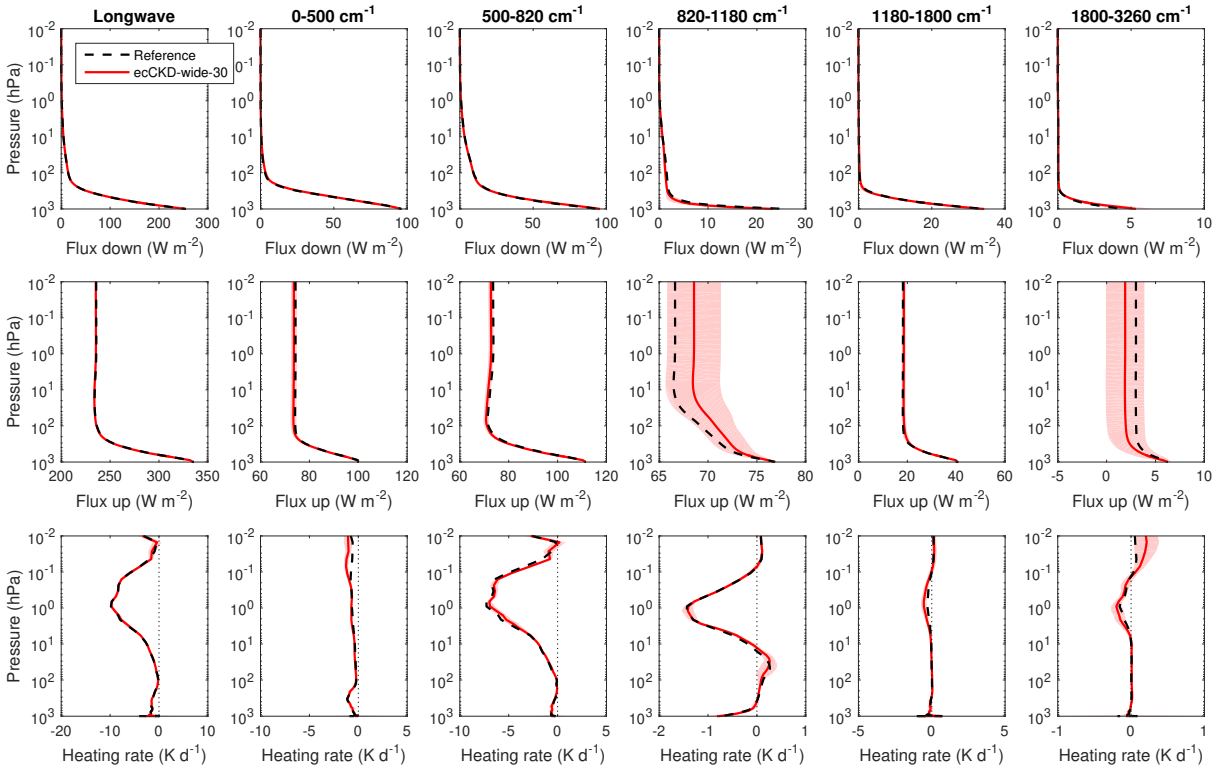

Evaluation of irradiances and heating rates for the broadband (leftmost column of panels) and the 5 wide longwave bands (other panels) of the climate-wide-30 CKD model. The black dashed and red solid lines correspond to the average of the 50 profiles for the "present-day" scenario, while the shaded regions encompass 95% of the error.

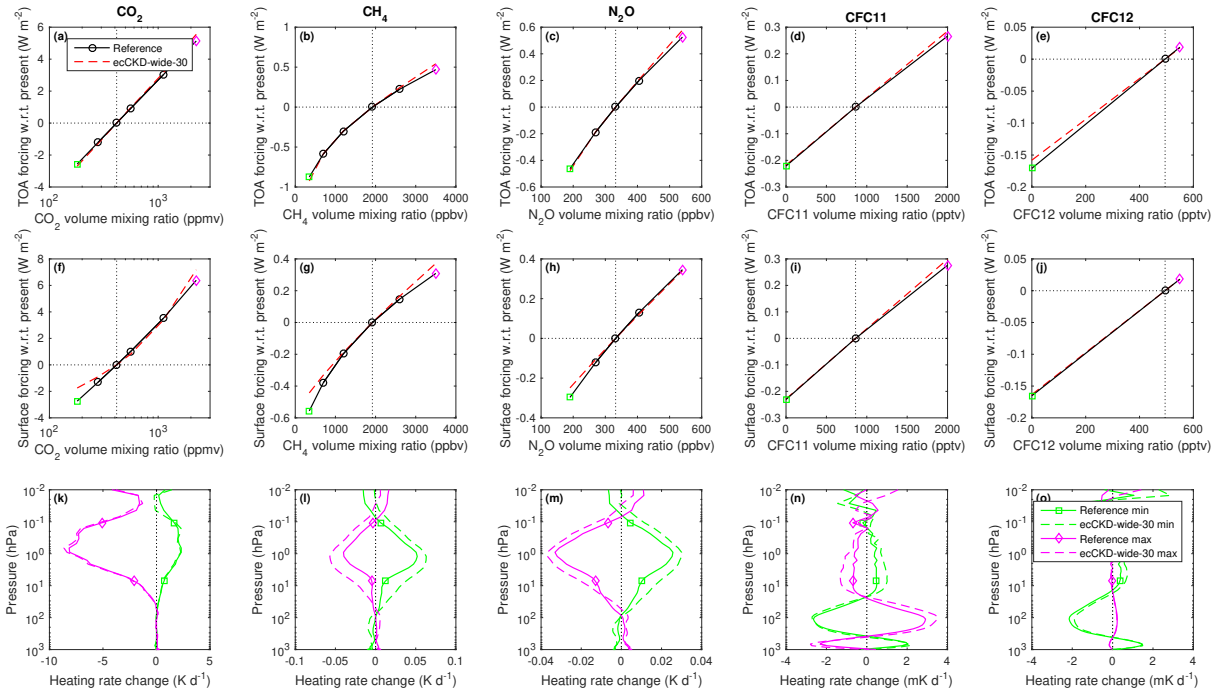

Comparison of reference line-by-line and calculations by the climate-wide-30 model of the instantaneous clear-sky radiative forcing from perturbing each of the five well-mixed greenhouse gases from their present-day values, at (top row) top-of-atmosphere and (middle row) surface, averaged over the 50 profiles of the Evaluation-1 dataset. The bottom row shows the mean change to heating rate resulting from perturbing the concentration of a gas from its present-day value to either the maximum or minimum value in the range for that gas.

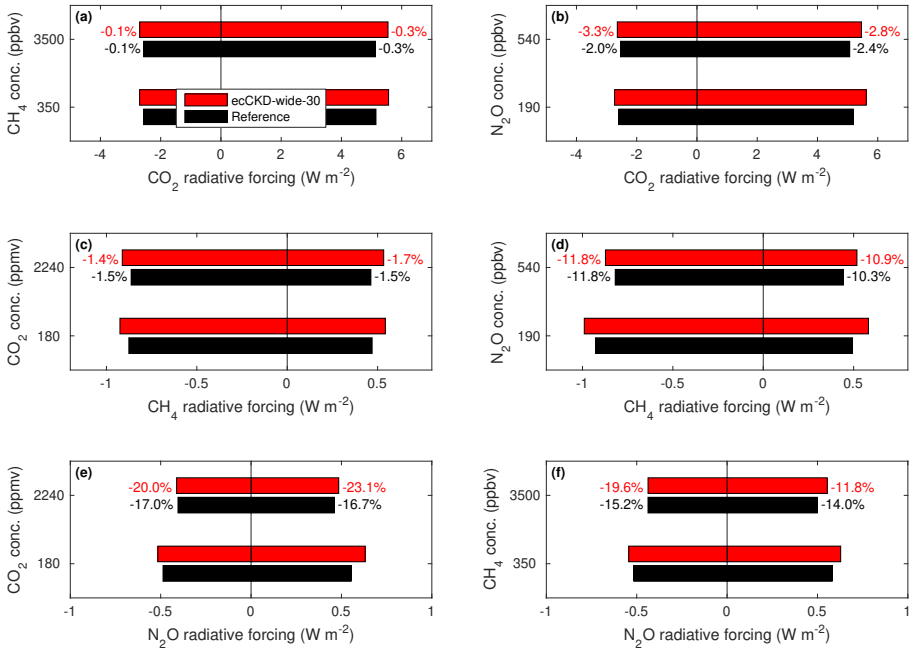

Evaluation of the representation of spectral overlap of CO_2, CH_4 and N_2O by the climate-wide-30 CKD model. In each panel, the abscissa shows the TOA radiative forcing from perturbing a gas to either its climatic minimum or maximum value. These radiative forcings are computed keeping the concentrations of all other well-mixed gases at their present-day values, except for the gas on the ordinate, which is perturbed to its own climatic minimum or maximum values.

Model 10: ecCKD climate-wide-43

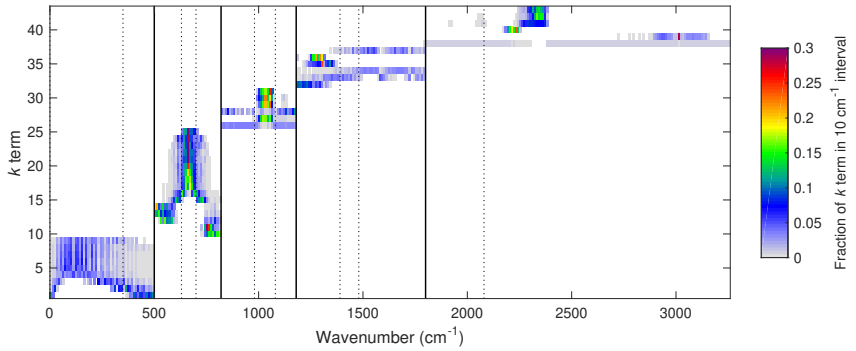

Illustration of the parts of the longwave spectrum that contribute to each k term of the climate-wide-43 model.

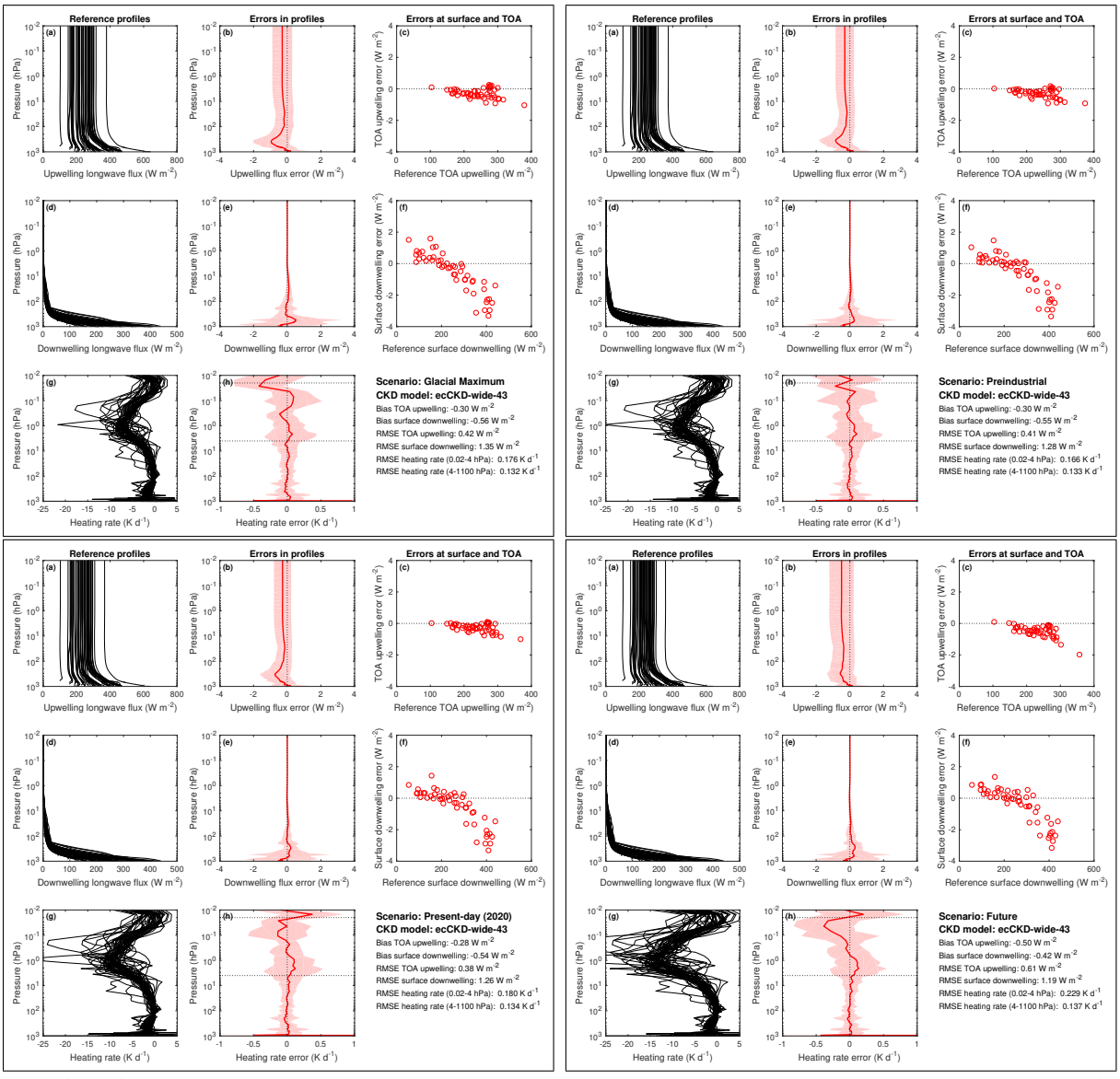

Each boxed groups of panels evaluate the climate-wide-43 CKD model for a single CKDMIP scenario. The left three panels in each group show the irradiances and heating rates from the reference line-by-line calculations. The red lines in the middle three panels show the corresponding bias in these quantities from the CKD model. The shaded regions encompass 95% of the instantaneous errors. Panels c and f depict instantaneous errors in upwelling TOA and downwelling surface irradiances. Error metrics are provided in the lower right.

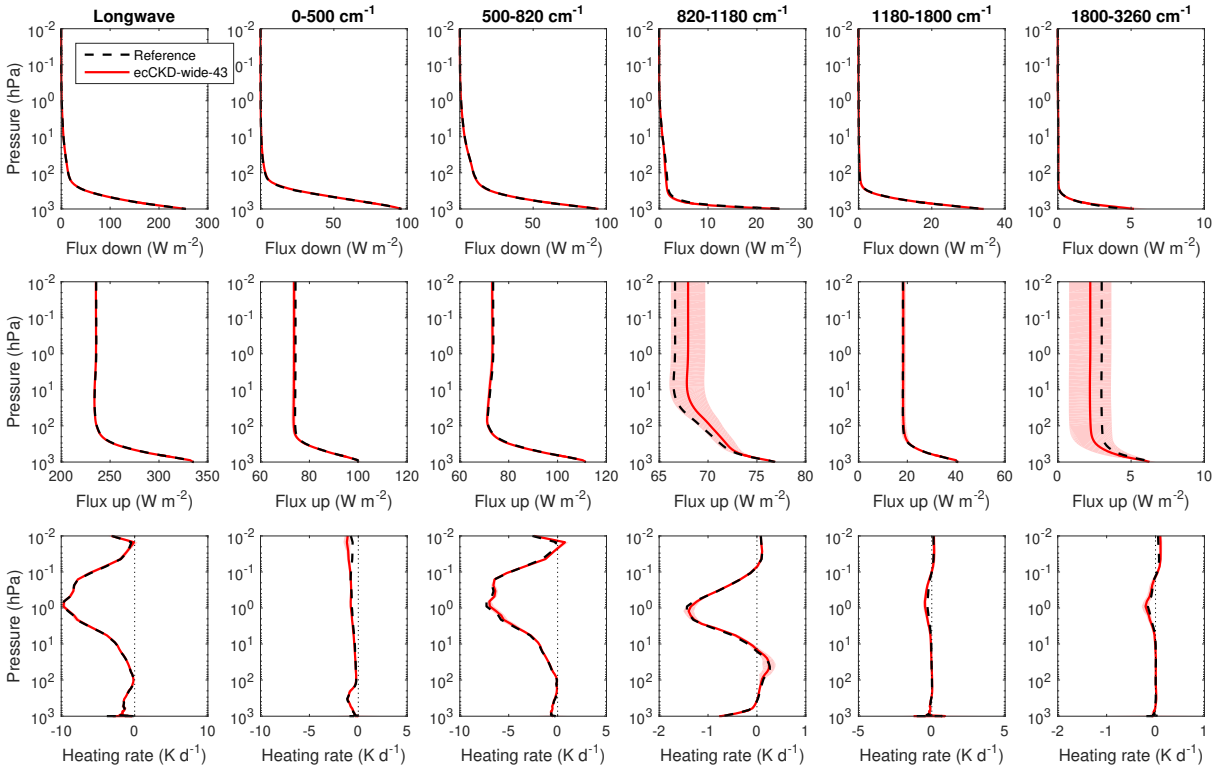

Evaluation of irradiances and heating rates for the broadband (leftmost column of panels) and the 5 wide longwave bands (other panels) of the climate-wide-43 CKD model. The black dashed and red solid lines correspond to the average of the 50 profiles for the "present-day" scenario, while the shaded regions encompass 95% of the error.

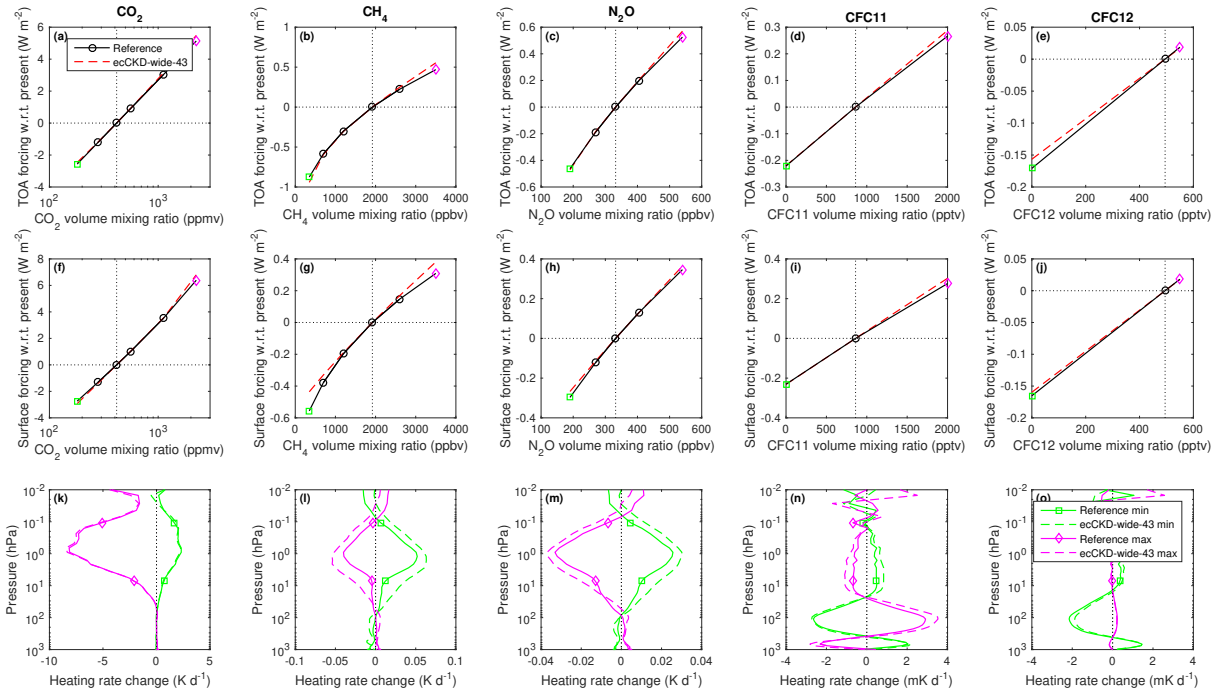

Comparison of reference line-by-line and calculations by the climate-wide-43 model of the instantaneous clear-sky radiative forcing from perturbing each of the five well-mixed greenhouse gases from their present-day values, at (top row) top-of-atmosphere and (middle row) surface, averaged over the 50 profiles of the Evaluation-1 dataset. The bottom row shows the mean change to heating rate resulting from perturbing the concentration of a gas from its present-day value to either the maximum or minimum value in the range for that gas.

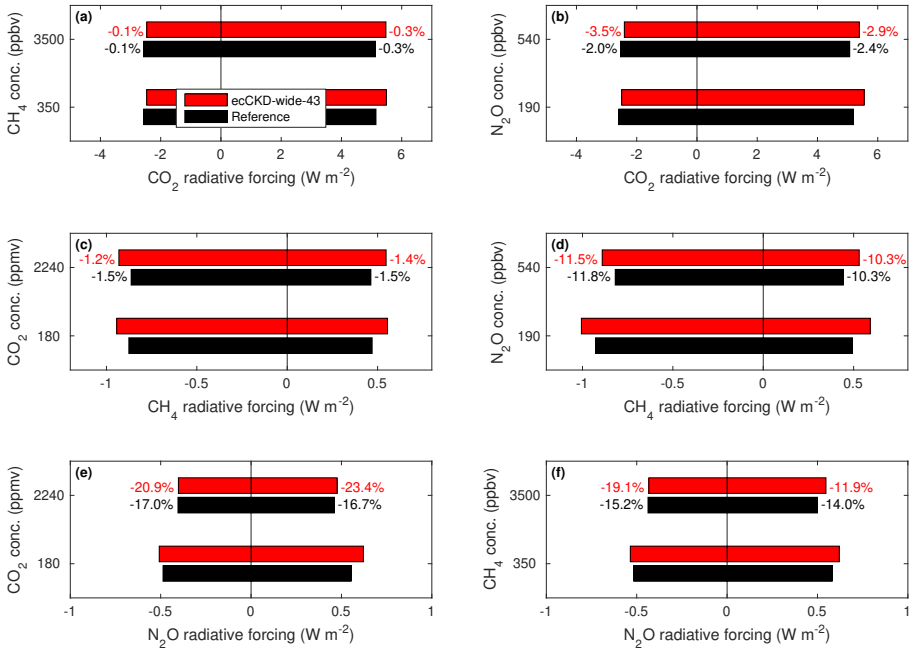

Evaluation of the representation of spectral overlap of CO_2, CH_4 and N_2O by the climate-wide-43 CKD model. In each panel, the abscissa shows the TOA radiative forcing from perturbing a gas to either its climatic minimum or maximum value. These radiative forcings are computed keeping the concentrations of all other well-mixed gases at their present-day values, except for the gas on the ordinate, which is perturbed to its own climatic minimum or maximum values.

Model 11: ecCKD climate-wide-57

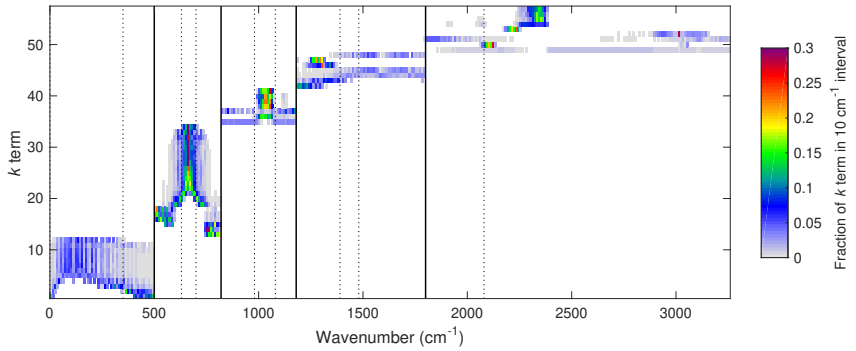

Illustration of the parts of the longwave spectrum that contribute to each k term of the climate-wide-57 model.

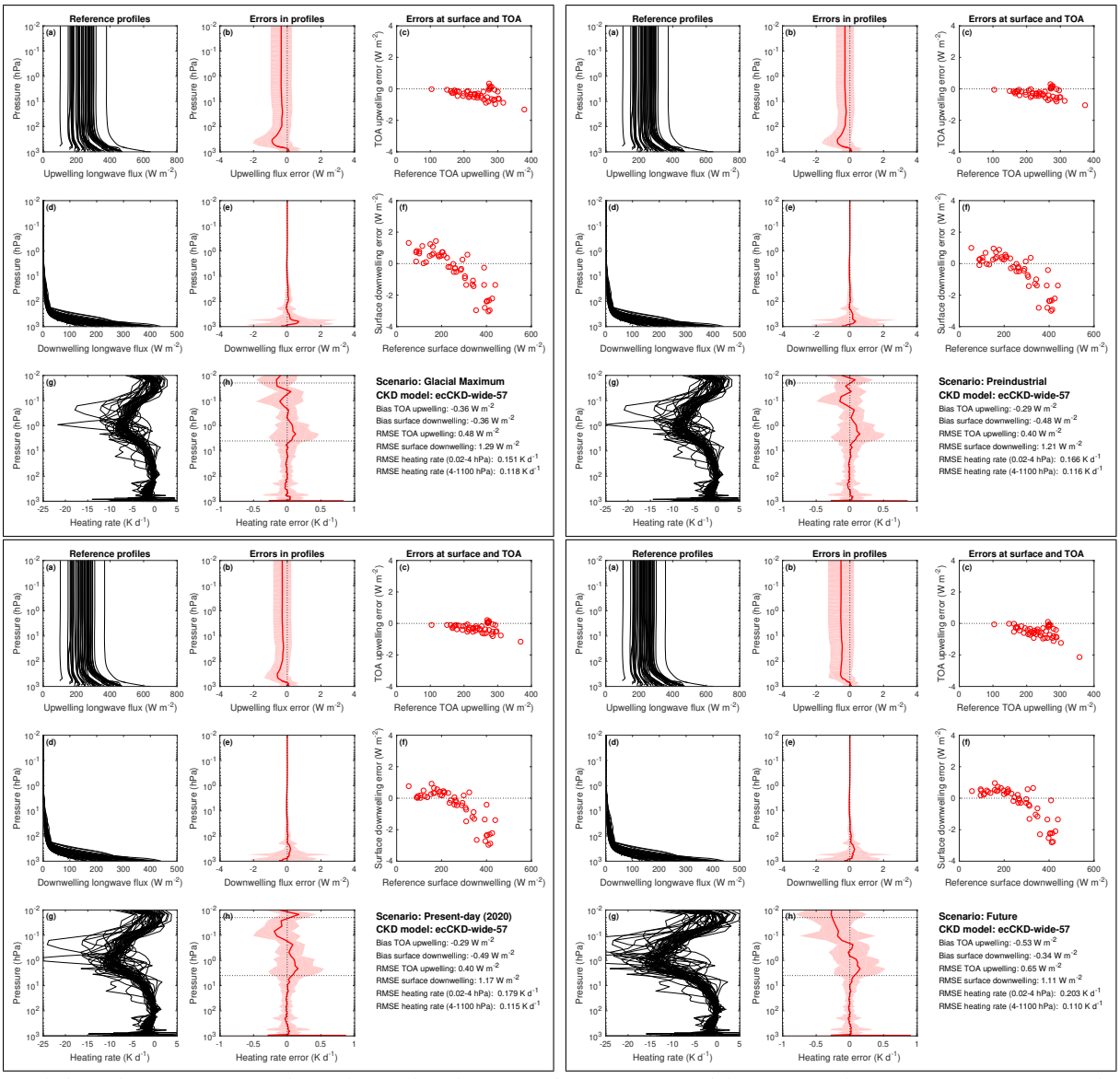

Each boxed groups of panels evaluate the climate-wide-57 CKD model for a single CKDMIP scenario. The left three panels in each group show the irradiances and heating rates from the reference line-by-line calculations. The red lines in the middle three panels show the corresponding bias in these quantities from the CKD model. The shaded regions encompass 95% of the instantaneous errors. Panels c and f depict instantaneous errors in upwelling TOA and downwelling surface irradiances. Error metrics are provided in the lower right.

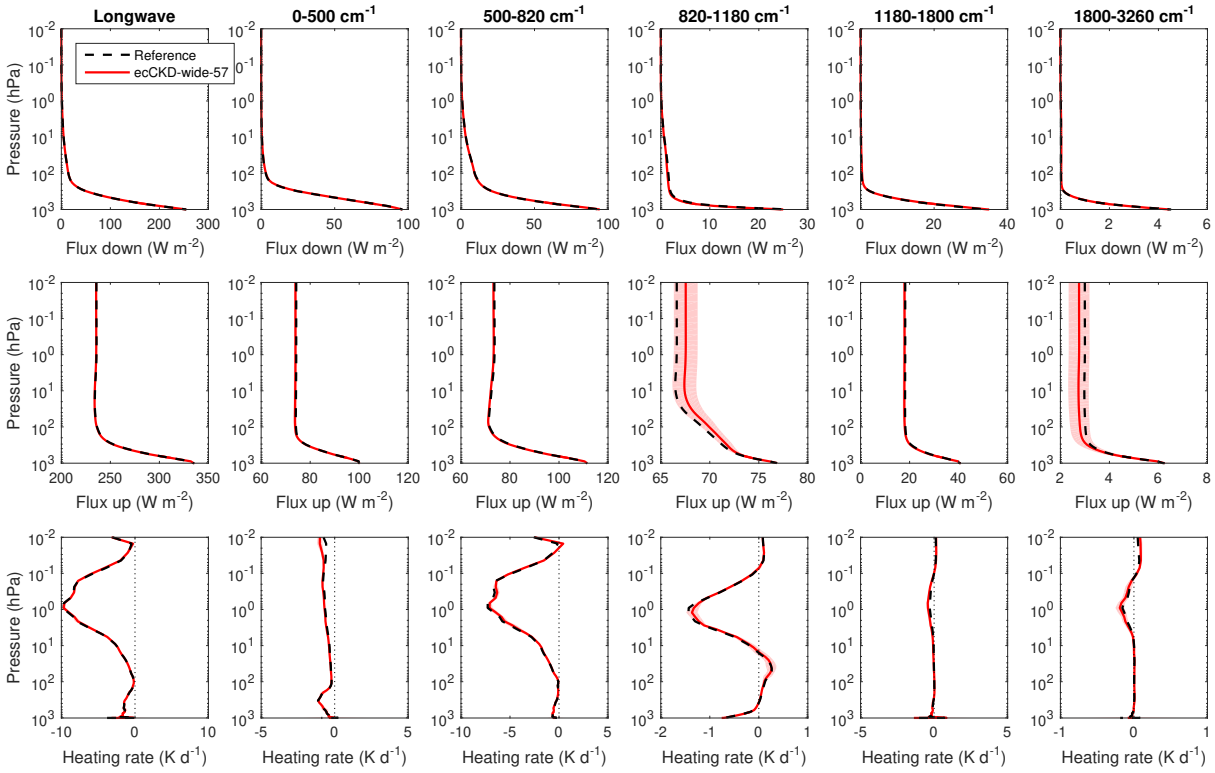

Evaluation of irradiances and heating rates for the broadband (leftmost column of panels) and the 5 wide longwave bands (other panels) of the climate-wide-57 CKD model. The black dashed and red solid lines correspond to the average of the 50 profiles for the "present-day" scenario, while the shaded regions encompass 95% of the error.

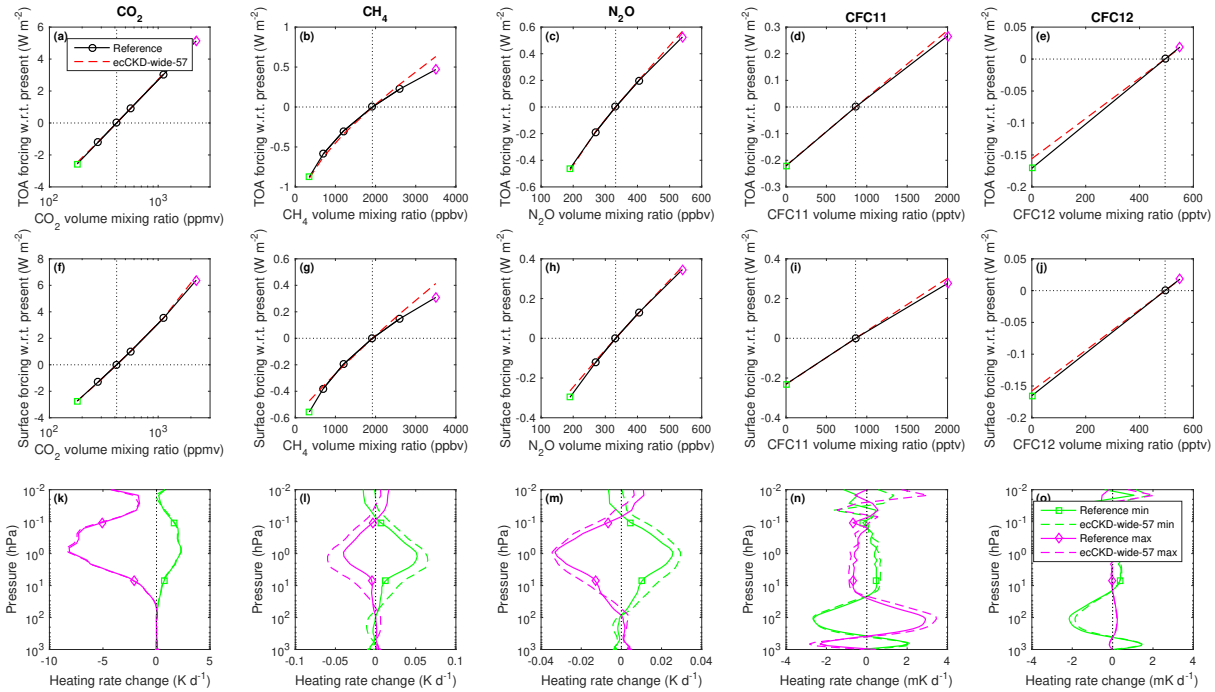

Comparison of reference line-by-line and calculations by the climate-wide-57 model of the instantaneous clear-sky radiative forcing from perturbing each of the five well-mixed greenhouse gases from their present-day values, at (top row) top-of-atmosphere and (middle row) surface, averaged over the 50 profiles of the Evaluation-1 dataset. The bottom row shows the mean change to heating rate resulting from perturbing the concentration of a gas from its present-day value to either the maximum or minimum value in the range for that gas.

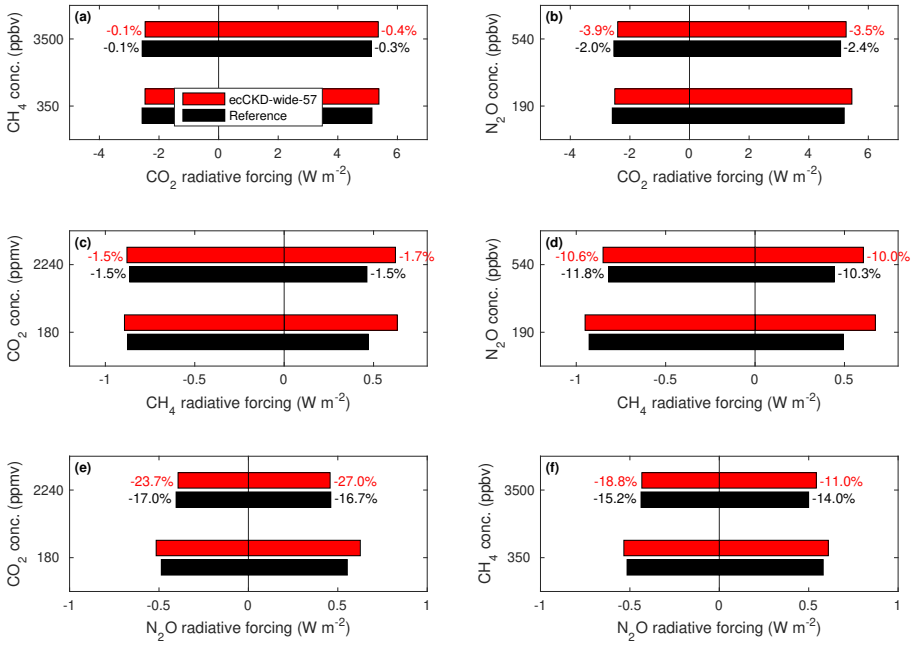

Evaluation of the representation of spectral overlap of CO_2, CH_4 and N_2O by the climate-wide-57 CKD model. In each panel, the abscissa shows the TOA radiative forcing from perturbing a gas to either its climatic minimum or maximum value. These radiative forcings are computed keeping the concentrations of all other well-mixed gases at their present-day values, except for the gas on the ordinate, which is perturbed to its own climatic minimum or maximum values.

Model 12: ecCKD climate-wide-87

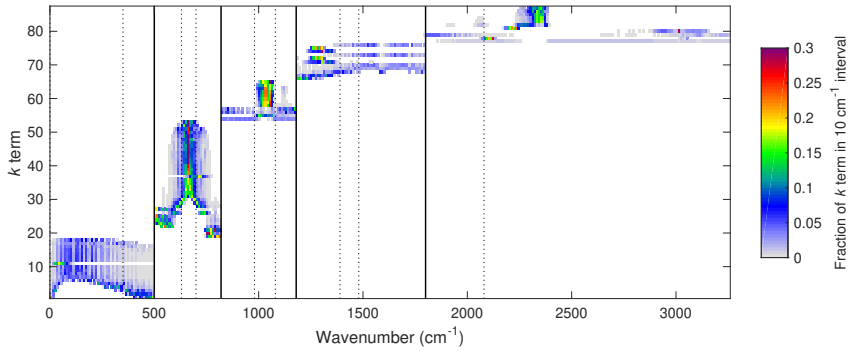

Illustration of the parts of the longwave spectrum that contribute to each k term of the climate-wide-87 model.

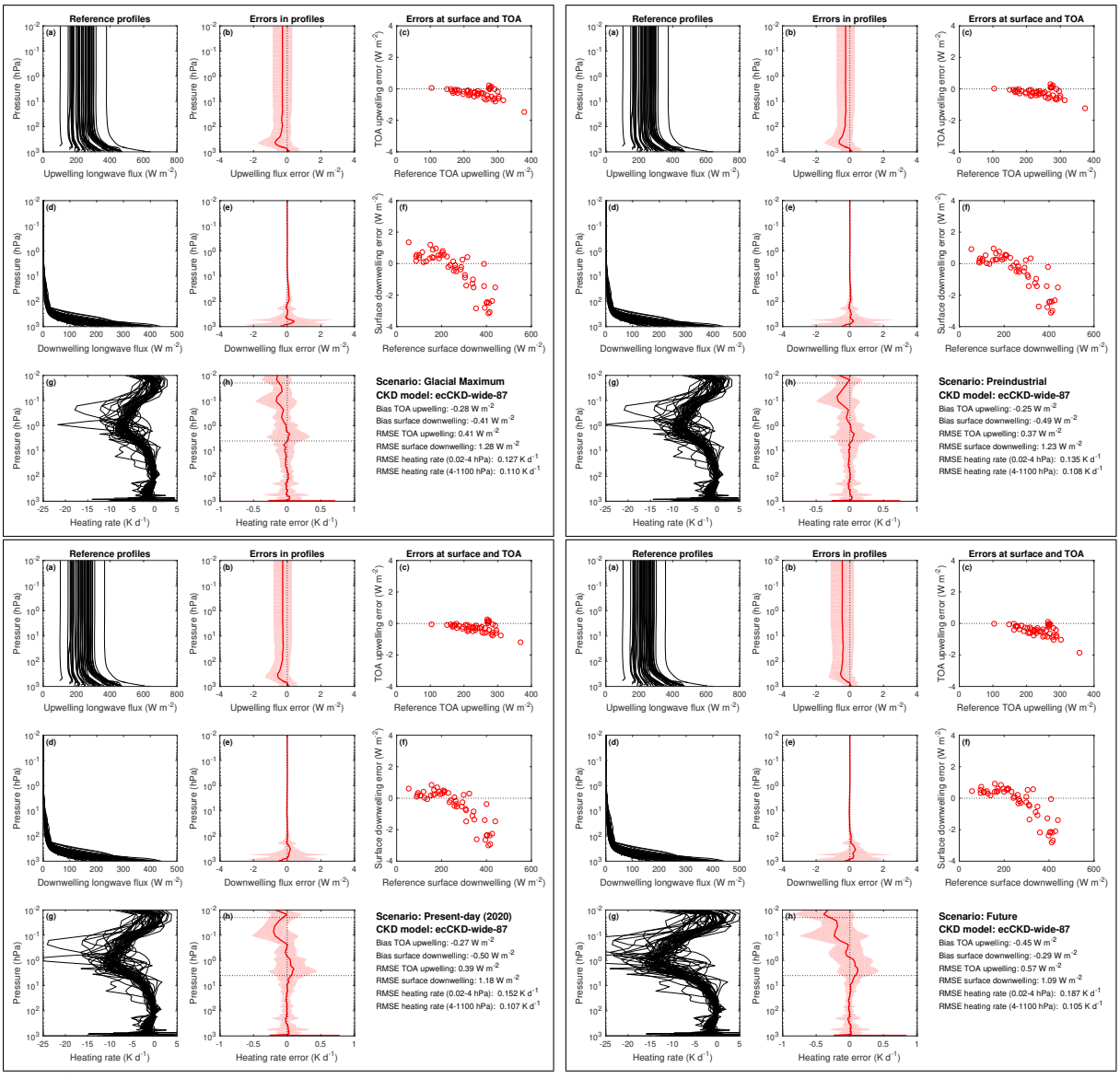

Each boxed groups of panels evaluate the climate-wide-87 CKD model for a single CKDMIP scenario. The left three panels in each group show the irradiances and heating rates from the reference line-by-line calculations. The red lines in the middle three panels show the corresponding bias in these quantities from the CKD model. The shaded regions encompass 95% of the instantaneous errors. Panels c and f depict instantaneous errors in upwelling TOA and downwelling surface irradiances. Error metrics are provided in the lower right.

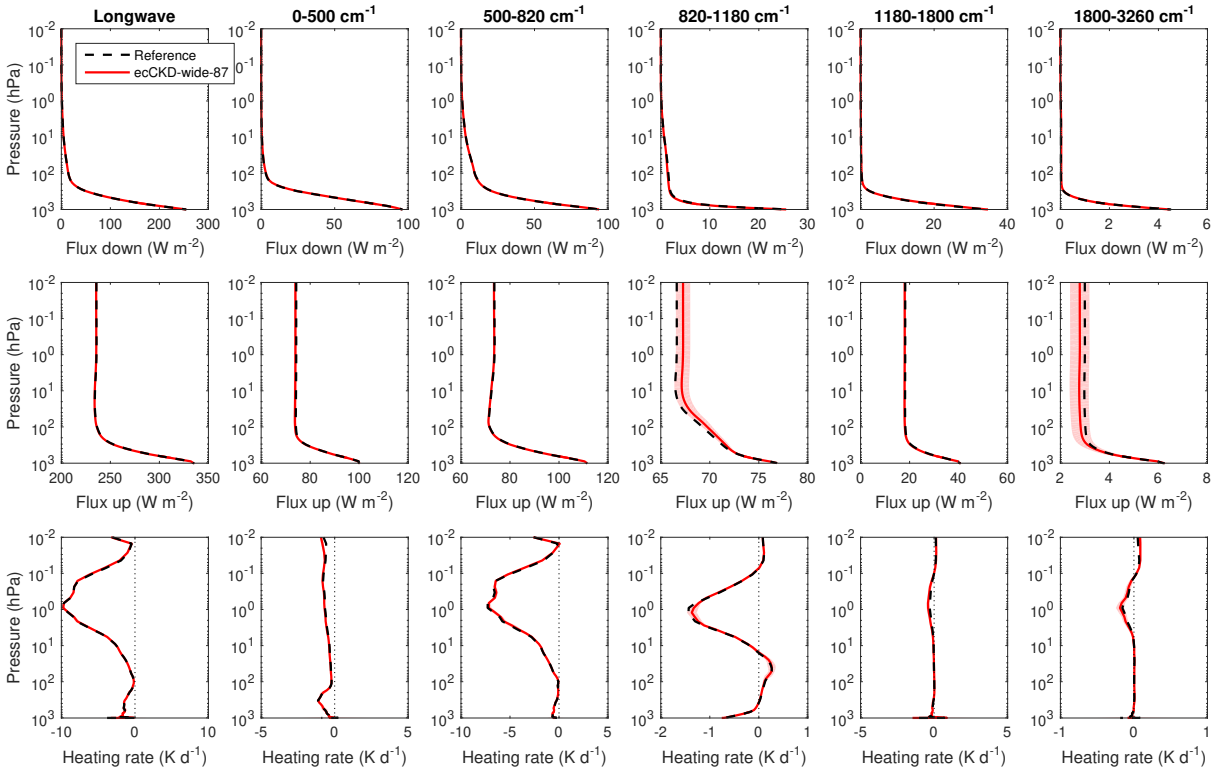

Evaluation of irradiances and heating rates for the broadband (leftmost column of panels) and the 5 wide longwave bands (other panels) of the climate-wide-87 CKD model. The black dashed and red solid lines correspond to the average of the 50 profiles for the "present-day" scenario, while the shaded regions encompass 95% of the error.

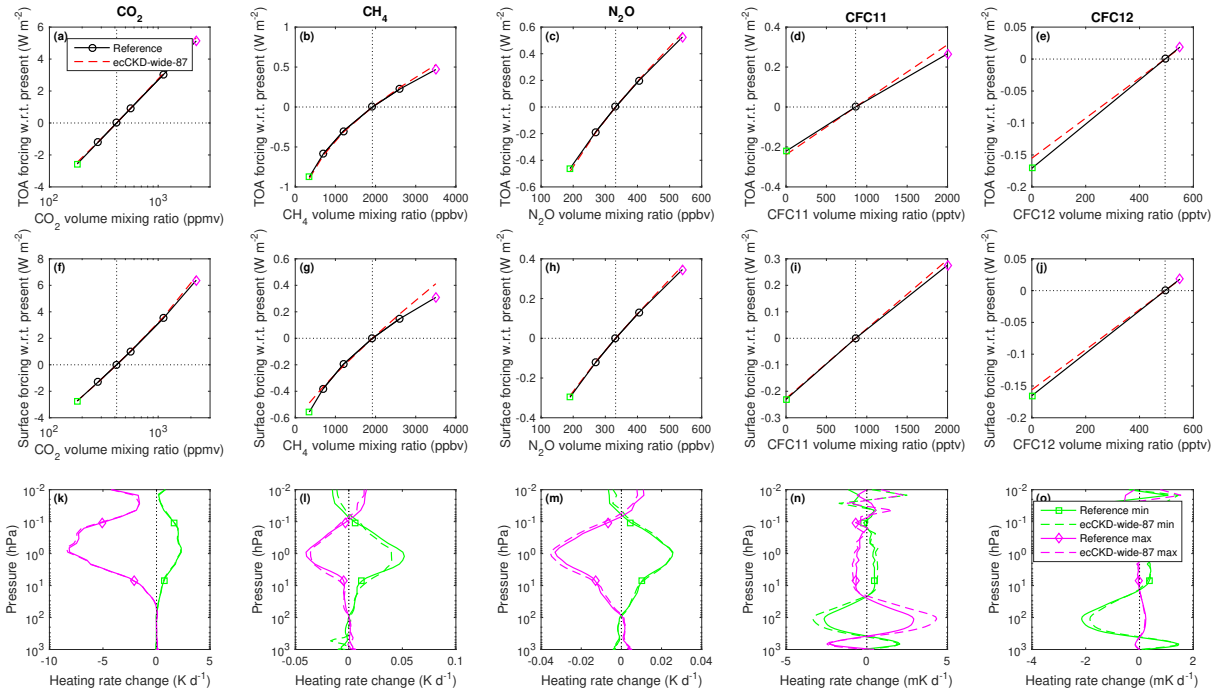

Comparison of reference line-by-line and calculations by the climate-wide-87 model of the instantaneous clear-sky radiative forcing from perturbing each of the five well-mixed greenhouse gases from their present-day values, at (top row) top-of-atmosphere and (middle row) surface, averaged over the 50 profiles of the Evaluation-1 dataset. The bottom row shows the mean change to heating rate resulting from perturbing the concentration of a gas from its present-day value to either the maximum or minimum value in the range for that gas.

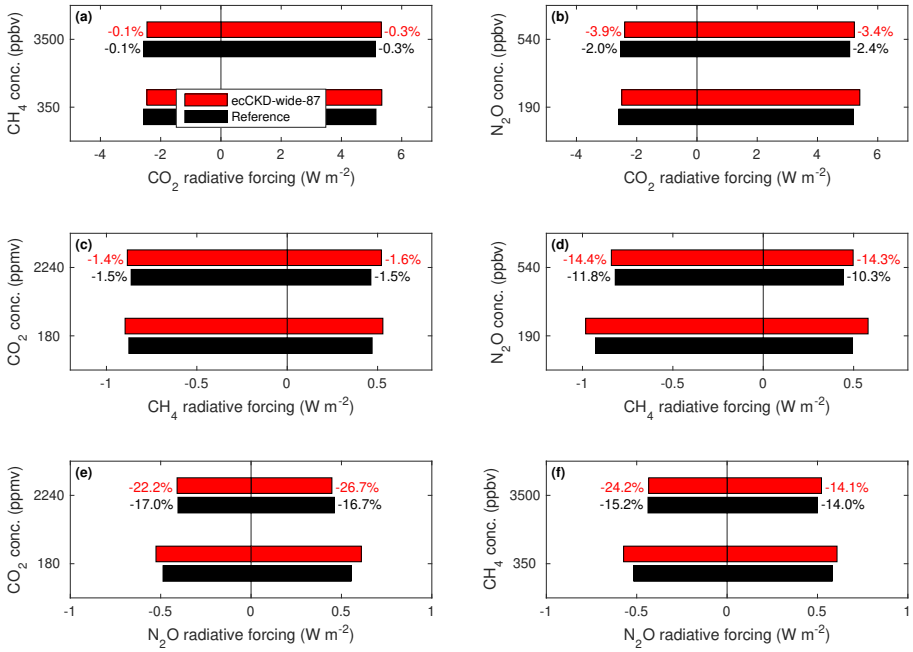

Evaluation of the representation of spectral overlap of CO_2, CH_4 and N_2O by the climate-wide-87 CKD model. In each panel, the abscissa shows the TOA radiative forcing from perturbing a gas to either its climatic minimum or maximum value. These radiative forcings are computed keeping the concentrations of all other well-mixed gases at their present-day values, except for the gas on the ordinate, which is perturbed to its own climatic minimum or maximum values.

Model 13: ecCKD climate-narrow-22

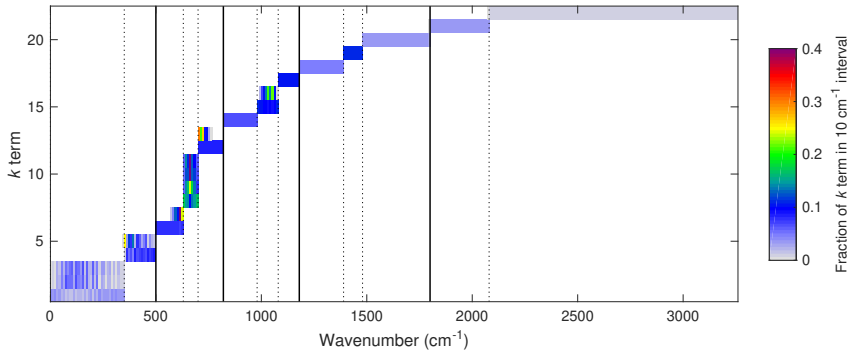

Illustration of the parts of the longwave spectrum that contribute to each k term of the climate-narrow-22 model.

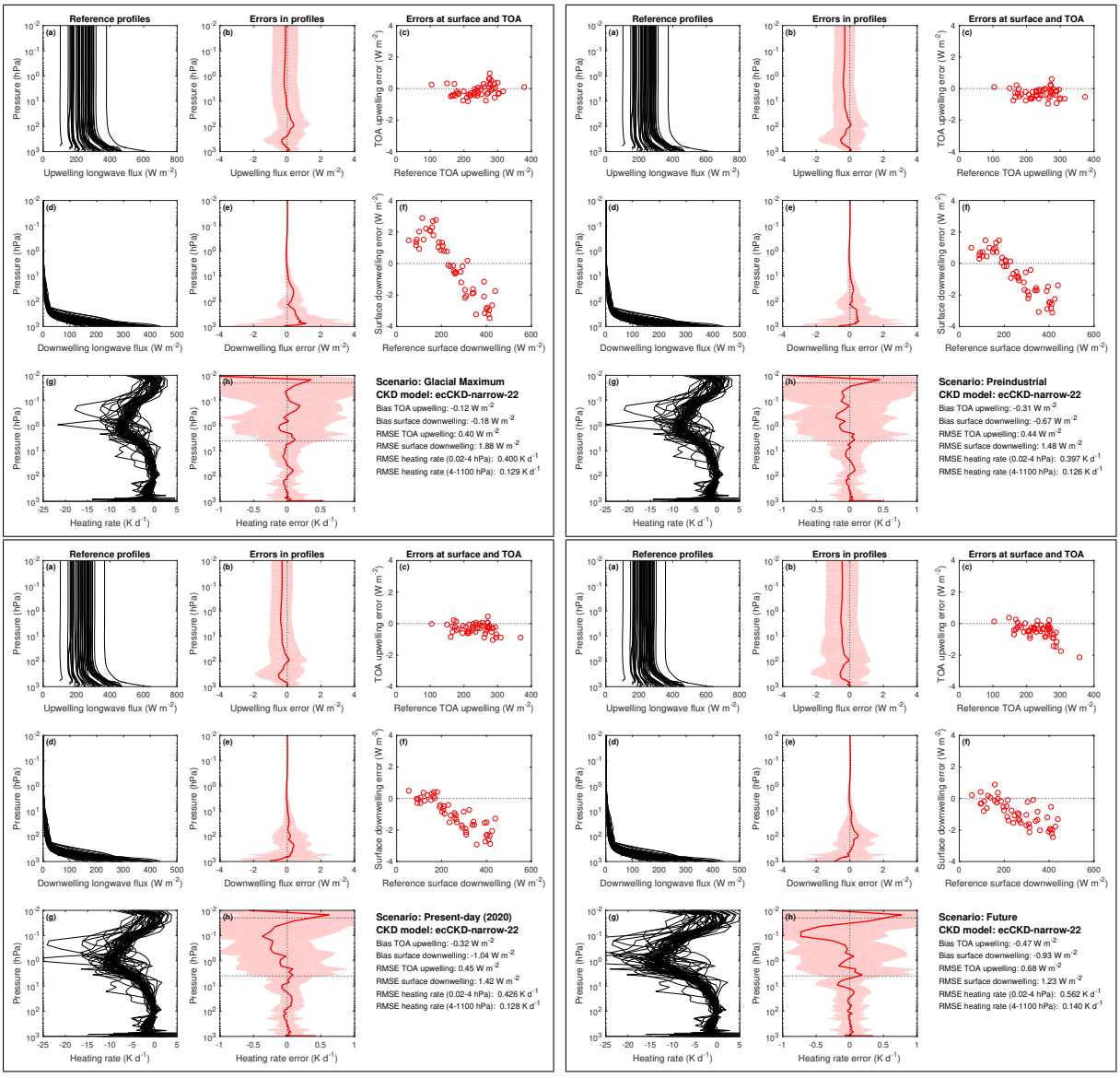

Each boxed groups of panels evaluate the climate-narrow-22 CKD model for a single CKDMIP scenario. The left three panels in each group show the irradiances and heating rates from the reference line-by-line calculations. The red lines in the middle three panels show the corresponding bias in these quantities from the CKD model. The shaded regions encompass 95% of the instantaneous errors. Panels c and f depict instantaneous errors in upwelling TOA and downwelling surface irradiances. Error metrics are provided in the lower right.

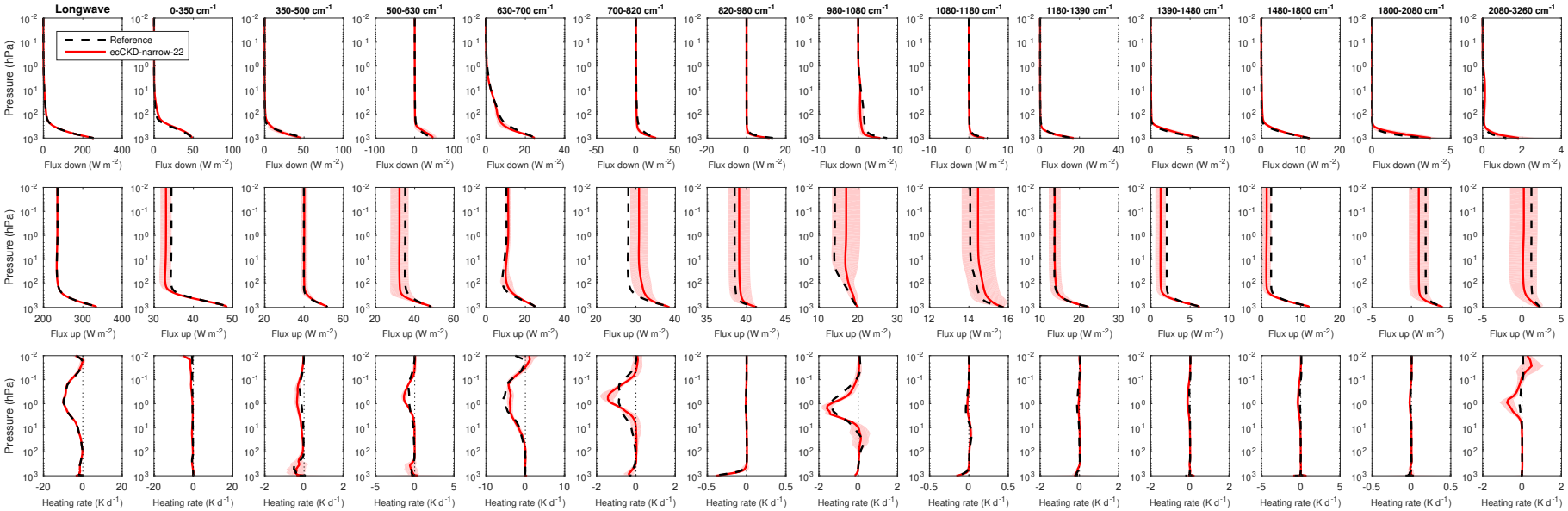

Evaluation of irradiances and heating rates for the broadband (leftmost column of panels) and the 13 narrow longwave bands (other panels) of the climate-narrow-22 CKD model. The black dashed and red solid lines correspond to the average of the 50 profiles for the "present-day" scenario, while the shaded regions encompass 95% of the error.

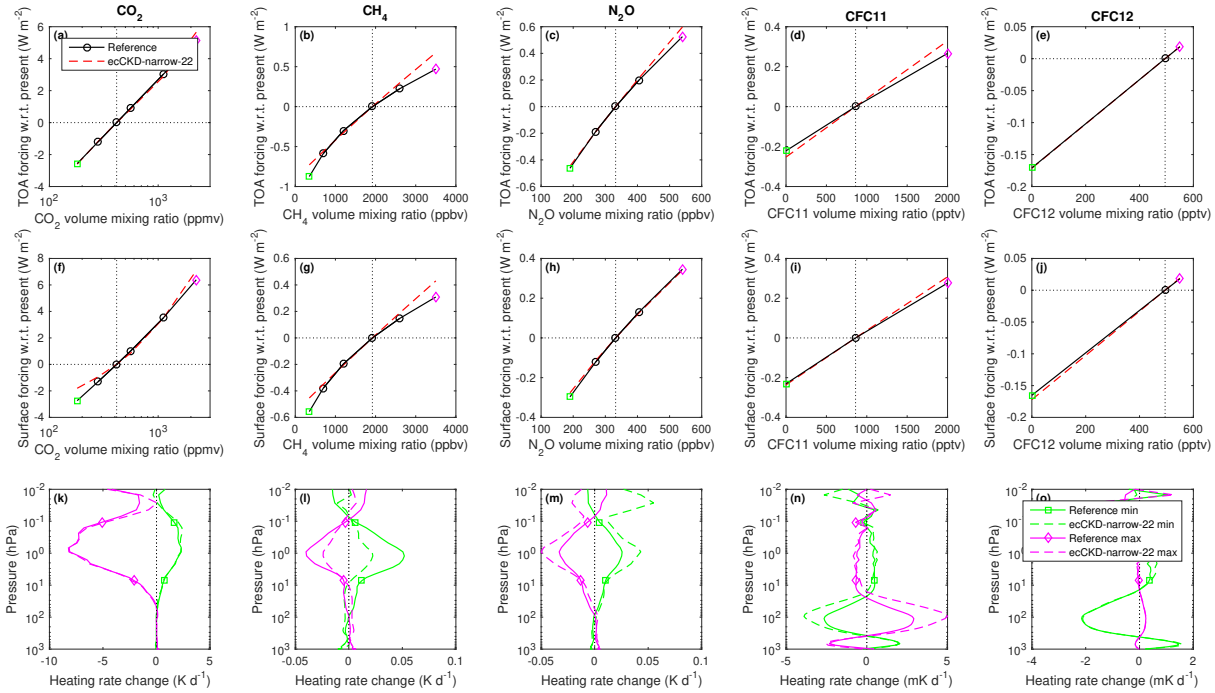

Comparison of reference line-by-line and calculations by the climate-narrow-22 model of the instantaneous clear-sky radiative forcing from perturbing each of the five well-mixed greenhouse gases from their present-day values, at (top row) top-of-atmosphere and (middle row) surface, averaged over the 50 profiles of the Evaluation-1 dataset. The bottom row shows the mean change to heating rate resulting from perturbing the concentration of a gas from its present-day value to either the maximum or minimum value in the range for that gas.

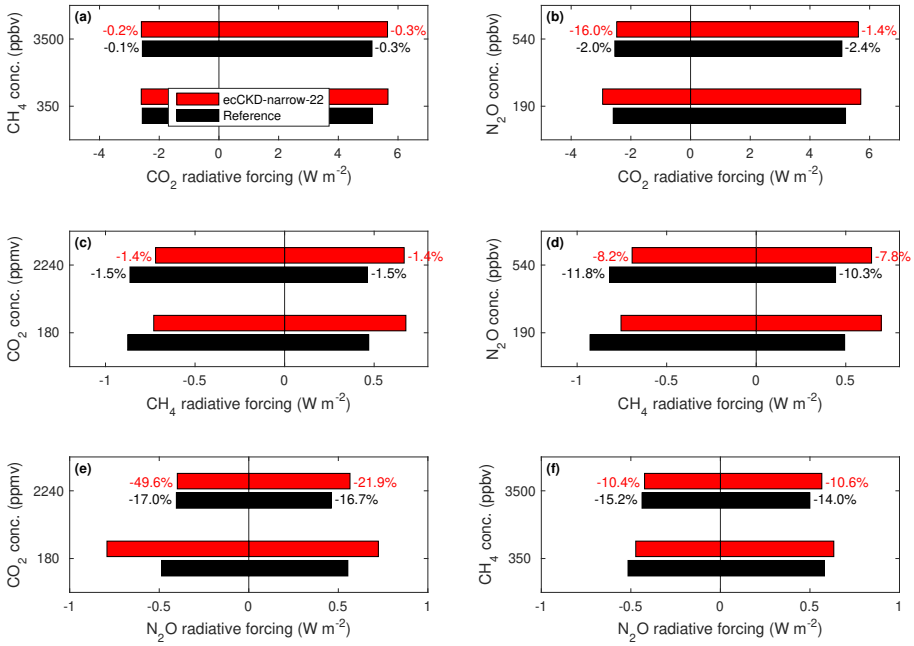

Evaluation of the representation of spectral overlap of CO_2, CH_4 and N_2O by the climate-narrow-22 CKD model. In each panel, the abscissa shows the TOA radiative forcing from perturbing a gas to either its climatic minimum or maximum value. These radiative forcings are computed keeping the concentrations of all other well-mixed gases at their present-day values, except for the gas on the ordinate, which is perturbed to its own climatic minimum or maximum values.

Model 14: ecCKD climate-narrow-28

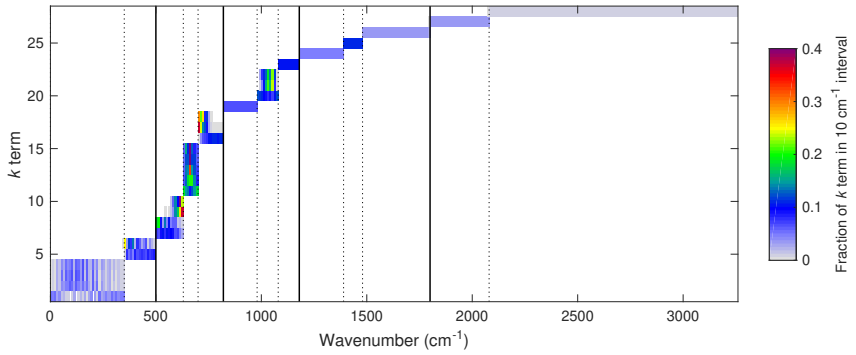

Illustration of the parts of the longwave spectrum that contribute to each k term of the climate-narrow-28 model.

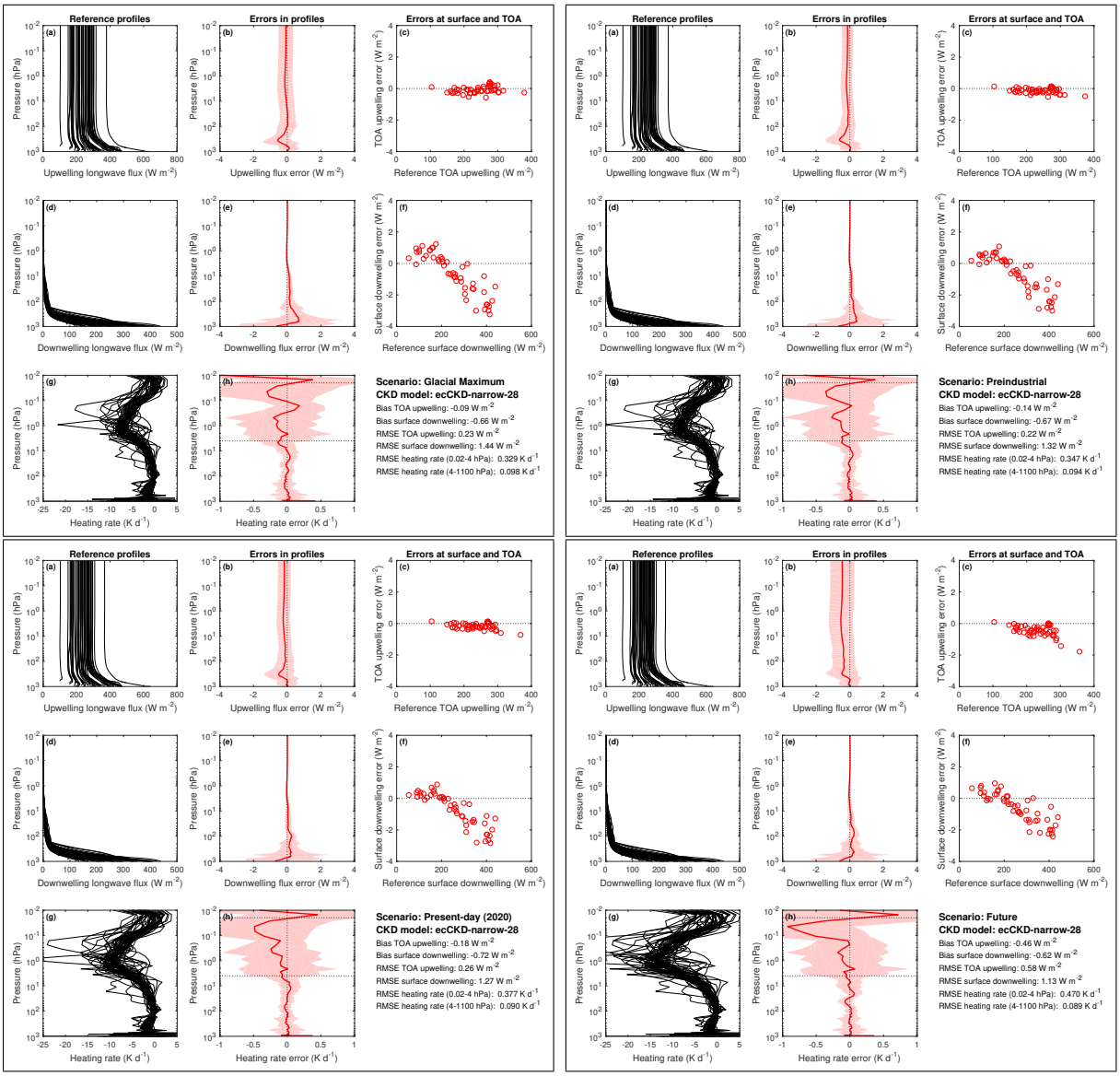

Each boxed groups of panels evaluate the climate-narrow-28 CKD model for a single CKDMIP scenario. The left three panels in each group show the irradiances and heating rates from the reference line-by-line calculations. The red lines in the middle three panels show the corresponding bias in these quantities from the CKD model. The shaded regions encompass 95% of the instantaneous errors. Panels c and f depict instantaneous errors in upwelling TOA and downwelling surface irradiances. Error metrics are provided in the lower right.

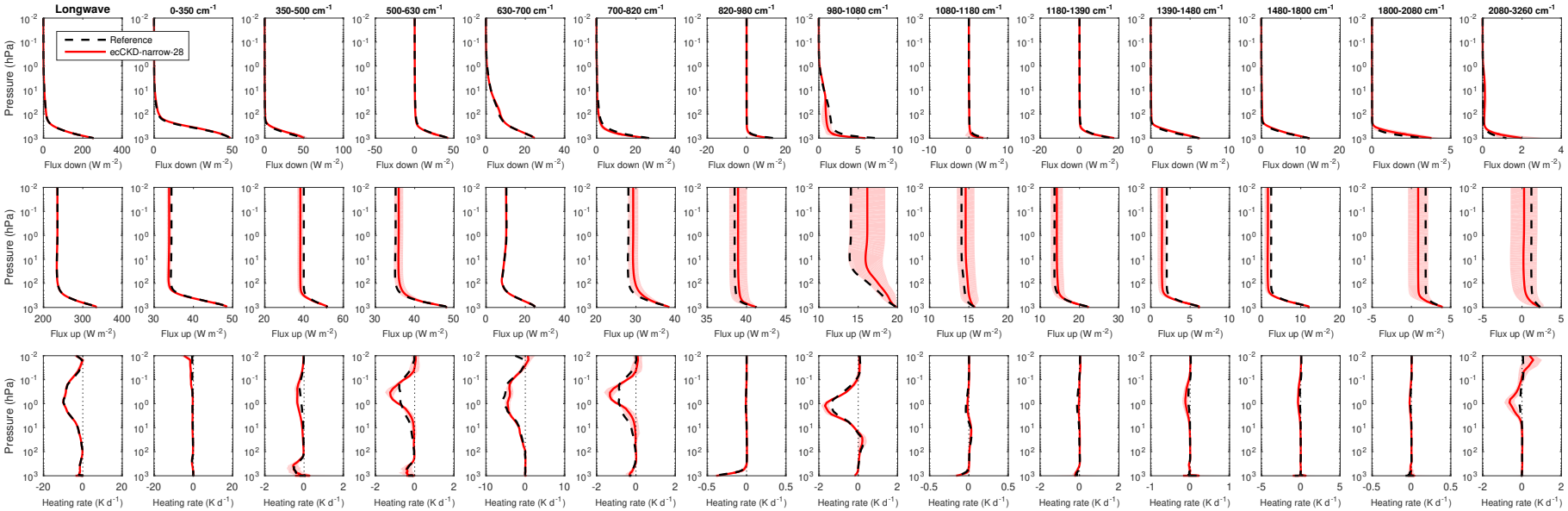

Evaluation of irradiances and heating rates for the broadband (leftmost column of panels) and the 13 narrow longwave bands (other panels) of the climate-narrow-28 CKD model. The black dashed and red solid lines correspond to the average of the 50 profiles for the "present-day" scenario, while the shaded regions encompass 95% of the error.

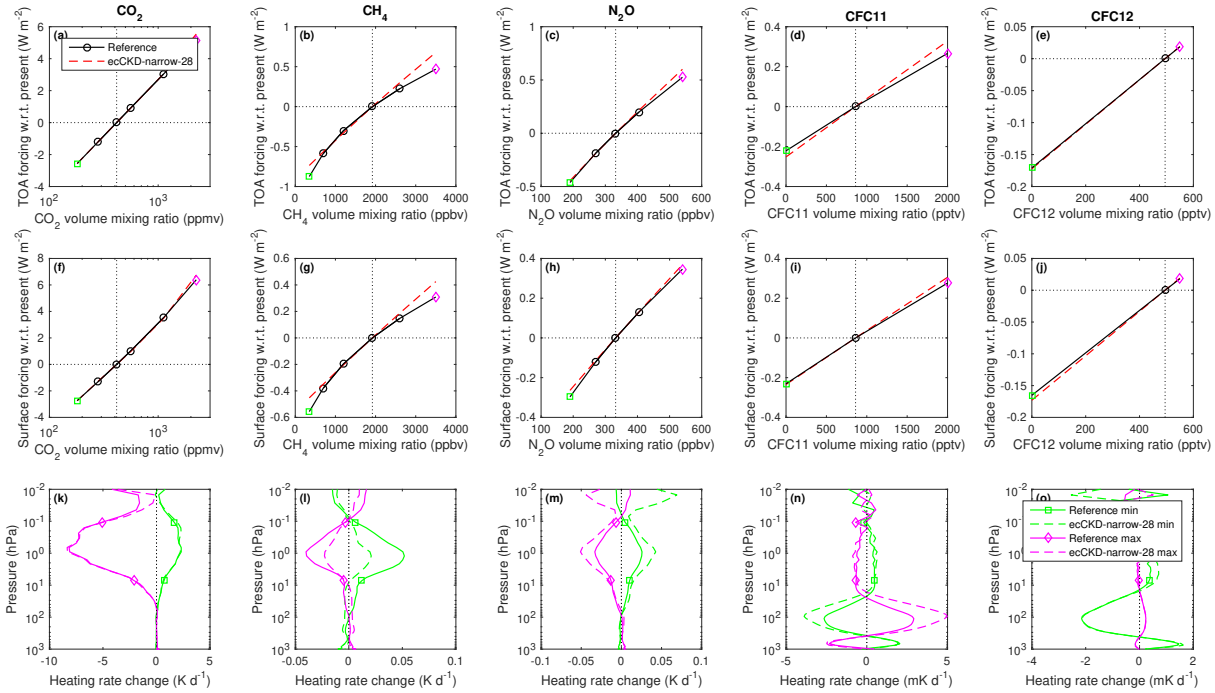

Comparison of reference line-by-line and calculations by the climate-narrow-28 model of the instantaneous clear-sky radiative forcing from perturbing each of the five well-mixed greenhouse gases from their present-day values, at (top row) top-of-atmosphere and (middle row) surface, averaged over the 50 profiles of the Evaluation-1 dataset. The bottom row shows the mean change to heating rate resulting from perturbing the concentration of a gas from its present-day value to either the maximum or minimum value in the range for that gas.

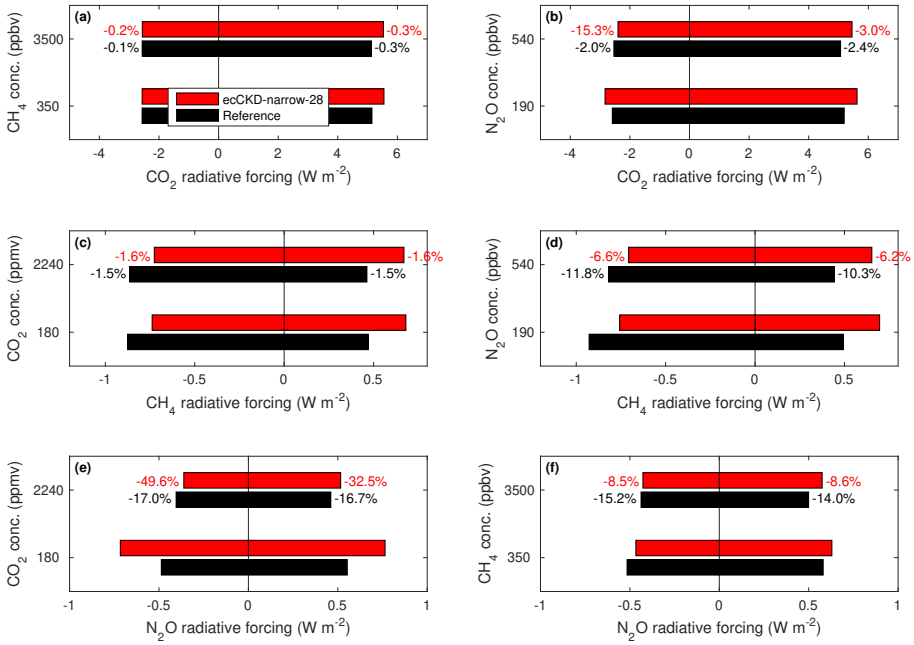

Evaluation of the representation of spectral overlap of CO_2, CH_4 and N_2O by the climate-narrow-28 CKD model. In each panel, the abscissa shows the TOA radiative forcing from perturbing a gas to either its climatic minimum or maximum value. These radiative forcings are computed keeping the concentrations of all other well-mixed gases at their present-day values, except for the gas on the ordinate, which is perturbed to its own climatic minimum or maximum values.

Model 15: ecCKD climate-narrow-37

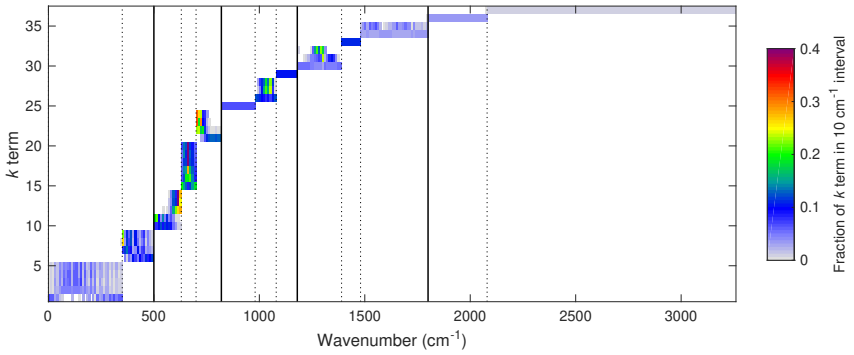

Illustration of the parts of the longwave spectrum that contribute to each k term of the climate-narrow-37 model.

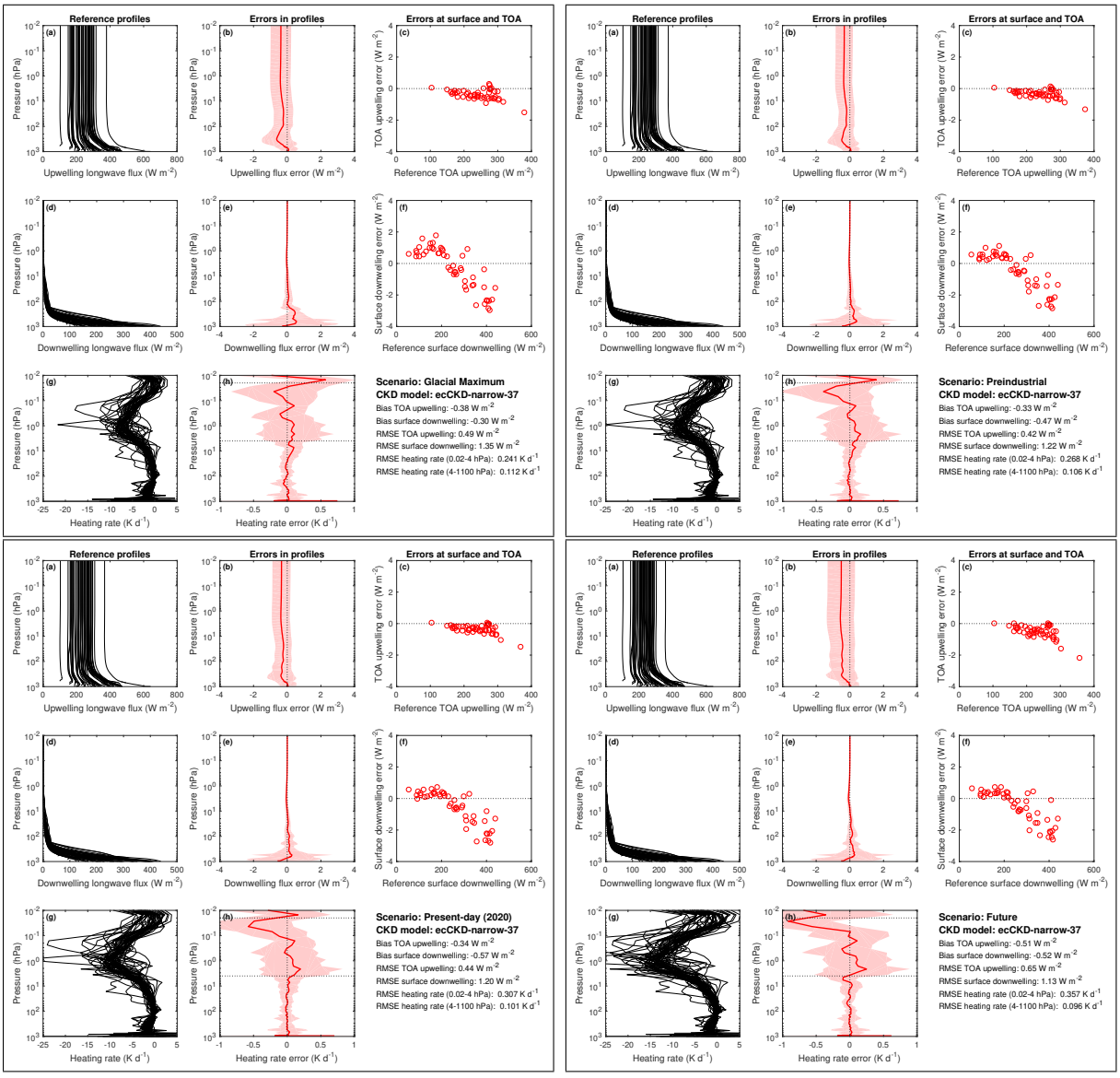

Each boxed groups of panels evaluate the climate-narrow-37 CKD model for a single CKDMIP scenario. The left three panels in each group show the irradiances and heating rates from the reference line-by-line calculations. The red lines in the middle three panels show the corresponding bias in these quantities from the CKD model. The shaded regions encompass 95% of the instantaneous errors. Panels c and f depict instantaneous errors in upwelling TOA and downwelling surface irradiances. Error metrics are provided in the lower right.

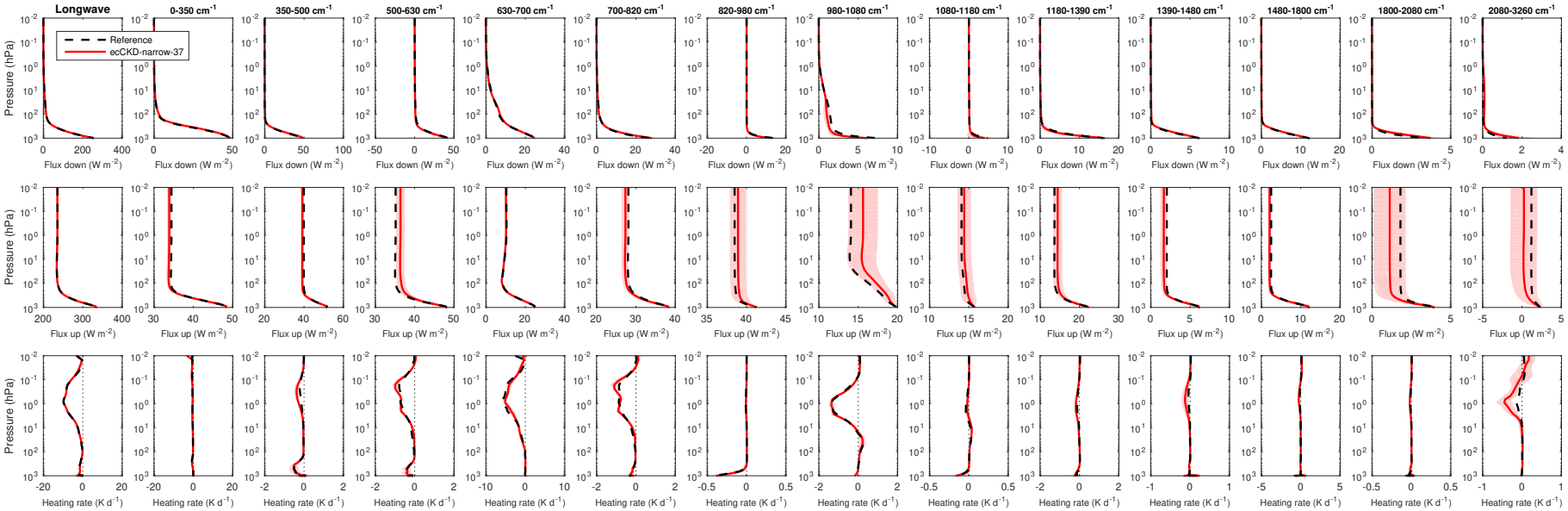

Evaluation of irradiances and heating rates for the broadband (leftmost column of panels) and the 13 narrow longwave bands (other panels) of the climate-narrow-37 CKD model. The black dashed and red solid lines correspond to the average of the 50 profiles for the "present-day" scenario, while the shaded regions encompass 95% of the error.

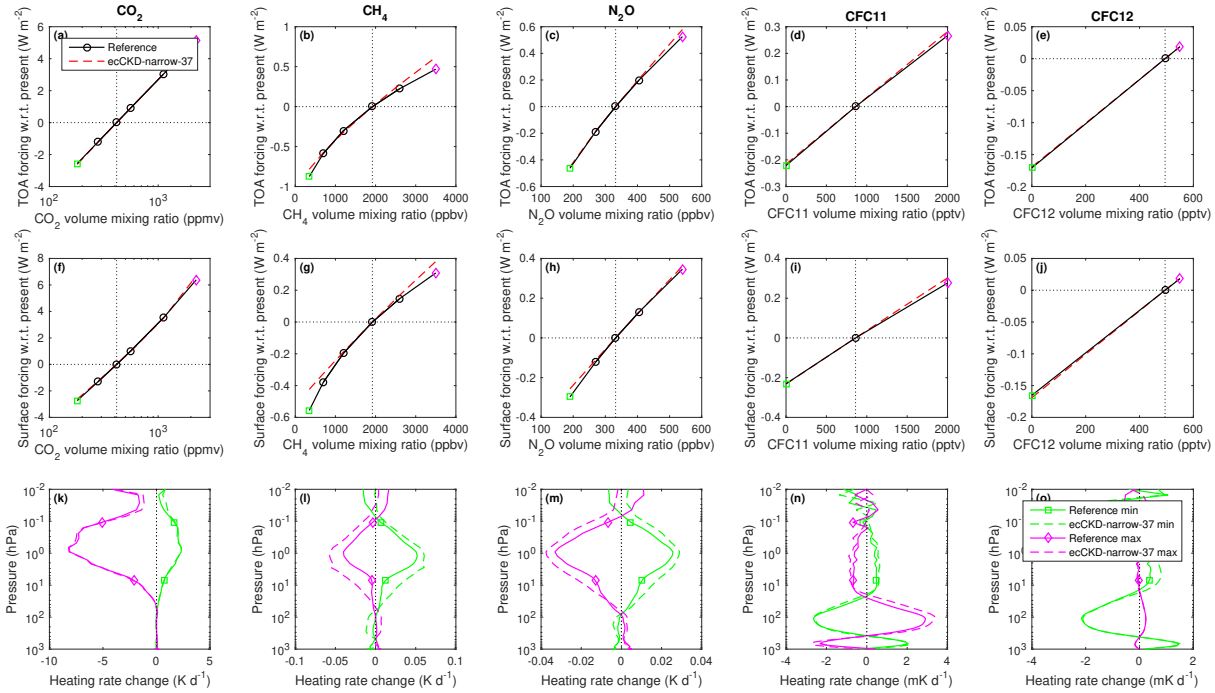

Comparison of reference line-by-line and calculations by the climate-narrow-37 model of the instantaneous clear-sky radiative forcing from perturbing each of the five well-mixed greenhouse gases from their present-day values, at (top row) top-of-atmosphere and (middle row) surface, averaged over the 50 profiles of the Evaluation-1 dataset. The bottom row shows the mean change to heating rate resulting from perturbing the concentration of a gas from its present-day value to either the maximum or minimum value in the range for that gas.

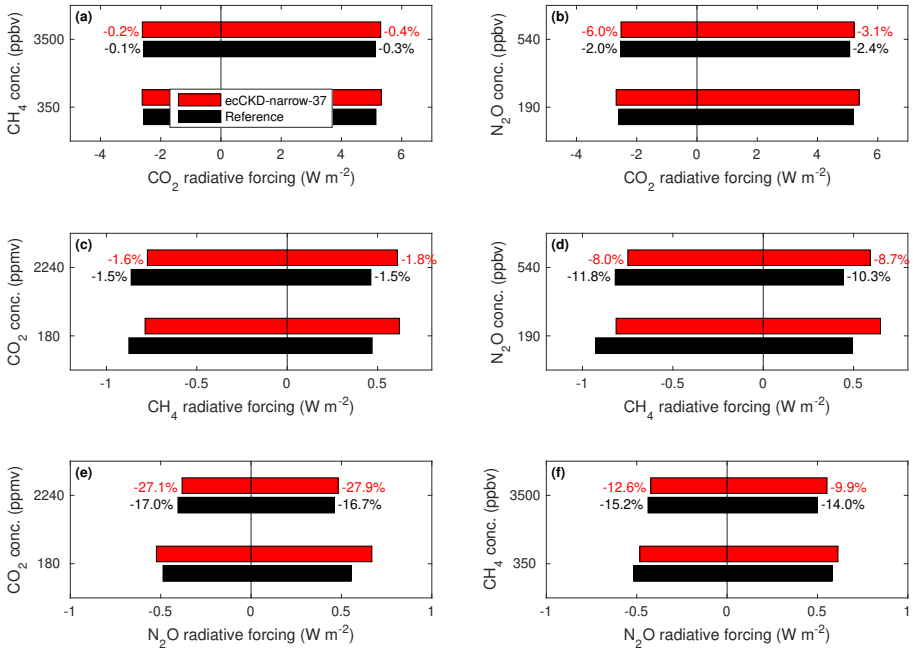

Evaluation of the representation of spectral overlap of CO_2, CH_4 and N_2O by the climate-narrow-37 CKD model. In each panel, the abscissa shows the TOA radiative forcing from perturbing a gas to either its climatic minimum or maximum value. These radiative forcings are computed keeping the concentrations of all other well-mixed gases at their present-day values, except for the gas on the ordinate, which is perturbed to its own climatic minimum or maximum values.

Model 16: ecCKD climate-narrow-48

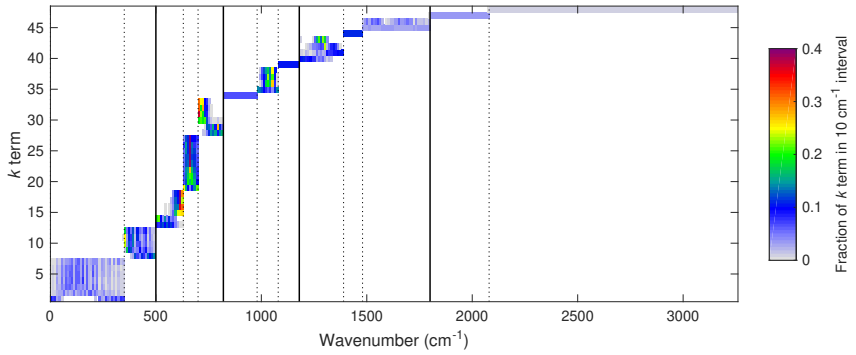

Illustration of the parts of the longwave spectrum that contribute to each k term of the climate-narrow-48 model.

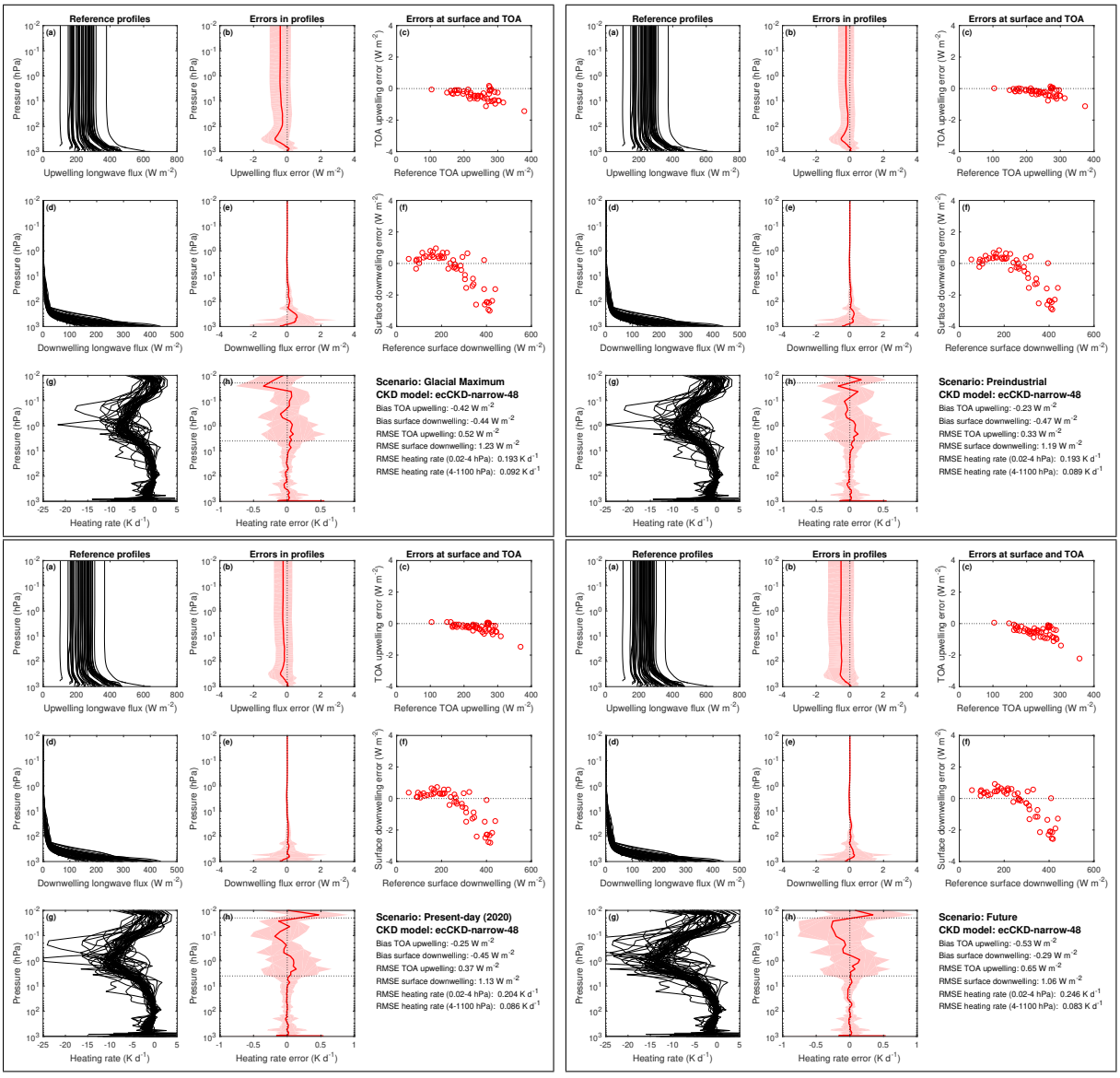

Each boxed groups of panels evaluate the climate-narrow-48 CKD model for a single CKDMIP scenario. The left three panels in each group show the irradiances and heating rates from the reference line-by-line calculations. The red lines in the middle three panels show the corresponding bias in these quantities from the CKD model. The shaded regions encompass 95% of the instantaneous errors. Panels c and f depict instantaneous errors in upwelling TOA and downwelling surface irradiances. Error metrics are provided in the lower right.

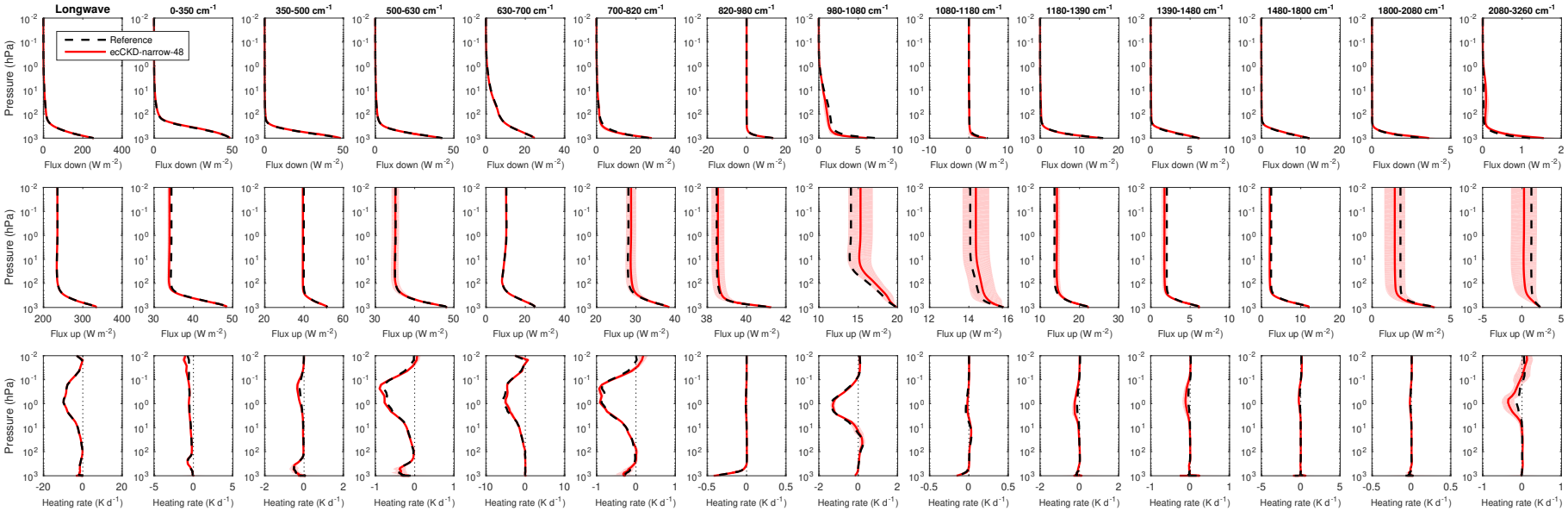

Evaluation of irradiances and heating rates for the broadband (leftmost column of panels) and the 13 narrow longwave bands (other panels) of the climate-narrow-48 CKD model. The black dashed and red solid lines correspond to the average of the 50 profiles for the "present-day" scenario, while the shaded regions encompass 95% of the error.

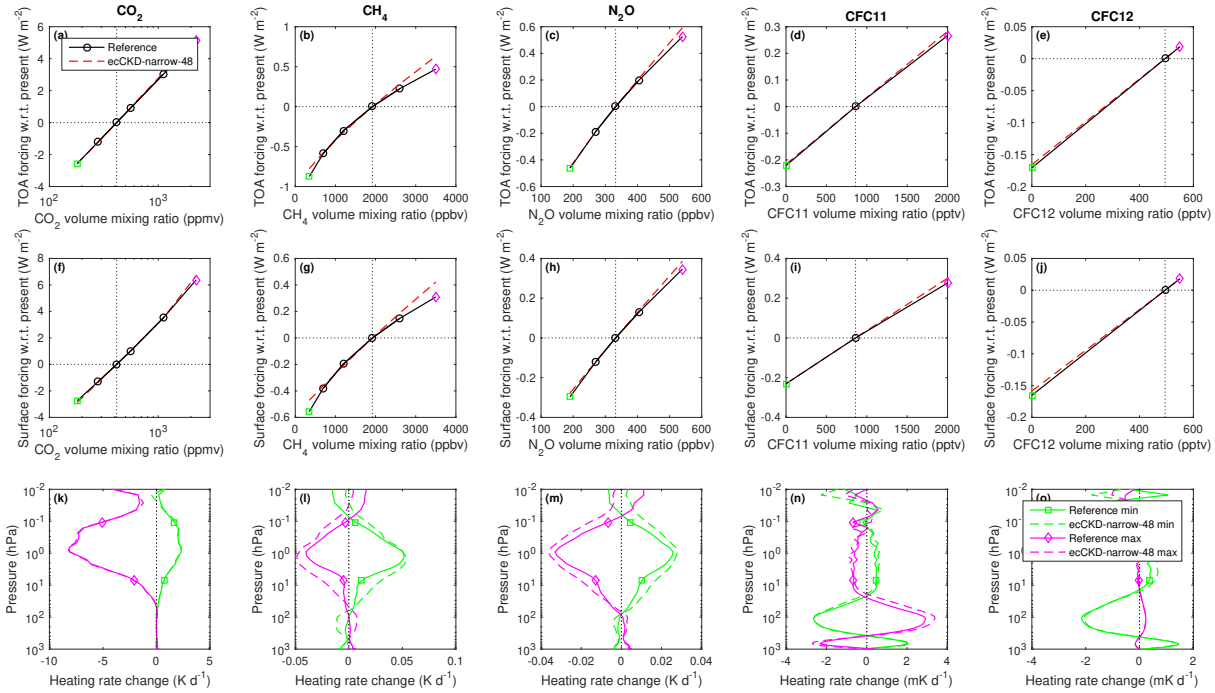

Comparison of reference line-by-line and calculations by the climate-narrow-48 model of the instantaneous clear-sky radiative forcing from perturbing each of the five well-mixed greenhouse gases from their present-day values, at (top row) top-of-atmosphere and (middle row) surface, averaged over the 50 profiles of the Evaluation-1 dataset. The bottom row shows the mean change to heating rate resulting from perturbing the concentration of a gas from its present-day value to either the maximum or minimum value in the range for that gas.

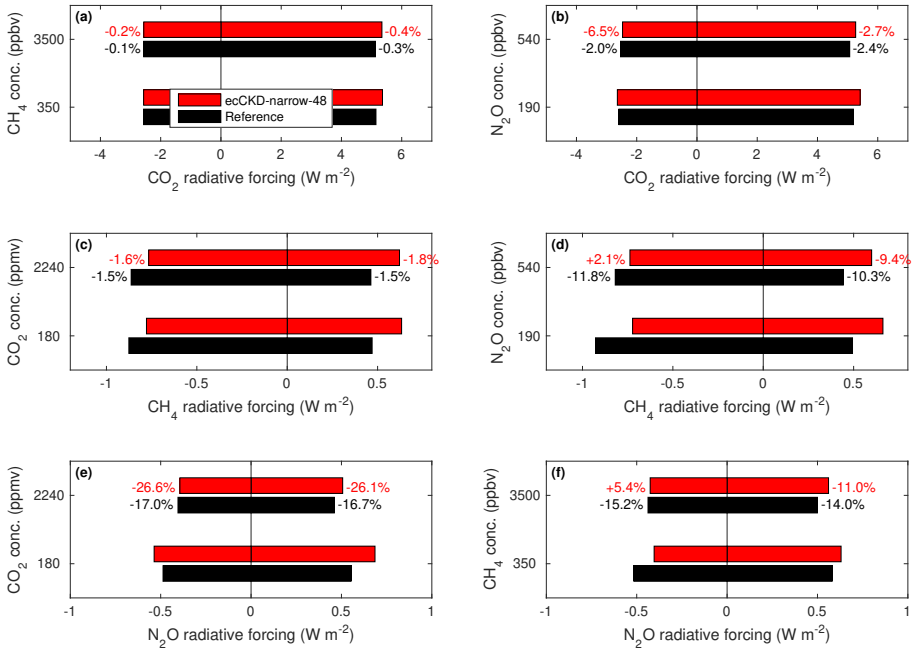

Evaluation of the representation of spectral overlap of CO_2, CH_4 and N_2O by the climate-narrow-48 CKD model. In each panel, the abscissa shows the TOA radiative forcing from perturbing a gas to either its climatic minimum or maximum value. These radiative forcings are computed keeping the concentrations of all other well-mixed gases at their present-day values, except for the gas on the ordinate, which is perturbed to its own climatic minimum or maximum values.

Model 17: ecCKD climate-narrow-69

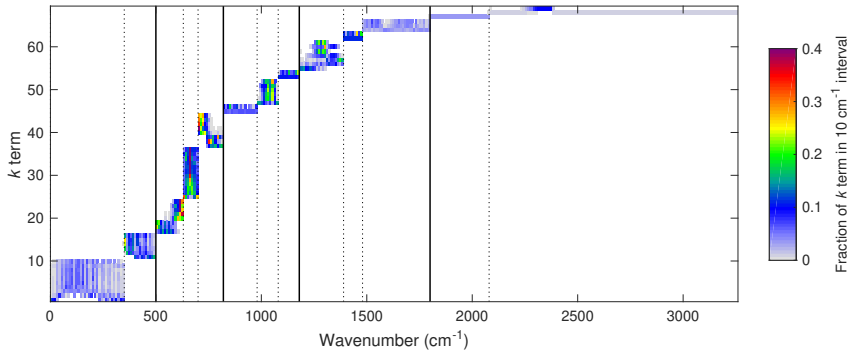

Illustration of the parts of the longwave spectrum that contribute to each k term of the climate-narrow-69 model.

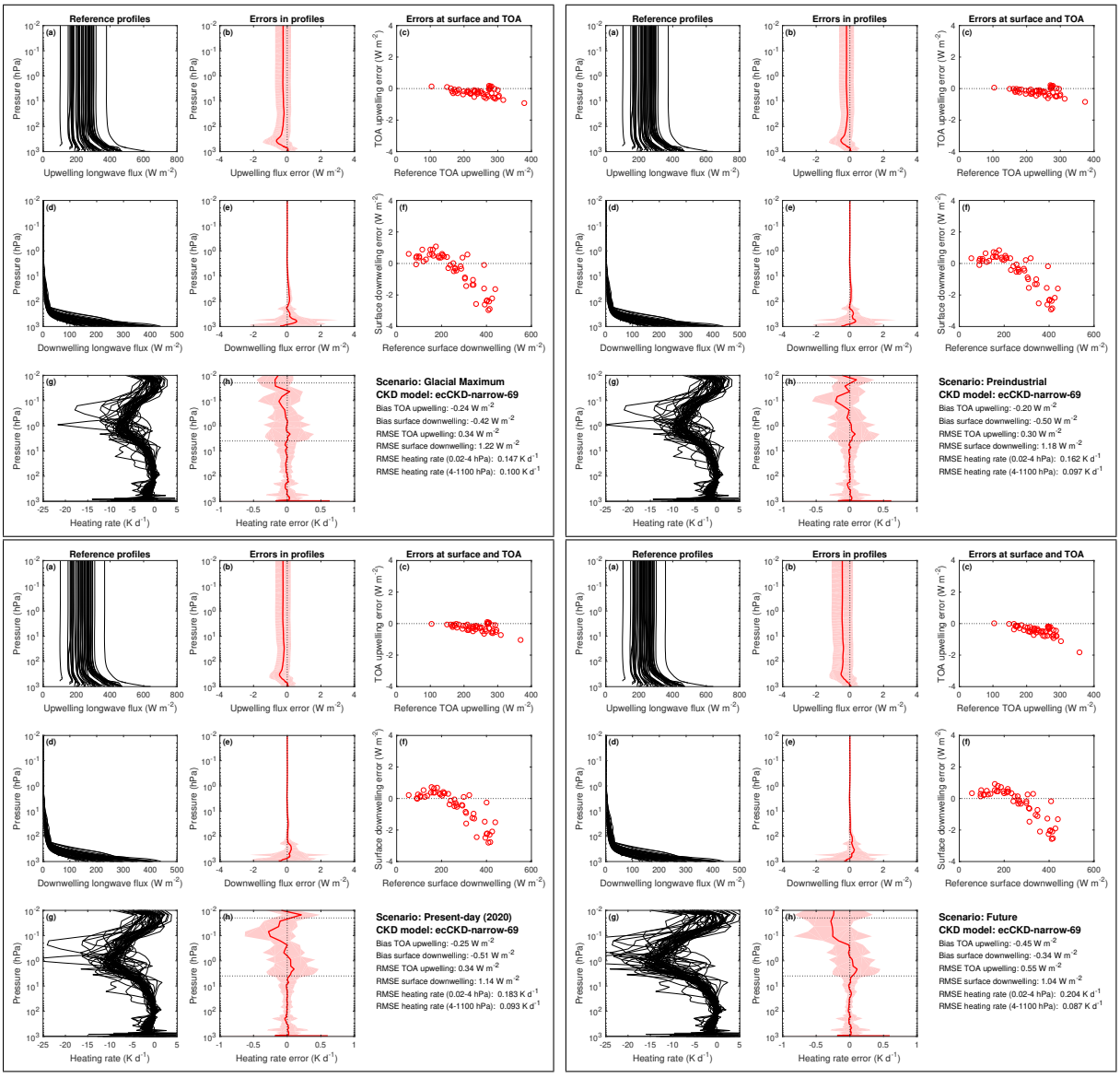

Each boxed groups of panels evaluate the climate-narrow-69 CKD model for a single CKDMIP scenario. The left three panels in each group show the irradiances and heating rates from the reference line-by-line calculations. The red lines in the middle three panels show the corresponding bias in these quantities from the CKD model. The shaded regions encompass 95% of the instantaneous errors. Panels c and f depict instantaneous errors in upwelling TOA and downwelling surface irradiances. Error metrics are provided in the lower right.

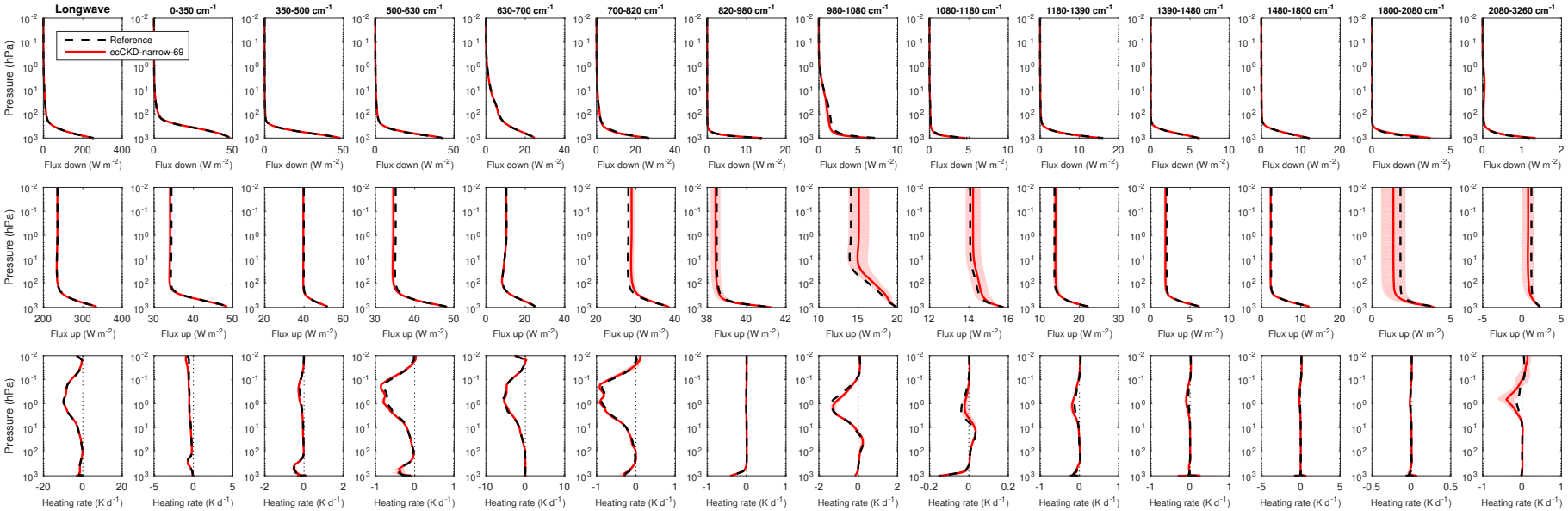

Evaluation of irradiances and heating rates for the broadband (leftmost column of panels) and the 13 narrow longwave bands (other panels) of the climate-narrow-69 CKD model. The black dashed and red solid lines correspond to the average of the 50 profiles for the "present-day" scenario, while the shaded regions encompass 95% of the error.

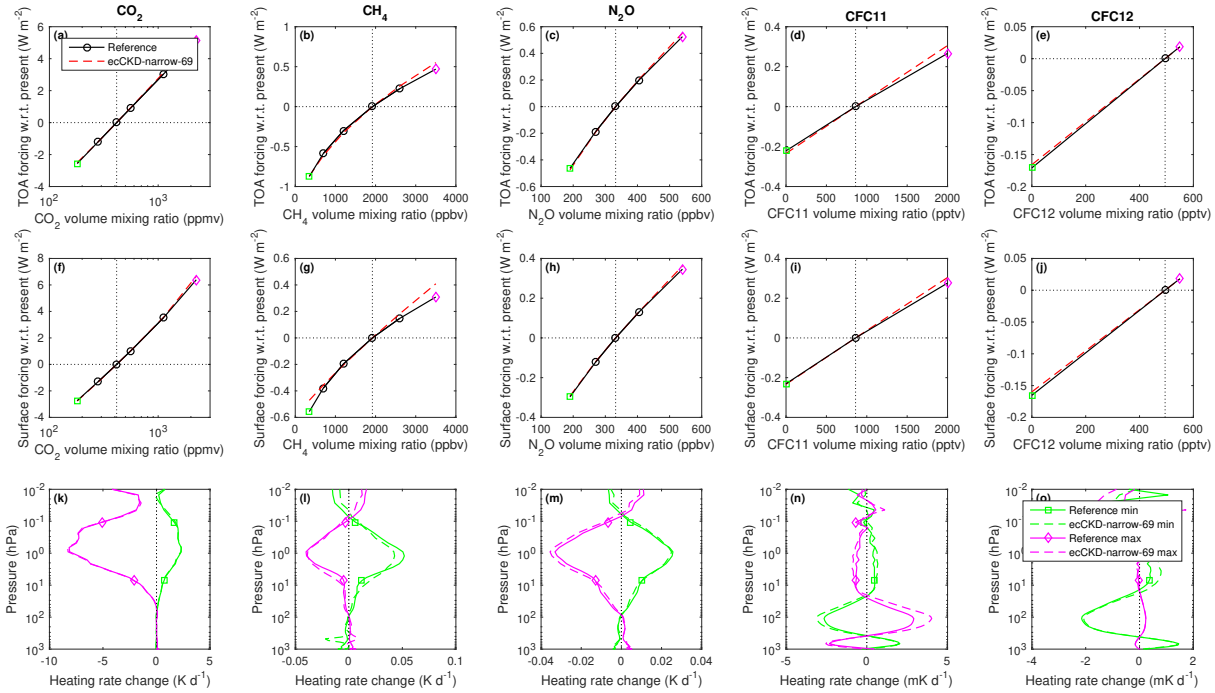

Comparison of reference line-by-line and calculations by the climate-narrow-69 model of the instantaneous clear-sky radiative forcing from perturbing each of the five well-mixed greenhouse gases from their present-day values, at (top row) top-of-atmosphere and (middle row) surface, averaged over the 50 profiles of the Evaluation-1 dataset. The bottom row shows the mean change to heating rate resulting from perturbing the concentration of a gas from its present-day value to either the maximum or minimum value in the range for that gas.

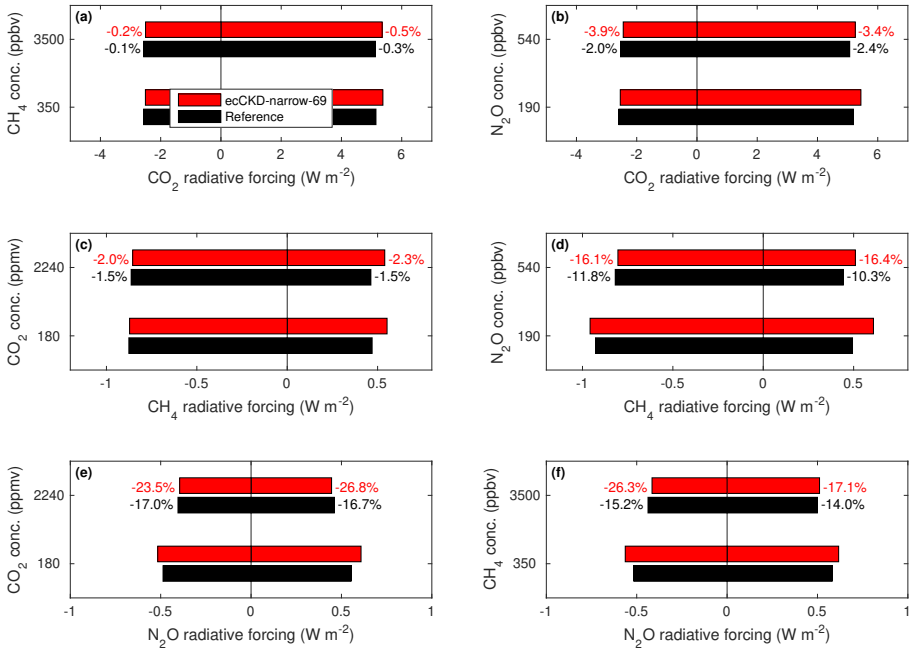

Evaluation of the representation of spectral overlap of CO_2, CH_4 and N_2O by the climate-narrow-69 CKD model. In each panel, the abscissa shows the TOA radiative forcing from perturbing a gas to either its climatic minimum or maximum value. These radiative forcings are computed keeping the concentrations of all other well-mixed gases at their present-day values, except for the gas on the ordinate, which is perturbed to its own climatic minimum or maximum values.

Model 18: ecCKD climate-narrow-101

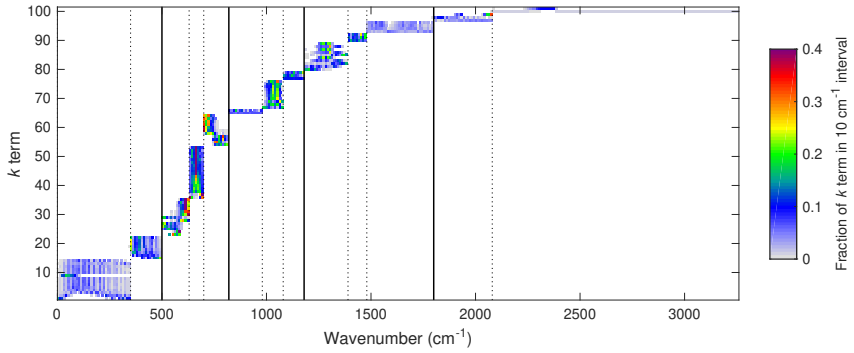

Illustration of the parts of the longwave spectrum that contribute to each k term of the climate-narrow-101 model.

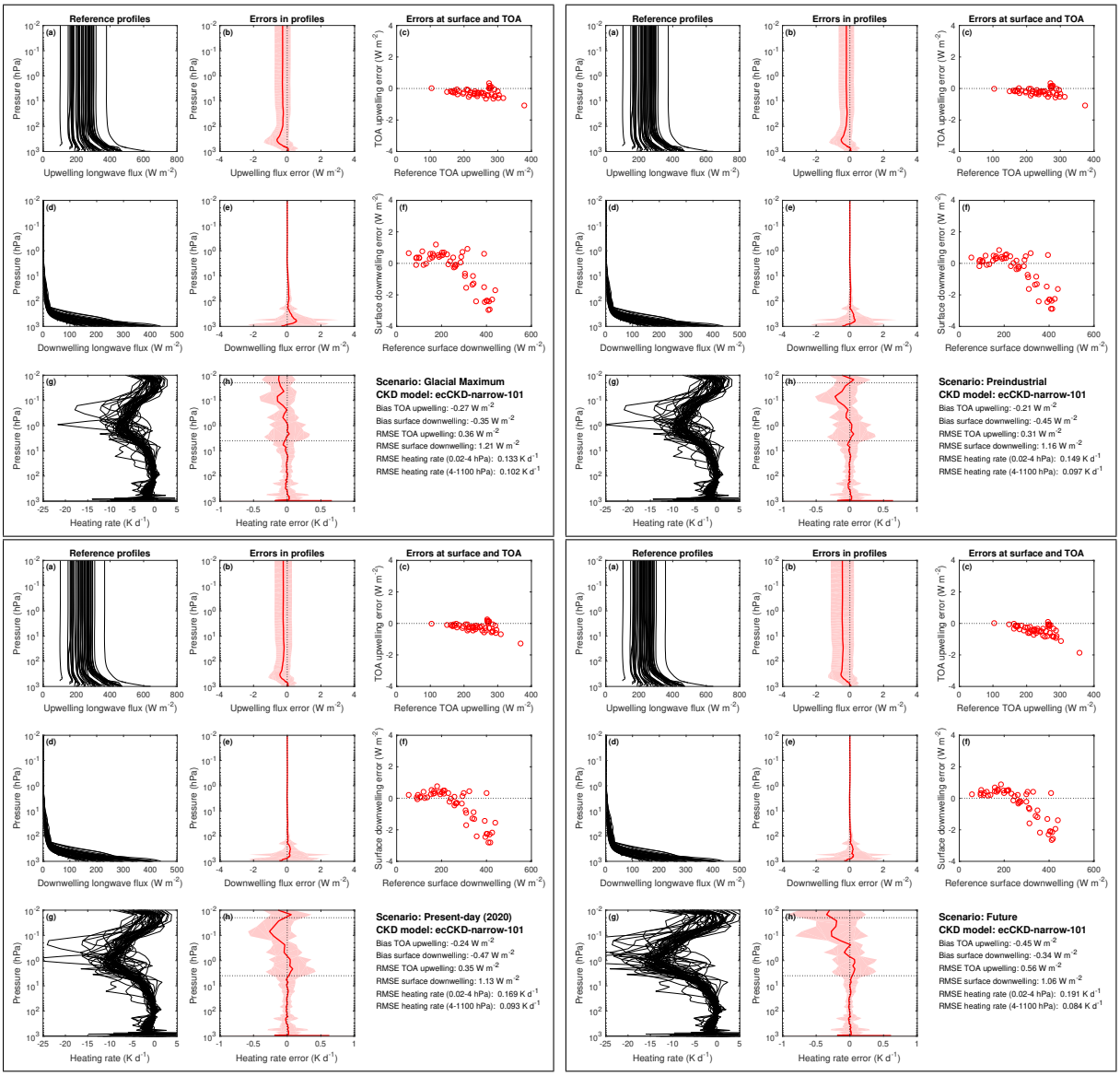

Each boxed groups of panels evaluate the climate-narrow-101 CKD model for a single CKDMIP scenario. The left three panels in each group show the irradiances and heating rates from the reference line-by-line calculations. The red lines in the middle three panels show the corresponding bias in these quantities from the CKD model. The shaded regions encompass 95% of the instantaneous errors. Panels c and f depict instantaneous errors in upwelling TOA and downwelling surface irradiances. Error metrics are provided in the lower right.

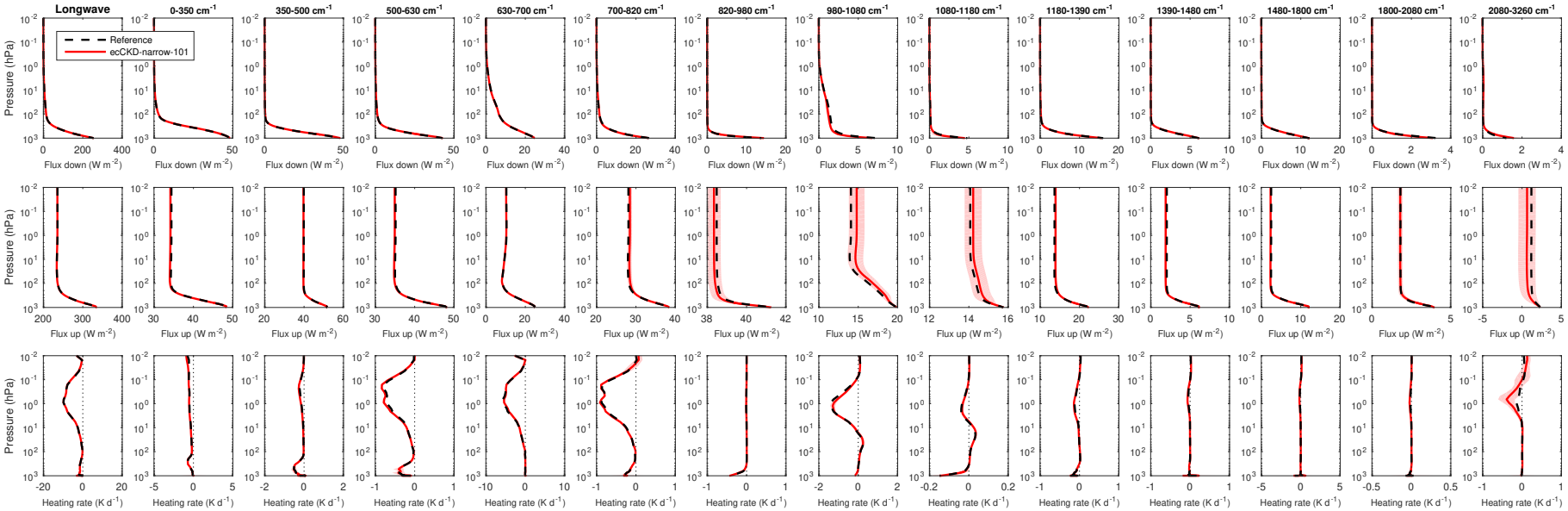

Evaluation of irradiances and heating rates for the broadband (leftmost column of panels) and the 13 narrow longwave bands (other panels) of the climate-narrow-101 CKD model. The black dashed and red solid lines correspond to the average of the 50 profiles for the "present-day" scenario, while the shaded regions encompass 95% of the error.

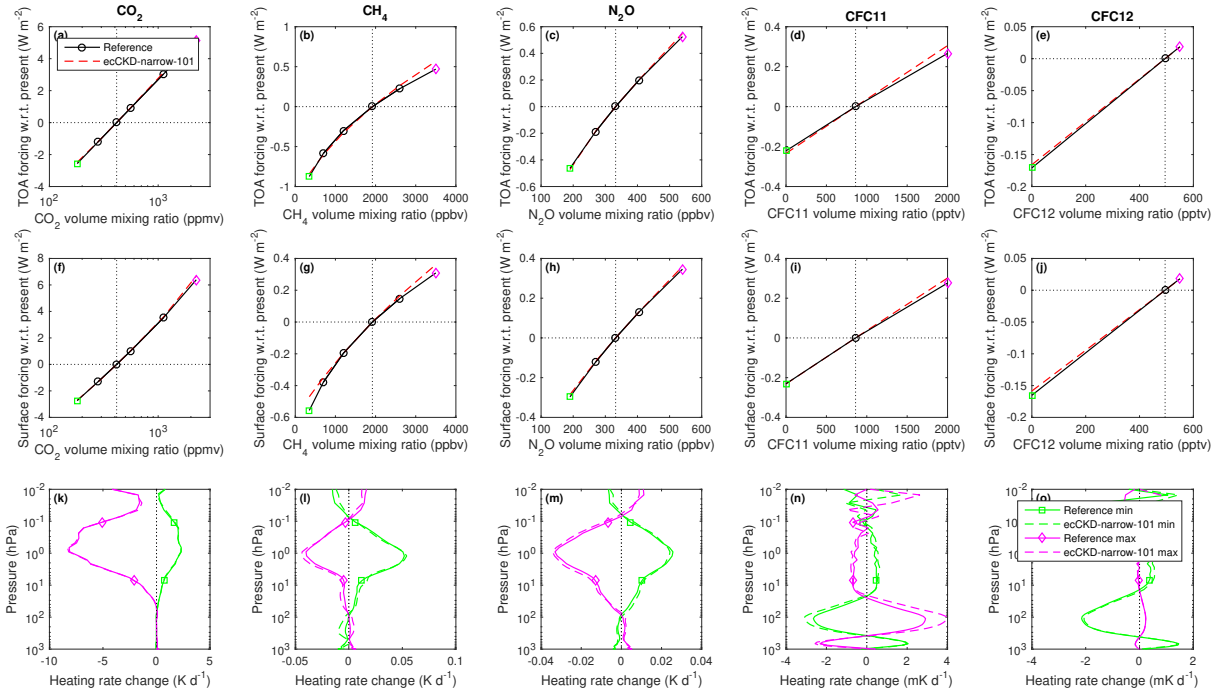

Comparison of reference line-by-line and calculations by the climate-narrow-101 model of the instantaneous clear-sky radiative forcing from perturbing each of the five well-mixed greenhouse gases from their present-day values, at (top row) top-of-atmosphere and (middle row) surface, averaged over the 50 profiles of the Evaluation-1 dataset. The bottom row shows the mean change to heating rate resulting from perturbing the concentration of a gas from its present-day value to either the maximum or minimum value in the range for that gas.

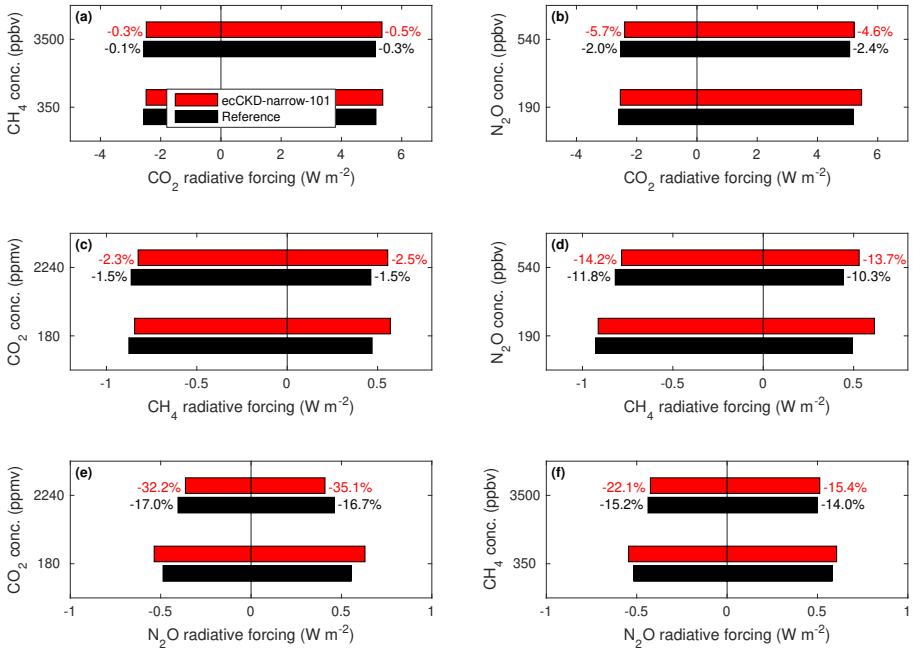

Evaluation of the representation of spectral overlap of CO_2, CH_4 and N_2O by the climate-narrow-101 CKD model. In each panel, the abscissa shows the TOA radiative forcing from perturbing a gas to either its climatic minimum or maximum value. These radiative forcings are computed keeping the concentrations of all other well-mixed gases at their present-day values, except for the gas on the ordinate, which is perturbed to its own climatic minimum or maximum values.